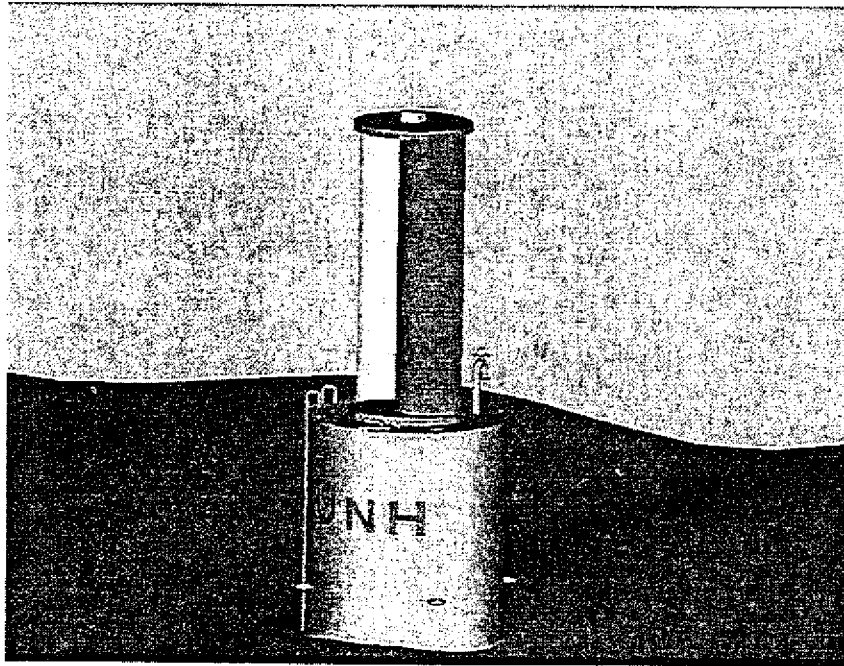


OSWEB

Offshore Wind Energy Powered Fish Feed Buoy



Open Ocean Aquaculture Engineering
Ocean Projects Course, 2002-2003
University of New Hampshire

TEAM MEMBERS

Angela Pelletier, Austin Ganly, David Parker,
Gita George, John Gagne, Phillip Perrinez

PROJECT ADVISOR

Dr. Barbaros Celikkol



Acknowledgments

We would like to thank our advisor, Dr. Barbaros Celikkol, for the opportunity to work on this project, and for his guidance throughout the project. We also extend our sincerest gratitude to Dr. M. Robinson Swift; without Professor Swift's expertise much of this project would not have been possible.

We greatly appreciate the assistance of Professor Igor Tsukrov and Oleg Eroshkin in creating and analyzing the finite element models for the design. We would like to thank Judson DeCew for his assistance with the physical model testing.

We are very grateful for the electrical and wireless communication expertise of Dr. Lloyd Huff. We would also like to acknowledge the assistance of Colin Kerr of Windstream Power Systems Inc. with the turbine design and analysis.

We would like to thank the engineers of the NOAA - University of New Hampshire Cooperative Institute of New England Fisheries and Mariculture Open Ocean Aquaculture Engineering team, particularly Dave Fredriksson, Brett Fullerton, Glen Rice, Glenn McGillicuddy, Ken Baldwin, John Ahern, Michael Chambers, and Can Kurgan for their input and for answering our many questions.

We thank Larry Harris for leading the TECH 797 course, and Jon Scott for the management of our budget.

We would like to note that this work is the result of research sponsored in part by the National Sea Grant College Program, NOAA, and the U.S. Department of Commerce, under grant #NA16RG1035 through the New Hampshire Sea Grant Program.

Abstract

As fish populations decline in the Gulf of Maine, alternatives to traditional fishing are being explored. One of these alternatives is Open Ocean Aquaculture (OOA). The University of New Hampshire currently maintains an OOA facility near the Isle of Shoals. The goal of this facility is to eventually support four cages of cod and haddock with up to 50,000 fish per cage (Chambers, 2002). In order for these fish populations to survive they must have an adequate food supply. An interdisciplinary undergraduate research design team was tasked with designing a buoy that will hold enough food to feed four full cages for one week and deliver the feed to the fish in a manner that can be controlled remotely. The team was charged assessing feasibility from a technical standpoint

One design goal was that the buoy be self-supporting in terms of its energy needs. A renewable power source for the pumps, valves, and communication systems needed to be contained on the buoy. Because of continuous winds at the application site it was decided that a wind turbine would work well for the needs of this project. A vertical axis turbine, 1.8 meters in diameter and 4.4 meters tall, was designed by Windstream Power Systems. Eight marine batteries will be used to store energy produced.

The feed delivery is comprised of a screw auger and four lines, one to each cage. Each line has its own valve so each cage can be fed independently. Onboard the buoy is a system of pumps and valves that allow ballast water in and out of the buoy to maintain a constant draft as food is added and removed. All of the systems are capable of being controlled remotely using 900 MHz cellular communications.

The buoy was required to store food for 200,000 mature fish for one week without being refilled. A spar shape (long and slender) was chosen for the design of the buoy because of its general independence of wave motion (Berteaux, 1991). Dimensions of the buoy were largely determined by the projected volume of feed required for a maximum number of fish during a stage in their growth when food consumption is greatest. The proposed buoy is 3 meters in diameter and 16.6 meters in length. Scale models of the buoy were built for testing in the wave tank at the Jere A. Chase Ocean Engineering Laboratory at the University of

New Hampshire (UNH). Early testing revealed that the damped natural frequency of the spar buoy as designed was the same as that of storm seas. A large disc nine meters in diameter with eight holes 1.5 meters in diameter spaced evenly around the vertical axis was placed on the bottom of the buoy; lowering the damped natural frequency and avoiding resonant loading conditions. Finite element analysis was conducted for the buoy structure and showed that the factor of safety for the buoy is 9.5.

UNH Open Ocean Aquaculture engineers have recently designed a mooring system suited for the proposed four fish cages. The design team needed to design a method for incorporating the feed buoy into this system. An extended bridle system was developed where four bridle lines extend horizontally from the feeder buoy to smaller surface buoys, down to the grid, where a line extends from the bottom of the buoy to a chain on the sea floor. The purpose of the chain is to act as a restoring force, further reducing interaction between the waves and the buoy. Finite element analysis was also performed on the mooring grid and feed buoy system using Aqua-FE. Results showed stresses and displacements to be within acceptable ranges.

While the design of a feeder buoy capable of feeding 200,000 fish (50,000 fish per cage) for seven days is large, computational and physical tests show that it is possible. The structural integrity of the buoy and stability of the mooring system are sound. The buoy designed can withstand the harsh conditions in the Gulf of Maine. The project team asserts that this design is feasible, however, internal systems such as feed delivery and energy storage should be rigorously tested before construction.

Table of Contents

Title Page	i
Acknowledgments.....	ii
Abstract.....	iii
Table of Contents.....	v
List of Tables	vi
List of Figures	vii
I. Introduction	1
Background.....	1
Purpose	3
Approach	3
Site Description	4
Mooring System Design	9
III. Design	13
Buoy Structure Design.....	14
Feed Distribution System Design	17
Turbine Design	22
III. Physical Modeling	26
Model Design	26
Facility	29
Free Release Tests	31
<i>Test Plan</i>	31
<i>Method</i>	32
<i>Results</i>	33
<i>Discussion</i>	35
Sea Keeping Tests	36
<i>Test Plan</i>	36
<i>Method</i>	36
<i>Results</i>	39
<i>Discussion</i>	43
V. Computational Modeling	45
Finite Element Analysis of Buoy Structure.....	45
<i>Mesh</i>	45
<i>Load Cases</i>	46
<i>Results</i>	47
<i>Discussion</i>	53
Finite Element Analysis of Mooring System.....	53
<i>Load Cases</i>	56
<i>Results</i>	57
<i>Discussion</i>	60
VI. Conclusion	62
VII. References	63
VIII. Appendices.....	65
A. Detail Drawings	A-1
B. Buoy Feed System Operating Procedures.....	B-1
C. Prefabricated Component Specifications	C-1
D. Raw Data Plots of Physical Test Results.....	D-1
Free Release Tests.....	D-1
Moored Sea-Keeping Tests	D-2

List of Tables

Table 1: Masses and Centers of Structure.....	17
Table 2: Feed Distribution Component List	18
Table 3: Components Requiring Power	22
Table 4: Scaled Masses and Centers	27
Table 5: Model Scale Free-Release Heave Results	34
Table 6: Model Scale Free-Release Pitch Results	34
Table 7: Full Scale Free Release Heave Results.....	34
Table 8: Full Scale Free Release Pitch Results.....	35
Table 9: Summary of Free-Release Results.....	35
Table 10: Summary of Sea States	36
Table 11: Summary of Element Properties.....	56
Table 12: Summary of Load Cases.....	57
Table 13: Maximum Rope Stress at Anchor Points.....	57

List of Figures

Figure 1: UNH OOA Cage Deployment.....	2
Figure 2: Haddock.....	2
Figure 3: Location of OOA Demonstration Project Site.....	5
Figure 4: Bottom Bathymetry of the Site.....	6
Figure 5: Average Monthly Wind Speeds.....	9
Figure 6: Top View of Mooring System.....	10
Figure 7: Recommended Mooring Buoy	11
Figure 8: Side View of Mooring System	12
Figure 9: Sketch of Mooring System	12
Figure 10: Isometric View of Buoy Design.....	13
Figure 11: Close-up of Turbine and Buoy Top.....	14
Figure 12: Schematic of Buoy Structure.....	16
Figure 13: Schematic of Feed Distribution System	18
Figure 14: Communications Schematic	20
Figure 15: Horizontal Axis Turbine.....	23
Figure 16: Vertical Axis Turbine	23
Figure 17: Storage Batteries.....	25
Figure 18: Unfinished Buoy Model	28
Figure 19: Finished Buoy Model	29
Figure 20: Wave Paddle.....	30
Figure 22: OPIE Calibration	31
Figure 22: A Free-Release Trial.....	32
Figure 23: Free Release Heave Response.....	33
Figure 24: Free-Release Pitch Response.....	33
Figure 25: Sea-Keeping Test Schematic.....	37
Figure 26: OPIE Frame of a Sea-Keeping Test	38
Figure 27: A Sea-Keeping Test.....	38
Figure 28: Comparison of Raw and Average Data	39
Figure 29: Model Scale Sea-Keeping Test Results.....	40
Figure 30: Model Scale Free Release Test Pitch Results.....	41
Figure 31: RAO vs. Frequency	42
Figure 30: Pitch Transfer Function	43
Figure 33: 3 Dimensional View of Buoy Mesh	46
Figure 34: Downward Motion Load Cases	47
Figure 35: Upward Motion Load Cases	47
Figure 36: Maximum Stress of Shell (Downward Motion)	48
Figure 37: Maximum Stress of Disc (Downward Motion)	49
Figure 38: Maximum Stress of Shell (Upward Motion).....	50
Figure 39: Maximum Stress in Disc (Upward Motion)	51
Figure 40: Maximum Displacement of Disc.....	52
Figure 41: Maximum Displacement of Disc.....	52
Figure 42: Buoy Mesh for Mooring System FEA.....	54
Figure 41: Full Mooring Grid Mesh	55
Figure 44: FEA Results for Storm Seas	59
Figure 45: Input Wave Envelope and Buoy Heave as Modeled by AquaFE.....	60

I. Introduction

The University of New Hampshire (UNH) currently maintains an active Open Ocean Aquaculture (OOA) facility in the Gulf of Maine. This experimental aquaculture site, along with others like it, is of great importance due to rapidly decreasing native fish populations in the North Atlantic. The motivation for alternative solutions re-manifests itself as quotas decrease and restrictions are implemented on catches every season. This year alone some southern New England cod harvesters could see their limits drop from 2,000 lbs to 500 lbs per day. Contained Aquacultures could be the only long-term solution to the great problems facing the fishing industry, its economy, and the depletion of natural fish stocks.

Background

In June of 1999 UNH, as part of a regional effort, deployed the OOA demonstration project. An offshore location was chosen over a protected coastal site because of the high use of New England's coastal waterways by commercial fishing, recreational, and shipping vessels. An offshore site also provides greater water depths and a solution to space restrictions in crowded inland waters (Fredriksson et al., 2000). The project has been operational and has withstood all weather forcing conditions since that time. A mid-depth horizontal grid moors the system of two cages, each 15 meters in diameter. The cages were designed to raise bottom fish such as summer flounder and halibut. Figure 1 shows a photograph of the deployment of one of the current cages; haddock currently being raised at the site are shown in Figure 2.

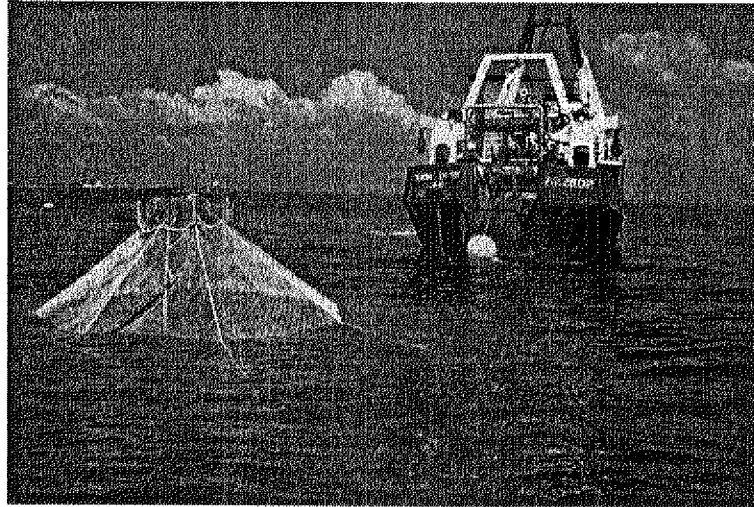


Figure 1: Deployment of one of the current cages in 1999 (www.ooa.unh.edu).

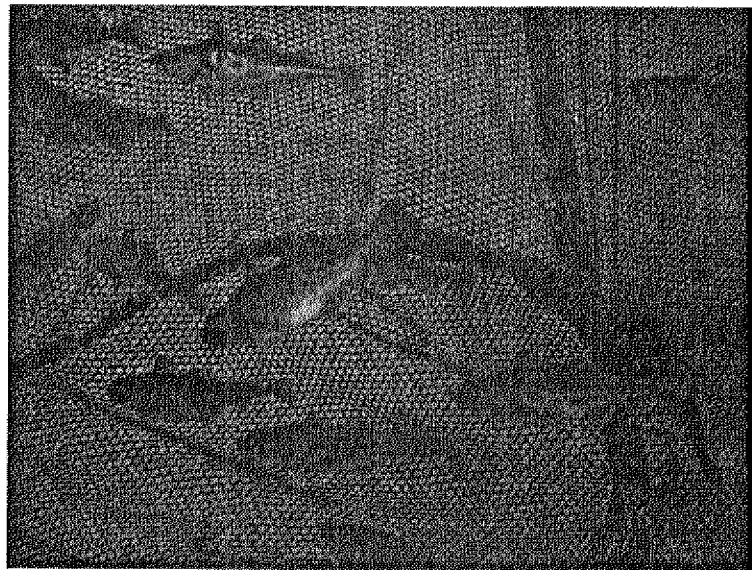


Figure 2: A view from inside the cage of the haddock being raised offshore (www.ooa.unh.edu).

Interest in aquaculture is increasing rapidly throughout the world in all areas of declining fish stocks. In the future the OOA group hopes to raise cod and haddock, which are important species to the New England economy. Funding from NOAA/Sea Grant supports the project (Tsukrov et al., 2000).

The OOA project at UNH has been a success thus far, and is constantly being updated to increase production and efficiency. Currently there is one wind and solar powered buoy that maintains the feed supply to one of the cages. It is effective, but must be refilled frequently as it has a maximum feed capacity of 500 lbs. The maximum density of mature fish in just one of the new proposed cages consumes 8,400 lbs of feed per week. It was decided that for production to increase the current buoy would need to be replaced with a design that could accommodate four cages and hold enough food for seven days of feeding. This would be an increased initial cost, but would cut down on boat travel, man hours, and improve overall fish production (www.ooa.unh.edu).

Purpose

The purpose of this project was to design a conceptual large-scale offshore wind powered fish feeding buoy to service four cages at the UNH OOA demonstration project site. Specific requirements for the buoy included remote communication and refilling of the feed silo every seven days. The group was not tasked with manufacturing, cost control, or deployment.

Approach

The task of designing a new conceptual spar buoy was undertaken by a group of six students in the Ocean Research Projects class, Tech 797, at the University of New Hampshire. The specific project goals included a concept design for a durable buoy structure to be maintained at the site within the stable mooring system designed by the OOA project team, a reliable design for pumping the feed, remote communication and monitoring capabilities, and that all the power generated is by the wind. Energy from the wind was a feasible clean solution to offshore power. The use of rechargeable batteries removed the need to change fuel cells often, and was a practical power alternative given the daily wind durations at the site. The buoy was designed to deliver sufficient feed to sustain every possible load of fish between empty and maximum capacity.

With these design goals in mind, the group split into smaller groups to tackle separate parts of the project. The project was broken down into the following areas:

1. Buoy structure- envelope design and ballast design,
2. Feed system- pumps, hoses, valves, and feed silo,
3. Remote Communication- feed system controls and monitoring,
4. Turbine-selection, power generation and storage,
5. Mooring system-stability, safety, and general sea keeping,

For each of these areas the design included studying feasibility, reliability, and durability of all components.

Each section was designed separately and agreed on by the group as a whole. After initial calculations and numerical models for theoretical performance were completed, an actual model buoy was constructed and physical tests were run to determine how the buoy would fare in the open ocean. Once the test results were analyzed, the model was modified accordingly and tested again. Finally, the systems were modified and their respective positions were fixed within the buoy structure and mooring design. The final model was constructed with all representative weights and components included. Free release tests and general sea keeping tests were run with and without the buoy anchored to the model mooring system and analyzed for stability and durability. Based on the performance of the model buoy recommendations were made for a full-scale buoy design.

Site Description

The OOA site is currently located in 55 meters of water approximately 9.6 kilometers (6 miles) off the coast of New Hampshire and 1.6 kilometers (one mile) south of the Isles of Shoals' White Island. The exact location, 42°57' North Latitude and 070°38' West Longitude, can be seen in Figure 3.

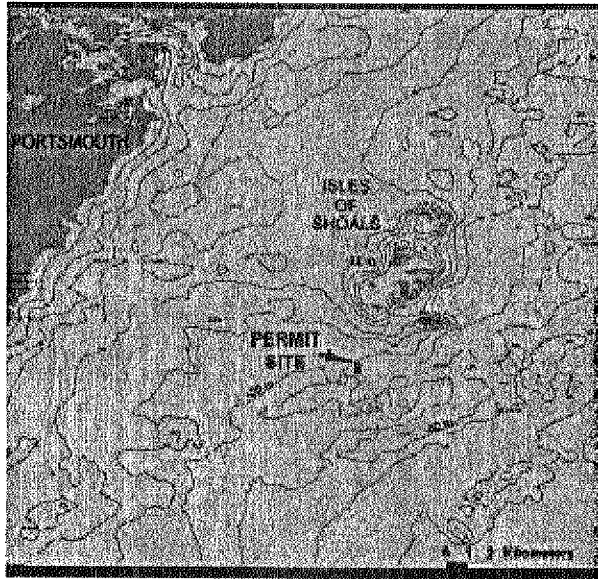


Figure 3: Location of the OOA Demonstration Project Site (www.ooa.unh.edu)

The site is rectangular and covers 121,405 square meters (30 acres) (www.ooa.unh.edu). There are two cages deployed at the site, containing haddock and halibut. They rest approximately 18 meters (30 feet) below the water's surface to decouple them from surface motion and damp wave and current interaction with the cages.

Bottom type in the area is mostly low organic sandy silt and is relatively flat. There is a small bedrock outcrop on the northern limit of the site skirted by a gravel or cobble apron. Figure 4 shows the sea floor. The flat bottom improves mooring stability (www.ooa.unh.edu).

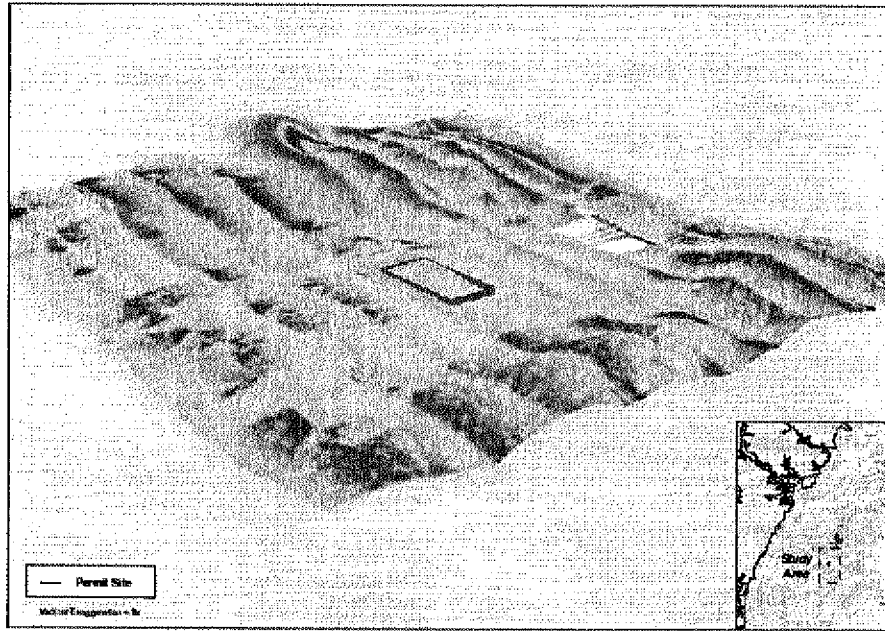


Figure 4: Bottom Bathymetry (www.oaa.unh.edu)

The buoy's design must withstand strong storm waves and breakers. The waves most frequently recorded at the site range from less than a meter to greater than five meters with periods of four seconds to a maximum of around 12 to 14 seconds (www.ndbc.noaa.gov). Tidal ranges at the site were gathered from data at the Isles of Shoals and from observations at the site itself. Maximum tidal ranges were determined to be approximately four meters (www.tidesonline.nos.noaa.gov).

Wind speeds are of great concern for power generation. The only historical average sustained wind speed data was found through NOAA maintained C-MAN Station IOSN3 located on the Isles of Shoals. The anemometer height is 19.2 meters above sea level; some error is introduced due to the difference between buoy elevation and station elevation. Once again, of highest concern were worst-case scenarios: strongest and weakest winds, which effect stability and energy production. The lowest sustained winds occur during the month of August. The month of August, falling in the height of the summer could be a very active fish growth time. This could mean that cages operating at maximum capacity would be relying on the lowest wind power supply of the entire year. General winds for the rest of the year range anywhere from zero knots to hurricane force winds (www.ndbc.noaa.gov).

II. Design Specifications

The buoy design is subject to many constraints and specifications. Design criteria included the number of fish cages to be serviced, the type and stage of development of the fish, the location of the site, the amount of power required of the turbine, the communication with the buoy, feed line behavior from the buoy to the cages, and integration of the buoy with the mooring system. In addition, the project team was given from September 2002 through April 2003 to complete the design and a budget of \$2,000 dollars for fabrication and testing of the model.

Feed Requirements

The primary purpose of the buoy is to feed the fish contained in four submerged cages. Cod was used as the prototype for the feed system requirements. Design specifications included the ability to sustain four 3000 m³ fish cages, each holding approximately 50,000 fish. At a consumption rate of 3% body weight per day, at stocking size, the population of 250-gram cod would require 375 kg of feed per day. At harvest size, the population of 700-gram cod would require 1000 kg of feed per day. Assuming all four cages are filled with harvest size cod, and given the design requirement of only one-grain silo refill per week, a silo capacity of about 35 metric tons is required. Feed volume flow rates are determined based on two 30 minute feed cycles per cage, per day. For the harvest size cod, mass flow rate of 0.29 kg/s is required. Given a sinking feed-pellet of specific weight 1.2, this translates to a 240 cm³/s volume flow rate (Chambers, 2002).

Sea-Keeping Requirements

The buoy's intended use makes it necessary to be a quasi-stable platform in the open ocean. This is difficult to accomplish given the conditions in the North Atlantic; currents, wave heights, and wave periods are often quickly changing. The team is concerned with the heave

and pitch motion of the buoy due to the buoy's integration with the mooring system that holds the fish cages. Motion of the buoy that is very dependent on wave heights and periods will cause excessive strain on the mooring system and fish cages. The buoy must be designed to remain relatively stable in various sea states, and to withstand severe storm conditions.

Wave heights seen at the site vary from less than one meter to greater than five meters on a regular basis. The average significant wave height is taken to be 1.2 meters, based on observations from Boston and Portland data buoys (www.ndbc.noaa.gov). June and July are the least active months, and see maximum wave heights measuring 4 meters; in comparison, during the most active months (the winter months) waves can reach heights of 7 m. The group was most concerned with worst-case scenarios that were determined to be waves with periods of 8 to 12 seconds and heights of 9 to 11 meters. Water temperatures vary from 2.5 to 10 °C.

Energy Constraints

When placing a wind turbine on a buoy, there are many design factors that must be considered beyond those normally taken into account when designing a rigidly mounted wind energy system. Most of these factors result from the harsh sea environment described above, and may include accelerated corrosion, temperature variation, and general buoy dynamics. Due to the seawater environment, sea-spray may have an adverse affect on the wear of certain turbine components. Off the coast of New Hampshire, the buoy system will experience large temperature variation over the four distinct seasons. Furthermore, because the feed buoy is able to pitch and heave under a varying number of sea states the turbine will also experience additional dynamic forces not taken into consideration for a rigid system. In storm conditions, winds can be very high and waves will likely crash over the buoy hitting the turbine.

Investigating data from the National Data Buoy Center revealed that the month with the lowest average wind speed (6 m/s) is August (www.ndbc.noaa.gov). A monthly average of wind speed can be seen in Figure 5.

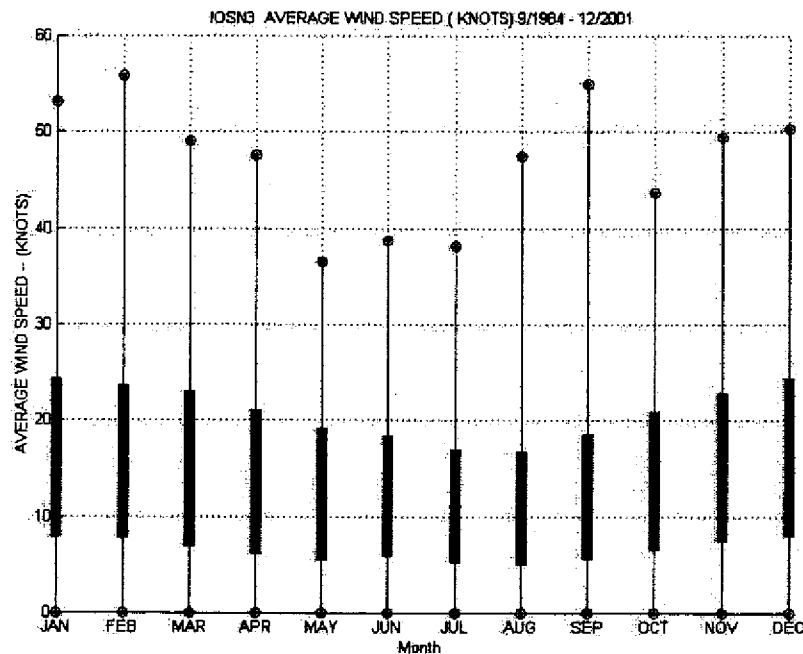


Figure 5: This plot of wind speeds near the Isle of Shoals from 1994 to 2001 shows maximum, average, and one standard deviation for each month. (www.ndbc.noaa.gov)

Mooring System Design

The UNH OOA project team designed the mooring system for the proposed four fish cages. The buoy must be incorporated into this system and have a minimal effect on the motion of the cages located below it. As mentioned previously, stability is incredibly important in this system; the buoy must be somewhat stable to increase energy yield and prevent damage to the turbine and to the feeding lines. The mooring system must be stable to decrease motion of the fish cages themselves.

The current two fish cages are moored on submerged single cage grids approximately 18 meters below the mean water surface. An interlocking grid of four squares has been developed to moor four fish cages, and will also rest approximately 18 meters below the

surface. The large grid design has a footprint of 22,952 m². Figure 6 shows a top view of the proposed grid system. The main grid is 16,900 m² (130 meters per side), with legs extending 151.5 meters (horizontally) from the centerlines (Celikkol et al, 2002).

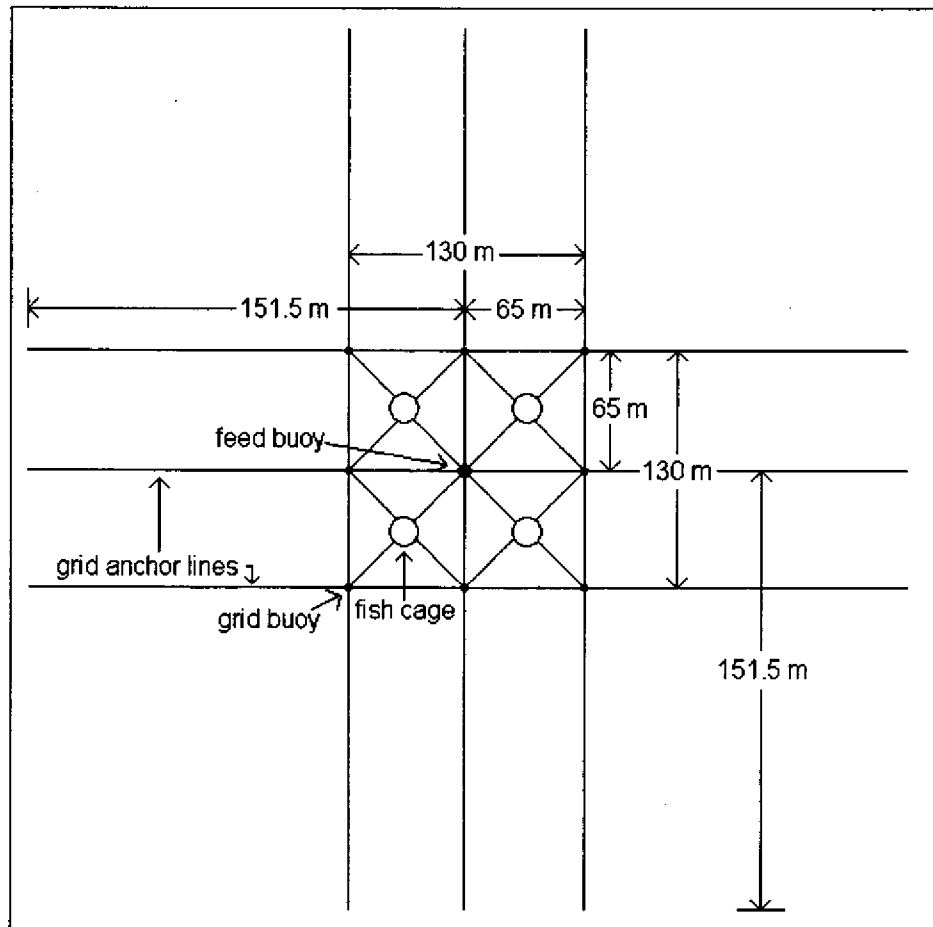


Figure 6: Top View of the Mooring System

The feed buoy is to be located above and moored to the center of this grid. Eight submerged buoys are used to keep the grid neutrally buoyant at the proper depth. The submerged buoys at the corners of the grid have a net buoyancy of 11,120 N (2,500 lbs). The submerged buoys in the center of the edge lines have a net buoyancy of 3,225 N (725 lbs) (Decew, 2003). Polyform A-5 buoys are to be used at the surface and are approximately 0.7 meters in diameter, 0.9 meters long, and yield 179.6 kg (396 lbs) of net buoyancy. The A-5 buoy can be seen in Figure 7.

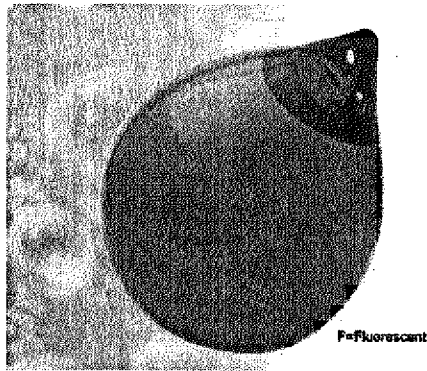


Figure 7: Polyform A-Series Buoy (www.polyformus.com)

The feed buoy is moored by a vertical line extending from its base to the center point of the grid. A second vertical length of line extends from the grid center point to the ocean floor. This line is not anchored to the ocean floor; rather, a length of chain is located at the bottom of the line. This chain is a restoring mechanism that opposes the vertical (heave) motion of the buoy. To reduce pitching of the feed buoy four bridle lines are tethered from the ocean surface to the grid. These bridle lines extend 16 meters from the feed buoy on the surface at 90° angles from each other, to the four surface buoys, before descending to the center of each side grid (Celikkol et al, 2002). Figure 8 is a side view of the complete mooring system.

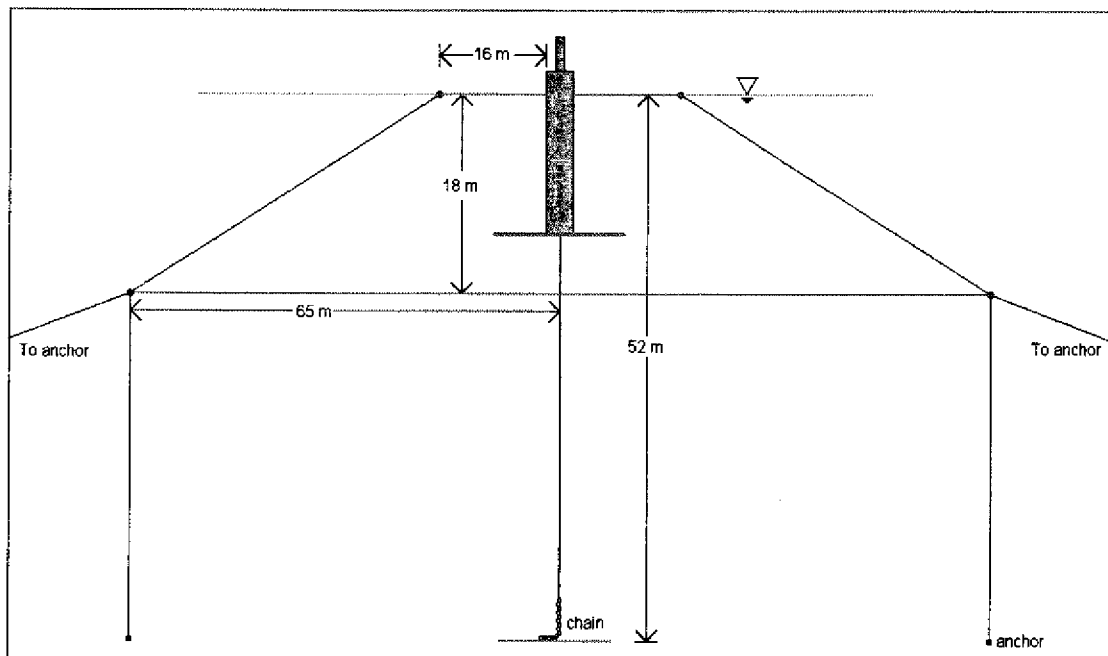


Figure 8: Side View of Mooring System

The rope used in this design is typical heavy-duty mooring line and has a diameter of 0.0756 meters, an elastic modulus of 3.579 GPa, and a mass density of 1,025 kg/m. The total length of rope utilized in the design is 2,199 meters. To obtain the desired effective spring constant, the chain must have a mass per length of 680 kg/m.

Figure 9 shows an isometric view of the mooring system. Though complex, the system is very robust, and the multiple anchor points serve as a safeguard against failure.

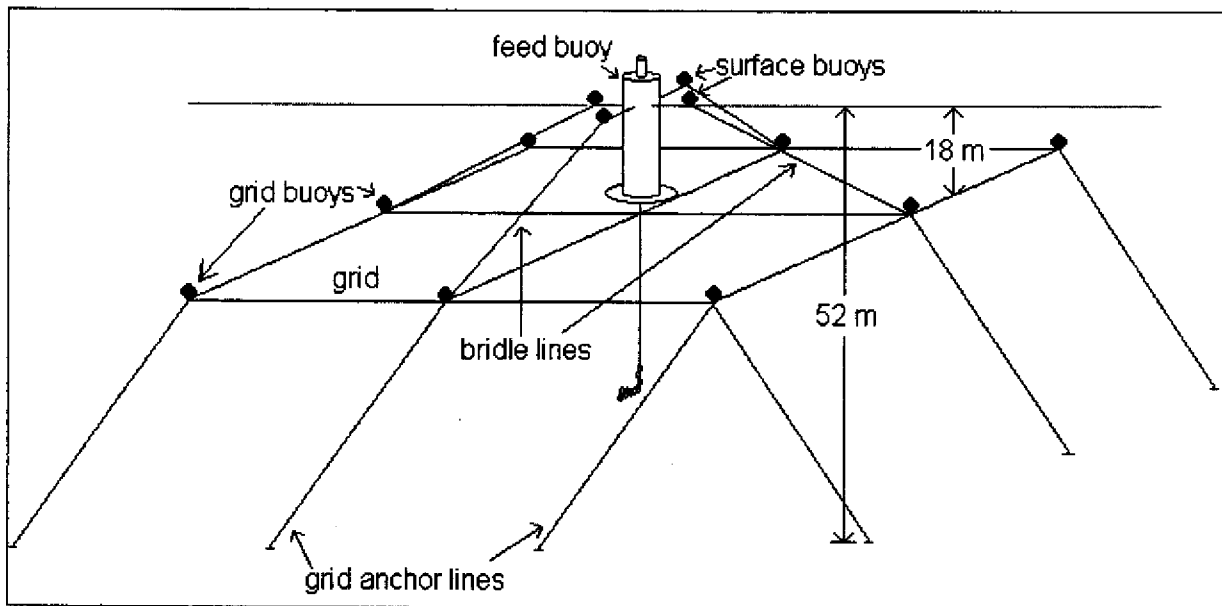


Figure 9: Sketch of Complete Mooring System

III. Design

The focus of this project is the design of a feed buoy to fit the specifications presented by the Open Ocean Aquaculture Demonstration Project Team at UNH. The final design consists of a steel structure 16 meters high and three meters in diameter. The turbine mounted to the top of the buoy is four meters tall and 1.8 meters in diameter. The damping disc located at the base of the buoy is nine meters in diameter. Figure 10 is an isometric view of the design.

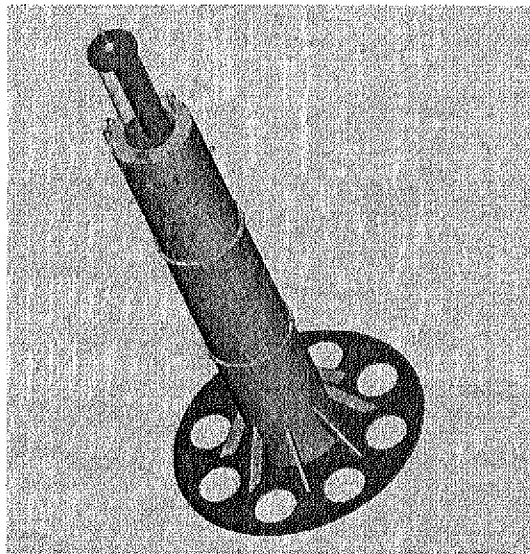


Figure 10: Isometric View of Buoy Design

The size of the buoy structure dwarfs the details located on the top of the buoy. Figure 11 is a close-up of the turbine and top surface of the buoy.

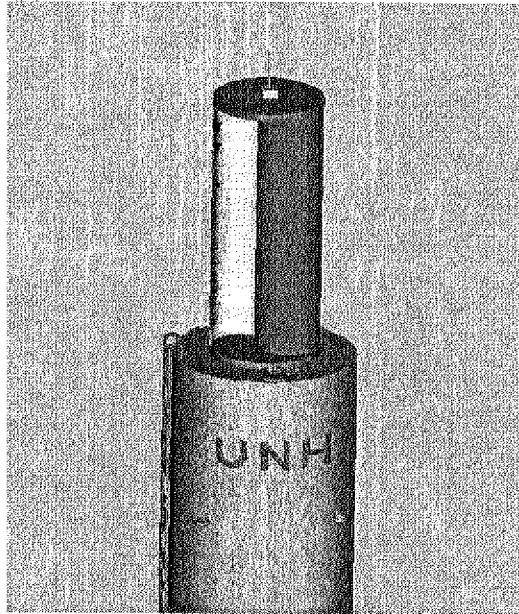


Figure 11: Close-up of Turbine and Top of Buoy

This chapter describes finalized design in detail. The design has been divided into four main components that will be discussed separately. The buoy structure consists of the buoy, damping disc, and internal structural components. The feed system consists of the pumps, valves, lines, and communications network necessary to deploy feed to the submerged cages. The turbine description will explain the turbine selection and power conversion system chosen to maximize the energy yield from the wind field at the site.

Buoy Structure Design

As described above, the intended purpose for the buoy located within the Aquaculture site is to feed four fish cages. Knowing this purpose enabled the buoy structure and other systems to be designed. The structure of the buoy is the most important aspect to be considered when investigating the feasibility for this buoy. Due to the large scale of the proposed buoy, the importance of having a sound structural design is clear. Equally important is how the buoy will interact with the wave field. To minimize the motion of the buoy within the wave field, the buoy was designed with spar-like characteristics. The long and slender, cylindrical shape

of the buoy will decouple its motion from that of the waves (Berteaux, 1991). The damping disc increases heave and pitch damping within the wave field.

As shown in Figure 12, the designed buoy is 16.6 meters long and has a cross-sectional diameter of three meters. The structural steel shell thickness of the buoy is prescribed to be 0.02 meters. The dimensions of the overall buoy structure allow for a feed silo capable of holding the necessary volume of feed (see chapter *II. Design Specifications, Feed Requirements*). The designed silo is 14.8 meters long and 1.6 meters in diameter and has a volume capacity of approximately 35 cubic meters. Attached to the bottom of the buoy is a damping disc that helps damp out the motion of the buoy. It is designed to have a thickness of 0.05 meters and have a diameter of 9 meters. There are eight holes cut out of the disc; each has a diameter of 1.52 meters. The disc has a mass of approximately 14,660 kilograms. The outer shell of the buoy will be painted with a rust-resistant paint to increase the life span of the buoy. Detail drawings of the buoy structure can be found in Appendix A.

To keep the buoy draft constant, the buoy will take on ballast water as the feed is distributed to the cages. The ballast water will be housed between the feed silo and the outer shell as shown in Figure 12. The water will be let in through a 3-inch normally closed solenoid valve in the shell. As the silo is filled water will be pumped out through another 3-inch normally closed valve at the bottom of the ballast tank, using the feed system pumps (B/C Valve, 2003). For every cubic meter of feed emptied from the buoy, 1.2 cubic meters of seawater will be added to the ballast tank. Capping the top and bottom compartments of the ballast tank are two steel bulkheads, three centimeters thick, which secure the silo to the shell. The top bulkhead is located one meter from the top of the buoy. This top bulkhead supports the batteries charged by the turbine that are used to power feed system and ballast valves, as well as the communication equipment used to deploy feed. The lower bulkhead is located 0.75 meters from the bottom of the buoy and supports steel cubes that serve as ballast in order to lower the center of gravity and raise the draft. The compartment below the lower bulkhead houses the feed distribution system. This bulkhead will be watertight to prevent flooding of the feed distribution compartment.

In each bulkhead there is a hatch that allows access to the lower compartment as seen in Figure 12. There is a ladder connecting each bulkhead near the hatch. The ladder runs perpendicular to the outer shell and is supported on either side by the shell and silo. The ladder is 0.7 meters wide. The hatches and ladder allow access to the ballast tank as well as the feed distribution system for upkeep and repair. To access the lower compartment, the silo should be filled to capacity so that there is no ballast water in the tank. However, if the ballast tank has water in it the lower compartment can be reached from within the tank by a diver through a double hatched, flooding compartment. Figure 12 shows a simple schematic of the overall buoy structure with important dimensions and compartment labels. Appendix A contains additional detailed figures.

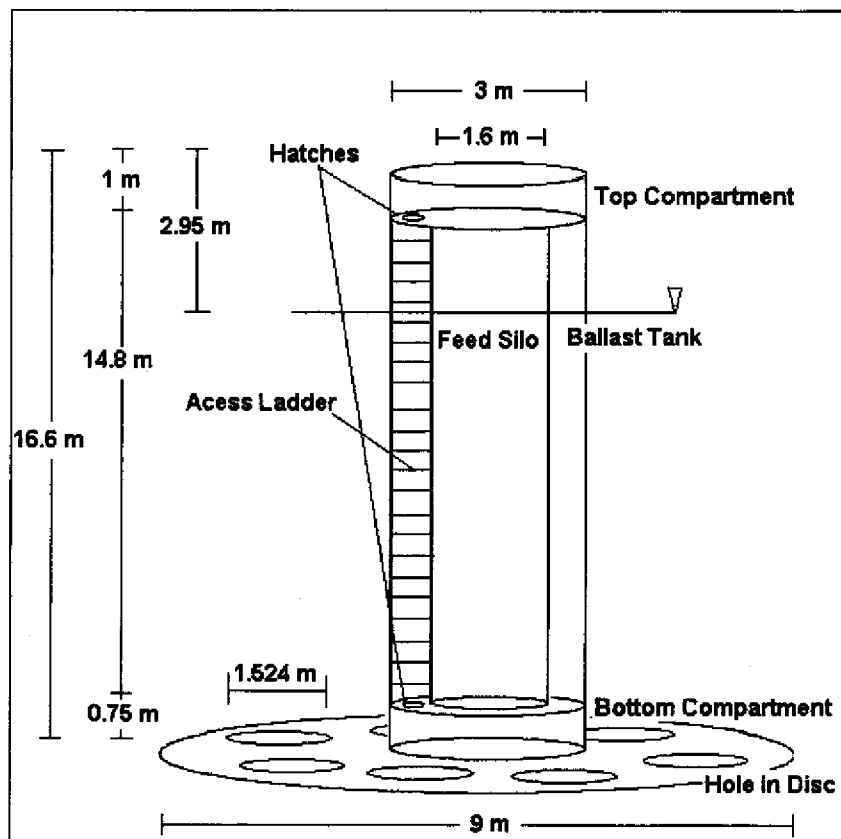


Figure 12: Schematic of Buoy Structure with dimensions

Hydrostatically, the buoy is very feasible. Using the weights and center of gravity heights for each material located within the buoy, a total weight and center of gravity were calculated. Steel cubes rest on the top of the lower bulkhead within the ballast tank to lower

the center of gravity and increase the draft. Table 1 shows the weights and heights of each element within the buoy as well as the buoy's total weight and total center of gravity. The buoy weighs 99,066 kilograms, centered 5.884 meters from the bottom of the buoy. The center of buoyancy is located 6.83 meters above the bottom of the buoy. The metacentric height of the buoy is 0.987 meters (Savory, 2003). This positive value indicates that the buoy design is stable (www.fas.org). The draft of the buoy is 13.66 meters; approximately three meters remain above water.

Table 1: Masses and centers of large-scale buoy structure

	Mass (kg)	Height of Center of Gravity (m)*
Shell	26580	8.306
Feed	35560	8.181
Silo**	1000	8.181
Pump**	100	0.5
Turbine**	600	19.66
Damping Disc	14660	-0.01905
Auxiliary**	400	15.946
Steel Cubes	16920	1.1
Upper Bulkhead	1621	15.612
Lower Bulkhead	1625	0.75
Buoy	99066	5.884
* measured from the bottom of the buoy		
** approximate weights		

Prefabricated elements that fit this design for the buoy structure were unattainable in the dimensions and capabilities that are necessary. Therefore, all the parts of the buoy structure must be fabricated.

Feed Distribution System Design

The silo capacity, along with an approximately equal volume of ballast tank, dictated the dimensions of the buoy. (Refer to *Buoy Structure Design*). A basic schematic of the feed system and a list of each component can be seen in Figure 13 and Table 2, respectively. Specifications for each component are found in Appendix C.

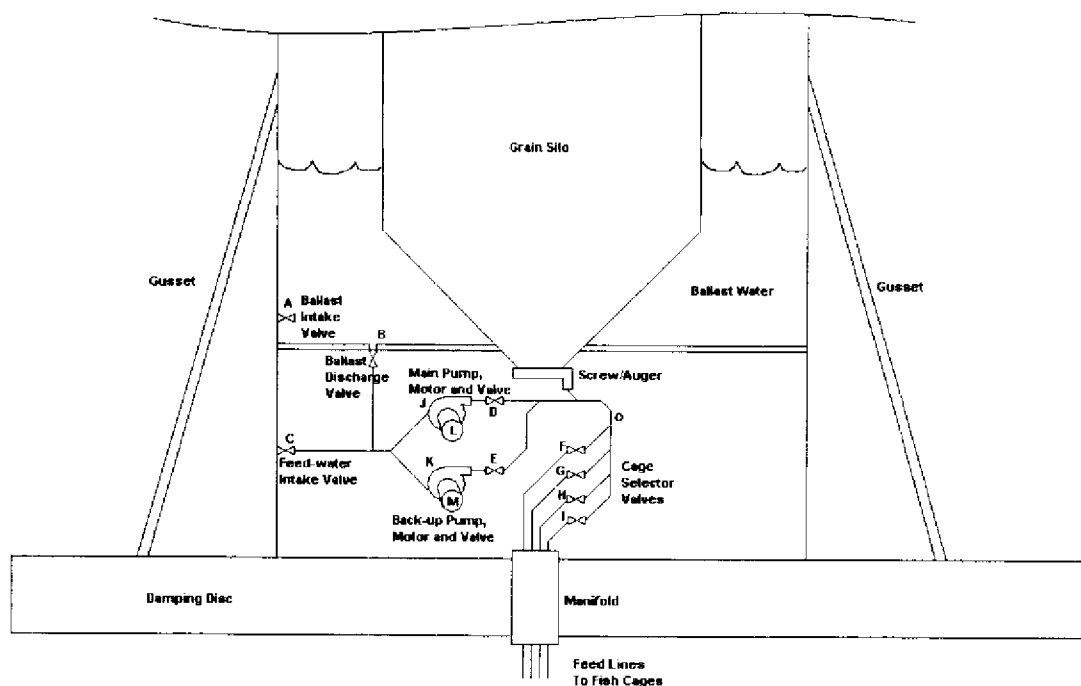


Figure 13: Schematic of feed distribution system.

Table 2: Feed Distribution Component List

Part Label	Part Name	Description
A	Ballast Intake Valve	Normally Closed 2-Way Solenoid Valve
B	Ballast Discharge Valve	Normally Closed 2-Way Solenoid Valve
C	Feed-water Intake Valve	Normally Open 2-Way Solenoid Valve
D	Pump-Side Feed Line Valve	Normally Closed 2-Way Solenoid Valve
E	Backup Pump-Side Feed Line Valve	Normally Closed 2-Way Solenoid Valve
F,G,H,I	Cage Selector Valves	Normally Closed 2-Way Solenoid Valve
J	Main Water Pump	Pedestal-Mount Type 316 Stainless Steel Centrifugal Pump
K	Backup Water Pump	Pedestal-Mount Type 316 Stainless Steel Centrifugal Pump
L	Main Pump Motor	NEMA C-Face DC Motor
M	Backup Pump Motor	NEMA C-Face DC Motor
N	Silo Emptier	Screw/Auger Feeder
O	Feed-water Lines	3" Flex-Hose
P	Electronics Enclosure	NEMA 6 Enclosure

The feed delivery system uses a Lucky-Pond Horizontal Screw/Auger Feeder (see part N in Figure 13) to empty the silo. The screw auger is capable of delivering 250 cm³ of feed per second. (www.aquaticceco.com). The feed pellets are forced into the stream of sea-water that flows through 3 inch diameter flex hose, pumped at rate of 55 gpm, using a Pedestal-Mount

Type 316 Stainless Steel Centrifugal Pump (J) driven at 1800 rpm by the ½ Hp DC motor (L) (www.mcmaster.com). Feed-water is prevented from entering the silo because of the airtight connection between the auger threads and the interior walls of the device. However, the pump-side feed line valves, which are 3-inch normally closed, (D, E) are required to prevent any backflow of the water/feed-pellet mixture (feed slurry) into the unused pump (backup pump) (www.mcmaster.com). The backup pump and drive motor (K, M) were included in the design for redundancy in case of a failure in the primary pump (www.mcmaster.com). This pumping system is integrated with the ballast tank system; the feed pump is also used to empty the ballast tank when the silo is being restocked. A feed restocking port is located at the top of the buoy. The feed is directed to the proper cage by a series of normally closed 3 inch solenoid valves (F, G, H, I) (www.bcvalve.com). Three valves remain closed while the valve in line to the cage being fed is energized and opened.

The feed slurry flows through 3" flex hose (O) (www.mcmaster.com). At the bottom of the buoy, where the feed lines enter the water, there is a manifold where four 3" holes are machined through the bottom of the buoy, as well as the damping disc. Four 3" OD pipes are fed through these holes and welded securely so that no water will enter the buoy. The appropriate tube fittings will be connected to the interior and exterior ends of these four pipes to make the transition from interior feed lines to exterior feed lines. All connections will be of NPT type. The design calls for the feed lines to be lashed to the central mooring line that goes from the center of the bottom of the buoy to the center of the grid. Extra feed line should be used so as to account for any stretch that may occur in the central mooring line, or the grid. (Refer to the mooring system description in chapter II. *Design Specifications, Mooring System Design*). The lashing can be accomplished by placing flanges at the end of each length of feed line. The 3" flex hose is sold in lengths of ten feet. The bolt holes of the flange will be used as a means of connecting the feed line to the mooring line. Locking carabineers are an ideal means of connection because of their low-wear characteristics (www.mcmaster.com). At the center of the grid, each feed line will branch off to the appropriate fish cage, lashed to the cage grid lines in a similar manner as mentioned above.

Communication from land to the buoy and its feed and ballast mechanisms is accomplished via 900 MHz cellular communication. Figure 14 is a schematic of the communication system.

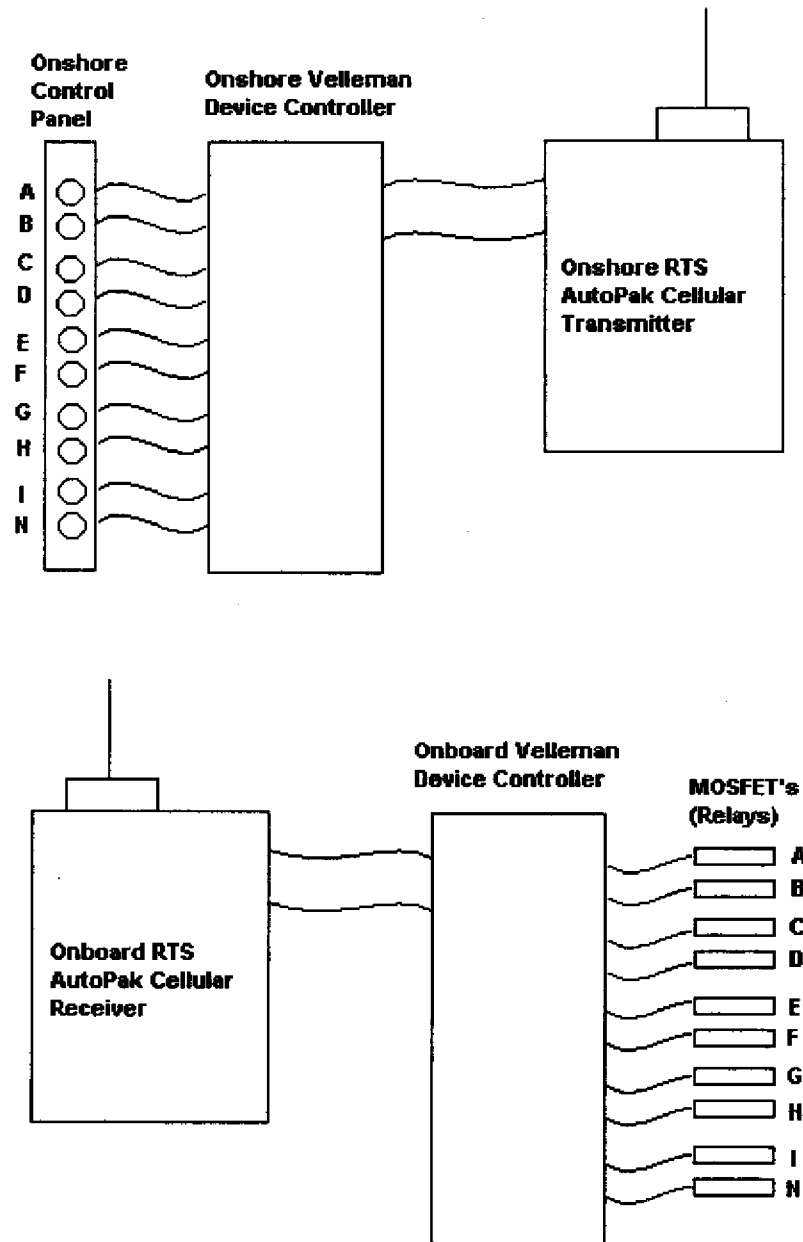


Figure 14: Communications Schematic

A 10-channel, 2-wire remote control from Velleman, Inc. will be used in concert with the RTS-AutoPak Remote Telemetry System, made by TransTel Group, Inc. (www.velleman-

www.transtelgroup.com). There are ten channels on the Velleman device controller, each corresponding to a feed system component on the buoy. There is one channel each for 7 solenoid valves; one for the screw auger, one for the main pump motor and valve, and one for the back up pump motor and valve.

The Velleman device controller has two components. One is located on land, and the other on board the buoy. Inputs to the onshore portion will be pushbutton controlled. No interlocks are included in the design, so the user will have explicit feeding, ballast intake and ballast discharge directions. These directions are found in Appendix B. The onshore device controller generates the 10 different dial tones, according to the user input. It is wired to the onshore RTS AutoPak, a wireless modem that sends these dial tones to its receiving counterpart onboard the buoy.

The onboard RTS AutoPak receiver collects the 900 MHz signals, and wires them to the onboard half of the Velleman device controller, which takes the dial tones and closes the appropriate circuit, energizing the appropriate device control relays, a.k.a. MOSFETs (metal-oxide semiconductor field-effect transistors) onboard. The cellular transceiver will require a constant phone-line connection to prevent others from dialing in and sending false instructions to the buoy. Since the feed buoy's batteries will provide DC electricity, MOSFETs will be used (instead of standard power relays) to avoid the potential problem of relay contactors welding shut (www.digikey.com). When a component's MOSFET is energized the component is allowed to draw power from buoy's batteries.

The onboard RTS AutoPak, Velleman device controller, and MOSFET's will be enclosed in a 19.6" x 17.8" x 18.8" fiberglass NEMA 6P electrical enclosure, located in the top compartment. The wiring to the pumps and valves at the bottom of the buoy will be laid in a single conduit, with waterproof seals through both the upper and lower bulkheads. The NEMA 6P enclosure is submersible, watertight, dust tight, and sleet (ice) resistant (www.mcmaster.com). This is the most durable type of electrical enclosure, capable of being submerged up to 30 minutes in up to 6 feet of water without harm to the contents. Data

sheets on all of these components can be found in Appendix D. The components requiring electricity generated by the turbine are shown in Table 3.

Table 3: Components Requiring Power

Part Name	Voltage	Amps	Watts	Hrs/day	Hrs/Wk	Amp-Hrs/Wk	kW-Hrs/wk
Ballast Intake Valve	24	0.42	10	0.5	3.5	1.46	0.04
Ballast Discharge Valve	24	0.42	10	0.5	2.4	1.00	0.02
Feed Water Intake Valve	24	0.42	10	8	56	23.33	0.56
Main Pump-Side Feed Line Valve	24	0.42	10	8	56	23.33	0.56
Backup Pump-Side Feed Line Valve	24	0.42	10	0	0	0.00	0.00
Cage Selector Valves	24	0.42	10	2	14	5.83	0.14
Cage Selector Valves	24	0.42	10	2	14	5.83	0.14
Cage Selector Valves	24	0.42	10	2	14	5.83	0.14
Cage Selector Valves	24	0.42	10	2	14	5.83	0.14
Main Pump Motor	24	15.54	373	8.34	60.78	944.62	22.67
Backup Pump Motor	24	15.54	373	0	0	0	0.00
Silo Emptier	12	0.50	6	8	56	28	0.34
Cellular Transceiver	12	0.25	3	24	168	0	0.50
Device Controller	12	0.30	3.6	24	168	50.4	0.60
Device Control Relays	24	0.625	7.5	32	224	140	1.68
					TOTALS:	1235	26.93

Turbine Design

To pump food to the cages the feed buoy requires a source of power. One of the primary goals of the design team was to determine if the power needs of the feed buoy could be met by harvesting energy from the wind. As mentioned previously in *II. Design Specifications*, design constraints for this application include concerns relating to corrosion and the pitching motion of the buoy.

In general, corrosion problems and temperature concerns are addressed with material selection. Plastics and composite fiber materials will not corrode but sacrifice a little in strength. Where strength and corrosion resistance are needed there is a large range of stainless steels that will work, but these materials sacrifice weight and cost.

There are many types of wind turbines available. Design concerns such as the pitching of the buoy and waves crashing into the turbine directly impact which type of turbine will be chosen. Almost all turbines fall into two basic categories: horizontal axis, where the axis of rotation of the turbine is parallel to the direction of the wind, as in Figure 15, and vertical axis, in which the axis of rotation of the turbine is perpendicular to the direction of the wind as seen in Figure 16.

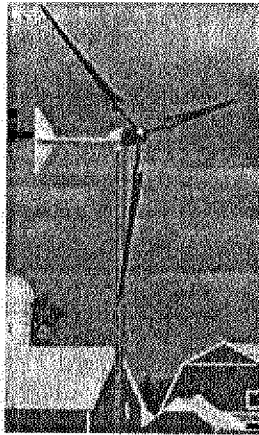


Figure 15: The Whisper H-80 is a horizontal wind turbine produced by wind stream power that can provide 1000 Watts in 28 mph winds (Windstream, 2003).

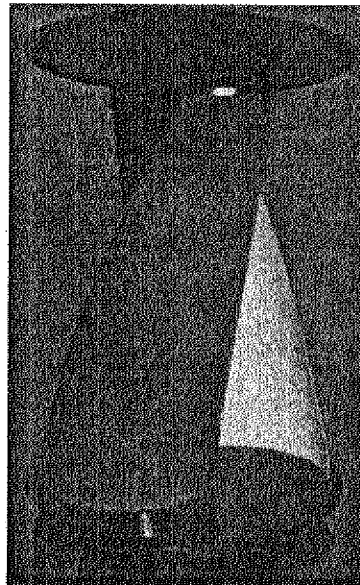


Figure 16: This is an example of a Helius turbine made by wind stream power (Windstream, 2003).

In general, a horizontal axis turbine will extract more energy than a vertical axis turbine of the same size. However, a horizontal axis turbine will undergo severe stresses when a wave hits it, especially on the blades. One design approach would be to design a weak spot where the blades meet the hub and generator. When the waves hit the turbine, the blades break off but leave the generator and other systems intact. The blades could be replaced when the feed is delivered. The downfall is that the power needs of the buoy combined with the wind available at the site necessitate that the blades be about 1.5 m long, and it could be difficult to manufacture these so that they could be replaced after every storm without significant cost. For a higher initial cost a vertical axis turbine could be designed to withstand moderate wave impact.

Another downfall of horizontal axis turbines in this application is the pitching motion of the buoy. When the turbine blade spins at a high rotational velocity all of the turbine's rotating parts have rotational inertia. Pitching effects a change in that rotational inertia resulting in a moment in the shaft supporting the turbine above the water, as well as the blades themselves. This means that the supporting shaft would have to be much larger and stronger than one used in a land based application. Also, most turbines use guide wires from the shaft to the ground to increase their strength; on the buoy there is little room to place guide wires. After weighing these factors and communicating with Colin Kerr, an engineer at Windstream Power Systems Inc., the design team decided that the best solution to the needs of this application would be a vertical axis turbine.

The Helius turbine is a vertical axis turbine that can be fixed directly on the top of the buoy and has been designed by Windstream Power Inc. This design group has a quote for a Helius turbine that is 1.8 m in diameter and 4.4 m tall (sketch in Appendix A). The turbine was designed to operate in minimum conditions. As quoted, the turbine will produce 20.3 kWh per week (Appendix C). This is 6.3 kWh less than the estimated energy needs of the buoy. Power generated by the turbine is proportional to the velocity of the wind cubed, so small increases in the average wind speed will lead to large increases in the energy produced. Months like November and December will produce much more energy than will be used. Using extra batteries will allow for the storage of energy during these high wind months to be

used in July and August when production is less than the demand. The amount of energy that will need to be stored, 6 kWh, is not much for the large batteries that will be used. The turbine will be constructed of aluminum and weigh 600 kg (see Appendix D). A more robust stainless steel model is available but costs approximately 30 percent more. Weekly trips will be made to the buoy so maintenance of the turbine should not be a problem. As quoted the Helius turbine costs \$11,980 (Windstream, 2003).

The batteries chosen for storing energy extracted from the wind are type 12 HHG 8DM produced by Rolls Battery, as seen in Figure 17. These are “deep cycle” batteries and are designed to withstand many charges and discharges. These are rated to supply 275 Amp-hrs over a 20 hr period. The design team has decided to implement eight of the type 12 HHG 8DM batteries in parallel. This should provide more storage capacity than will be needed for the systems on the buoy on a weekly basis.

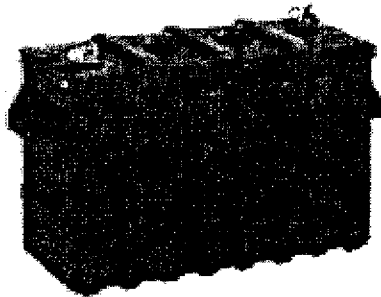


Figure 17: These batteries made by Rolls are designed for heavy cycling and have a 7-year warranty (www.rollsbattery.com).

IV. Physical Modeling

This chapter discusses the testing performed on a scale model of the buoy design. Using Froude scaling, a model was created to determine the damped natural frequency for heave and pitch motion. The physical model also underwent sea-keeping tests using a simplified mooring system in order to determine the buoy's heave and pitch response in certain sea states.

The scaling and construction of the model, description of the testing facilities in the Jere A Chase Ocean Engineering Laboratory (Chase Laboratory) at UNH, the free release tests and sea-keeping tests will be described and discussed.

Model Design

To scale the model to a size that could be tested in the UNH Ocean Engineering wave tank, Froude scaling of the full-scale design was implemented. Froude scaling utilizes the main principle that the Froude number remains the same for both the large-scale buoy and its small-scale model (Chakrabarti, 2003). Froude scaling was used due to the importance of gravitational, as well as inertial effects on the dynamics of the system. The length scale ratio for this model is 28.162/1. The diameter of the small-scale buoy is 0.107 meters and its height is 0.59 meters. The damping disc at the bottom of the buoy is 0.32 meters in diameter, has a thickness of 0.0011 meters and the holes in the disc are 0.052 meters in diameter.

Each element of the large buoy was scaled using the scaling number. Table 4 shows the required weights of each scaled element (proportional to scale ratio cubed) to be used within the scale model, along with their respective centers of gravity. To retain similitude for pitch motions, the major weight components were placed at the scaled component centers of gravity.

Table 4 - Masses and centers of large-scale buoy structure

Buoy Model	Weight (kg)	Height of Center of Gravity (m)*
Shell	1.190	0.29494
Feed****	1.592	0.29051
Silo****	0.045	0.29051
Pump***	0.0045	0.01775
Turbine	0.0270	0.27485
Damping Disc	0.656	-0.00068
Auxiliary**	0.018	0.56622
Steel Cubes***	0.758	0.03906
Upper Bulkhead**	0.073	0.55438
Lower Bulkhead***	0.073	0.02663
Buoy Model	4.436	0.206
* measured from the bottom of the buoy		
** combined to form top plate		
*** combined to form bottom plate		
**** combined to form the feed silo		

Several weights were combined together and new lumped centers of gravity within the scale-model were calculated for ease of construction. The scaled model has six main components (see Figures 18 and 19); the outer shell, a top and bottom plate, the silo, the damping plate and the wind turbine. Each component needed to match the weight of an equivalent element group on the full-scale buoy. The scaled outer shell is made of PVC with a density of approximately $1,550 \text{ kg/m}^3$ and a thickness of 0.0038 meters. The top plate has the combined weight of the top bulkhead and the auxiliary weights, which include the weight of the batteries and other power related equipment. This plate was made of aluminum with a density of 2700 kg/m^3 and has a thickness of 0.0065 meters. It is 0.08 meters in diameter and the plate was centered 0.56 meters from the bottom of the buoy.

The lower plate combines the weight of the steel ballast cubes, the bottom bulkhead and the feed distribution system. The steel plate has a density of $7,800 \text{ kg/m}^3$ and is 0.012 meters thick. Its diameter is the same as the inner diameter of the outer shell, 0.099 meters, and was centered 0.038 meters above the bottom of the buoy. The silo and feed were modeled as a cylinder centered 0.291 meters from the bottom of the buoy. This cylinder was made of the same density PVC as the outer shell and has a length of 0.461 meters. A copper rod of 0.0032 meters in diameter was fastened to the top of the aluminum rod representing the

height and weight of the wind turbine. The length of the rod is 0.108 meters with a density of 8,500 kg/m³.

Each modeled weight was fastened using nylon nuts to an aluminum-threaded rod that passes through the center of the buoy. The damping disc was bolted and sealed to be watertight on the bottom of the buoy. This keeps the buoy rigid and allows for easy placement of weights at their proper heights. The simulated feed silo was cut by 0.10 meters, to a length of 0.361 meters, to compensate for the excess weight of the aluminum rod and bolts used to hold the weights in place. The theoretical scaled weight of the model buoy is 4.436 kilograms. The actual buoy model weighs 4.421 kilograms. This gives a 0.294% error in weight between the theoretical and actual weights of the model. The draft of the model buoy using the actual weight is 0.485 meters, which leaves 0.105 meters of water above the waterline. Figure 18 is a picture of the separated buoy model with the elements distributed along the center axis. Figure 19 shows the assembled model, ready for testing.

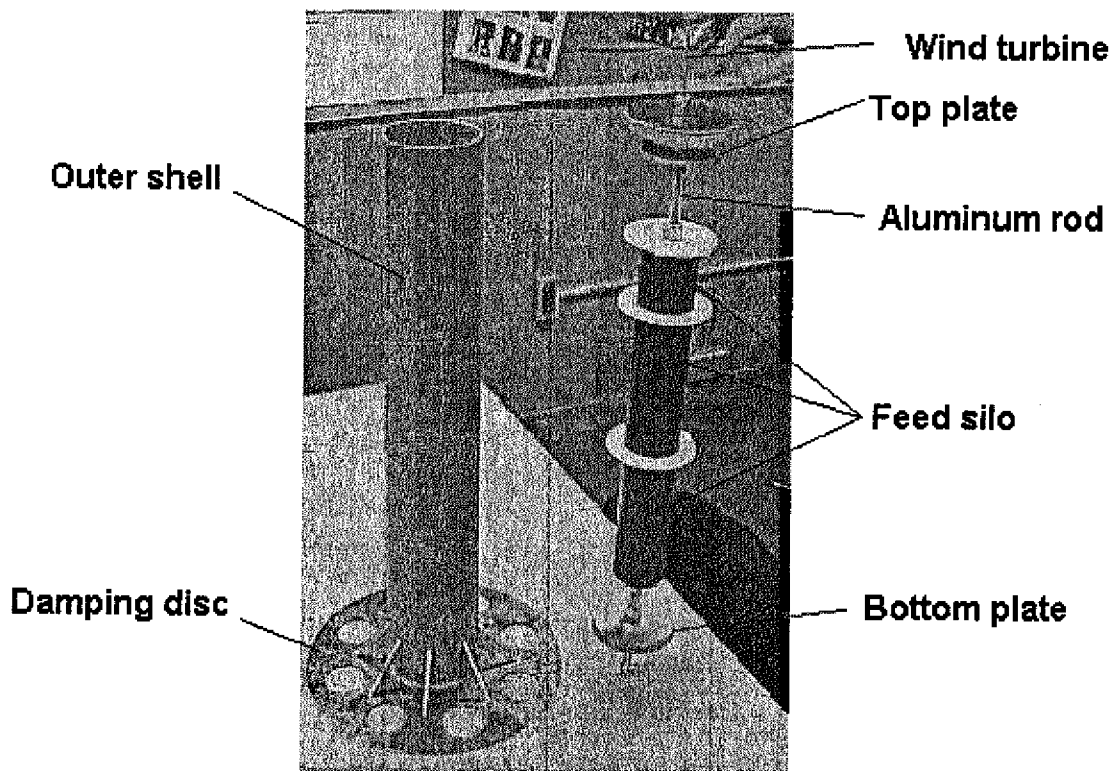


Figure 18: Separated Buoy Model

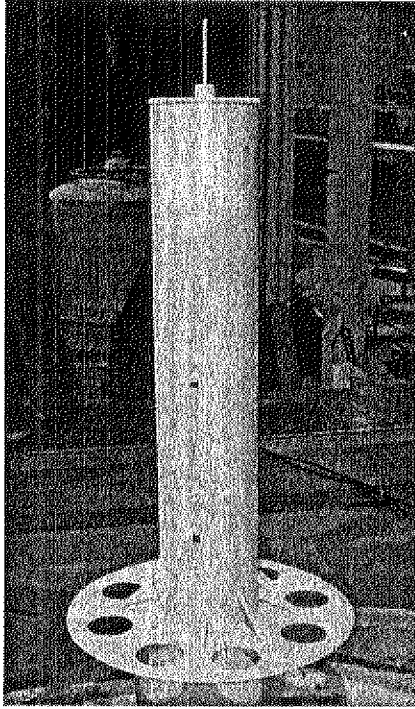


Figure 19: Finished Buoy Model

Facility

All tests performed on the buoy model were conducted at UNH in the Chase Laboratory.

Free release and sea-keeping tests were performed in the wave/tow tank. The tank is 120 ft long, 12 ft wide and 8 ft deep, and uses a single, hydraulically driven paddle to create waves.

Figure 20 shows the wave maker which is able produce waves with amplitudes up to 0.3 m and periods between 0.75 and three seconds (www.ooa.unh.edu).

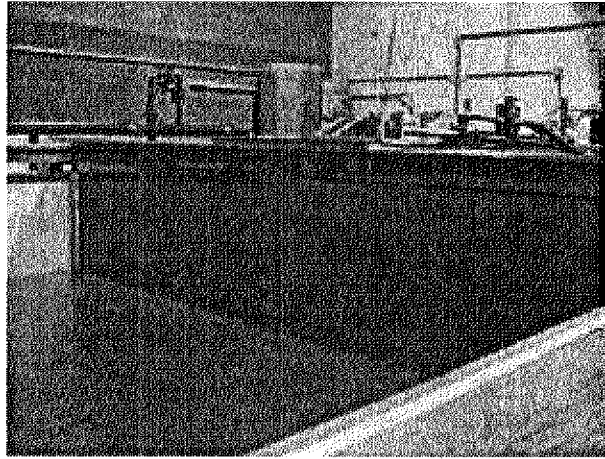


Figure 20: The wave maker can produce waves with amplitudes up to 0.3 m

Motion data from the model was acquired using the Optical Positioning Instrumentation and Evaluation system (OPIE). OPIE is an external, non-invasive measuring system that uses a black and white digital camera to follow up to two designated points based on contrast between light and dark pixels. The digital camera captures frames of the test at 30 Hz transmits the images to the computer. The OPIE software was written in Matlab which tracks the position of the dark pixels through time. From position, the velocity and acceleration in both vertical and horizontal directions were calculated. If two dots are placed along the axis of the buoy, then the pitch angle (angle from the vertical), angular velocity and angular acceleration can be calculated as well (Michelin and Stott , 1997).

OPIE is calibrated by placing a paddle with a large black circle next to the buoy at the start of the test, as shown in Figure 21. Within the program the user inputs the distance from one edge of the circle to the other in both the horizontal and vertical directions. The program then knows the correlation between number of pixels and physical distance.

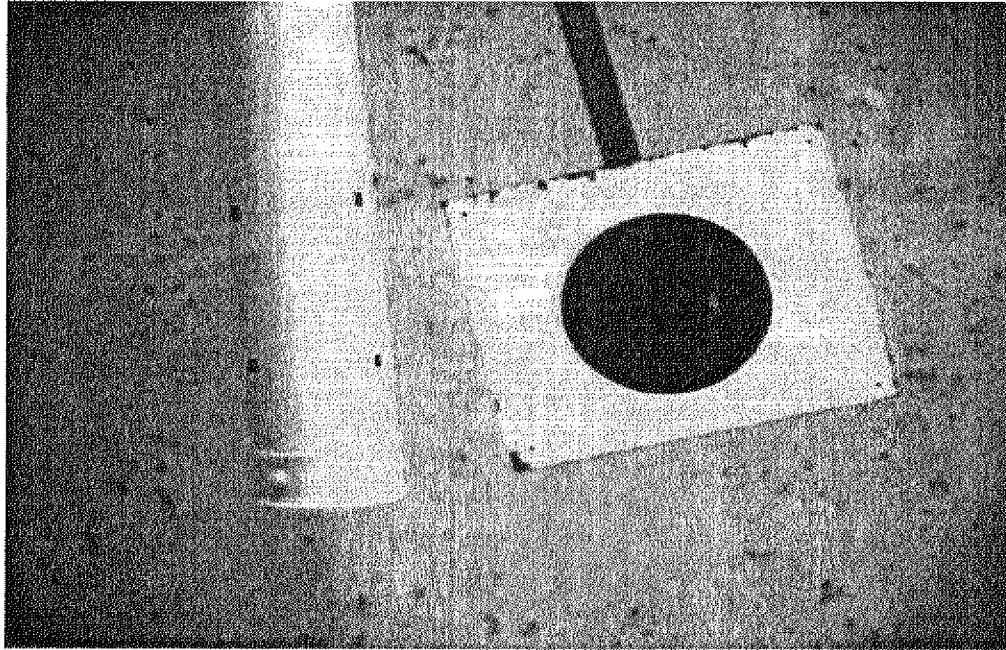


Figure 21: A screenshot from OPIE showing the calibration circle.

Free Release Tests

Test Plan

Evaluation of the design includes determination of the damped natural frequency (or period) of the heave and pitch motions of the buoy with no wave forcing present. It is important that this damped natural frequency is not within the targeted operating range of the full-scale buoy; waves at the site have frequencies ranging from 0.08 Hz to 0.3 Hz (3 second- 12 second periods). Avoiding this range of frequencies is important to prevent resonance, a situation where successive waves impacting the buoy cause increasing amplitudes of heave and/or pitch, which may cause mooring system failures to occur.

The testing plan included free release tests in the wave/tow basin in the Chase Laboratory, using the previously described OPIE system. For accurate results, several trials of both heave and pitch responses were conducted. From the data, heave natural period and pitch damped natural periods as well as the respective damping ratios were computed for each trial.

Method

In a free release test the buoy is slightly displaced from equilibrium and released to determine its response with no external forcing. The buoy was tested for heave response by lifting it slightly above its equilibrium position so that the initial motion was downwards (see Figure 22). Physically pushing the buoy downward from equilibrium has the same effect, however, it was more difficult to acquire clean heave data using this technique due to yaw or pitch motions induced. The pitch motion of the buoy was invoked by applying a disturbance force perpendicular to the vertical axis. Once released, the buoy bobbed up and down (or side to side in the case of pitch). The OPIE system was used to generate plots of the pitch and heave response. Four trials were performed to determine the heave response and three trials were performed to determine the pitch response.

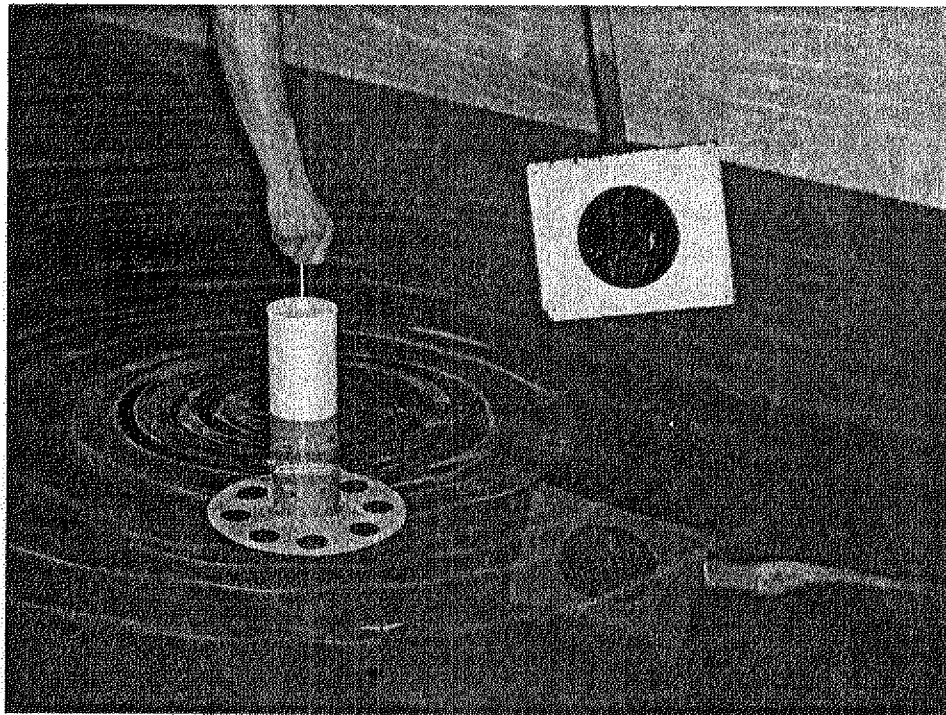


Figure 22: A picture of a free release trial

Results

OPIE generates several plots that describe the motion, including angular and linear position, velocity, and acceleration. The relevant plots for one heave test and one pitch test are shown in Figures 23 and 24.

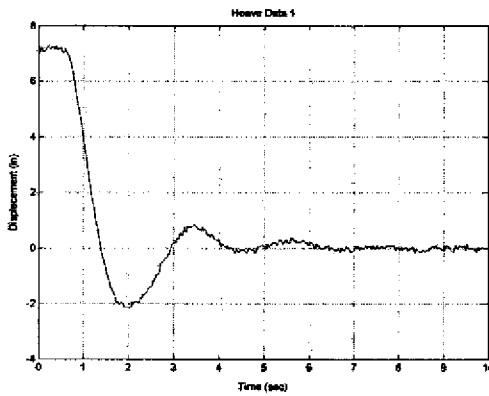


Figure 23: Heave Response

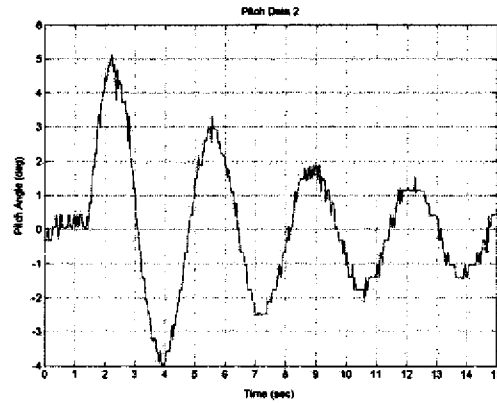


Figure 24: Pitch Response

Not all of the responses were as “clean” as those shown above. The OPIE program had a tendency to occasionally track a random dark spot on the wave tank wall before resuming tracking of the buoy motion. This “jump” corresponds to random peaks in the response plots, which were removed before analysis was conducted. Once the raw data had been “cleaned”, it was exported from *Matlab* to *Excel* where was manipulated.

The primary analytical tool used in determining the key second order system parameters was the Log Decrement Method. This technique analyzes the decrease in amplitude over a certain number of periods of oscillation to determine the important second order system parameters, including damped natural period and damping ratio. It is apparent from the plots shown above, that OPIE is unable to track the exact pixel location over the entire test. This type of error is characterized by the jagged edges observed along the curve profile. For the purposes of these tests, the jaggedness is overlooked, and the maximum and/or minimum values were used in the Log Decrement Method. Once the critical systems parameters were determined for each trial, the values were averaged over the number of trials for both pitch and heave. Tables 5 and 6 show the experimental results for each trial, as well as the average values.

Table 5: Model Scale Heave Motion

Test #	T_D (sec)	ζ	ω_n (rad/sec)	b (N/m/s)	M_v (Kg)
1	2.350	0.285	2.789	17.838	11.215
2	2.300	0.224	2.803	13.957	11.106
3	2.250	0.235	2.873	14.303	10.570
4	2.250	0.189	2.844	11.608	10.790
Mean	2.288	0.233	2.827	14.426	10.921

Table 6: Model Scale Pitch Motion

Test #	T_D (sec)	ζ	ω_n (rad/sec)	I_v (Kg*m ²)
1	3.333	0.073	1.890	0.187
2	3.333	0.068	1.889	0.187
3	3.300	0.089	1.912	0.183
Mean	3.322	0.077	1.897	0.186

In these tables, T_d represents the damped natural period of oscillation, ζ represents the damping ratio, ω_n the un-damped natural frequency, b the damping coefficient, M_v the virtual mass of the system, and I_v the virtual polar moment of inertia. In order for this information to be useful in determining the full-scale system characteristics, the results were re-scaled using the scale ratio. Froude scaling requires that periods are proportional to the square of the scale ratio. Once the model was “scaled-up” using the scaling number of 28.162 the data was compared with the calculations for the full-scale theoretical model. Tables 7 and 8 have tabulated values for the re-scaled second order parameters.

Table 7: Full Scale Heave Motion

Test #	T_D (sec)	ζ	ω_n (rad/sec)	b (N/m/s)	M_v (Kg)
1	12.471	0.285	0.526	75218.878	250972.160
2	12.206	0.224	0.528	58852.676	248526.151
3	11.940	0.235	0.541	60311.936	236536.605
4	11.940	0.189	0.536	48946.069	241463.037
Mean	12.139	0.233	0.533	60832.390	244374.488

Table 8: Full Scale Pitch Motion

Test #	T_D (sec)	ζ	ω_n (rad/sec)	I_v (Kg*m ²)
1	17.689	0.073	0.356	3314696.354
2	17.689	0.068	0.356	3317232.531
3	17.512	0.089	0.360	3240681.835
Mean	17.630	0.077	0.357	3290870.240

Table 9 summarizes the model-scale and full-scale results found for the free release tests.

Table 9: Summary of Heave and Pitch Damped Natural Period and Damping Ratio

Test Type	Model Scale		Full Scale	
	T_D (sec)	ζ	T_D (sec)	ζ
Heave	2.288	0.233	12.139	0.233
Pitch	3.322	0.077	17.630	0.077

Discussion

Table 9 shows that the average full-scale heave and pitch damped natural periods are approximately 12.1 seconds and 17.6 seconds, respectively. Data from UNH's Wave Rider Buoy shows that the average dominant period of wave excitation is about 5 seconds, with storm waves coming in at periods of 8-10 seconds. The heave and pitch damped natural periods of the buoy are both well above the dominant wave periods observed near the Isles of Shoals, even under storm conditions. The buoy has an excellent heave damping ratio of 0.233. While the system characterized as under-damped with respect to heave, the response showed that most of the heave motion was dissipated within 2 cycles. The pitch damping ratio is calculated to be about 0.077. While this is not as high as the damping ratio of the heave, the pitch amplitude is reduced by 85% within four cycles. In addition, these values can be compared with tests conducted before a damping plate was added to the buoy design. Without the plate, the buoy system was highly under-damped with heave and pitch damping ratios of 0.017, and 0.025 respectively. Damped natural periods without the damping plate were found to be in the middle of the wave excitation range of highest energy. The results of the free release tests with the damping disc confirmed that the pitch and heave motion are within acceptable limits for our design.

Sea Keeping Tests

The purpose of the sea-keeping tests was to determine the response amplitude operator (RAO) of the buoy. The RAO is the ratio of the response amplitude to the input amplitude (in this case, the buoy heave or pitch angle to the wave height), and is very useful in characterizing an object's behavior in the ocean. In this section the plan of testing and the method will be described; the results will be listed, and discussed.

Test Plan

The buoy was tested with a simplified mooring design, consisting of the large grid and vertical mooring line as described in the *Mooring System Design* in *II. Design Specifications*. It was assumed that the motion of this grid is very small in the ocean, allowing the grid to be fixed at the corners. The chain at the bottom of the vertical line was modeled with an elastic string with equivalent spring constant of the chain's motion. A series of single frequency tests were performed. Table 10 summarizes the periods and wave heights applied during each test. Data was recorded twice for each test, except test 7, which was recorded once.

Table 10: Summary of Test Parameters

	Model Scale		Full Scale	
	T (sec)	H (cm)	T (sec)	H (m)
Test 1	0.75	2	4	0.56
Test 2	1.0	4	5	1.12
Test 3	1.5	5	8	1.40
Test 4	1.8	7	10	1.96
Test 5	2.3	3	12	0.84
Test 6	3.0	5	16	1.40
Test 7	1.5	12	8	3.40

Method

A description of the buoy model can be found in *Model Design*, at the beginning of *IV. Physical Testing*. The mooring system was scaled with the same scale ratio (28.162/1) used in the fabrication of the physical model. Because of the width of the tank (see *Facility*), the grid was not as wide as scaling called for; the grid should have been 15 ft on each side, but tank constraints only allowed for a grid of 12 x 15 ft. The assumption that the grid is

decoupled from the wave motion, which allowed for the corners of the grid to be fixed, resulted in the width of the tank not being a concern. This is also confirmed by finite element analysis results in chapter VI. *Computational Modeling, Finite Element Analysis of the Mooring System*. In addition, the waves travel in the same direction as the fully proportioned model grid. Figure 25 shows a schematic of the test grid.

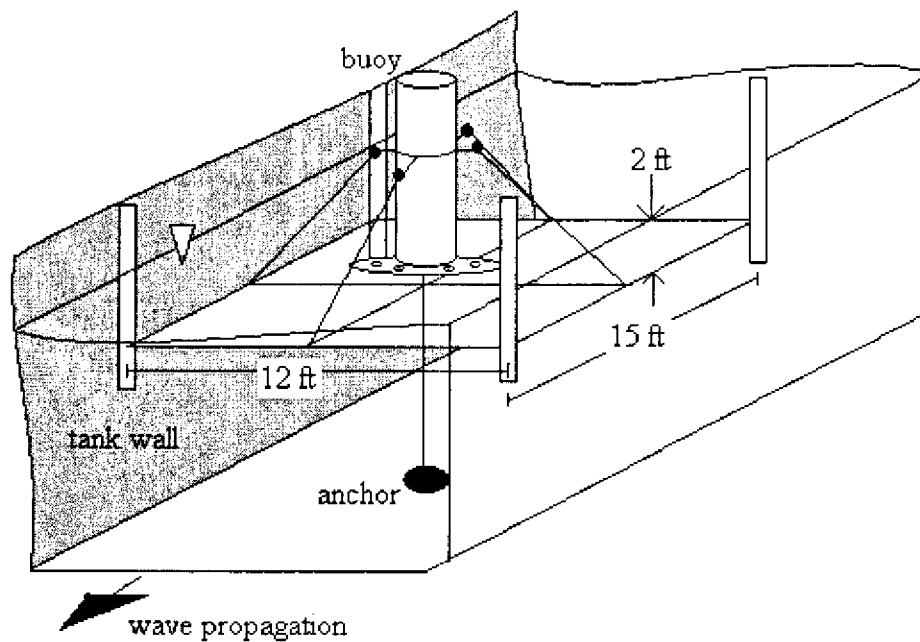


Figure 25: Sea-Keeping tests setup. The corners were fixed with 2x4's clamped to the walls of the tank.

Waves were generated by one, large, hydraulically driven paddle. The waves were dissipated at the other end of the tank with a turbulence inducing “beach”. The motions were recorded using OPIE (described in *Facility*) through the viewing window of the tank. Figure 26 is one frame of the movie taken by the digital camera. Figure 27 shows the buoy during a test.

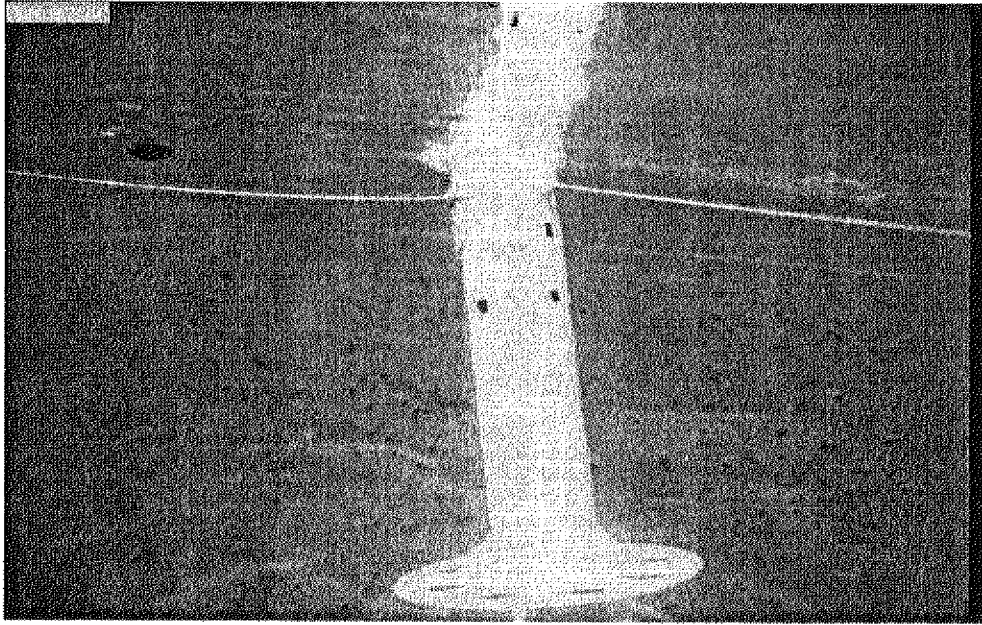


Figure 26: One image captured by the digital camera. OPIE tracks the black dots located on the side of the buoy, and the black lower surface of the wave-follower ball.

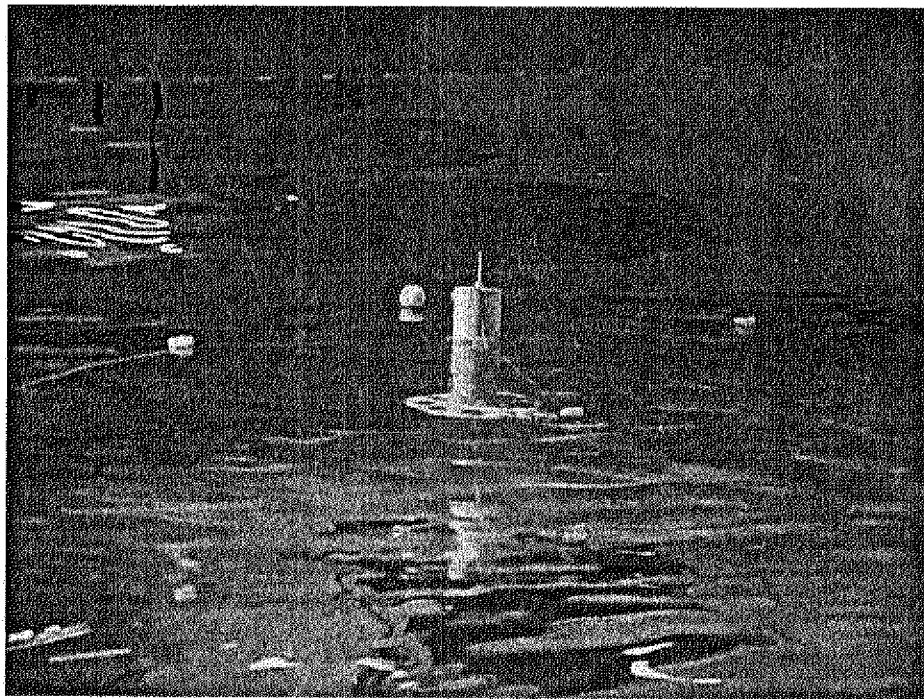


Figure 27: The Buoy During a Sea-Keeping Test

A wave follower ball was used to measure the wave heights independent of the buoy motion. The ball was allowed to move vertically on a taut string; the underside was painted black to allow OPIE to track the ball.

Results

Each test was analyzed using OPIE for the heave (vertical) and pitch motions. The data was then processed in *Matlab*. A ten-point running average was used to smooth the data, and the data mean was normalized to zero. Figure 28 shows the difference between the raw and averaged data.

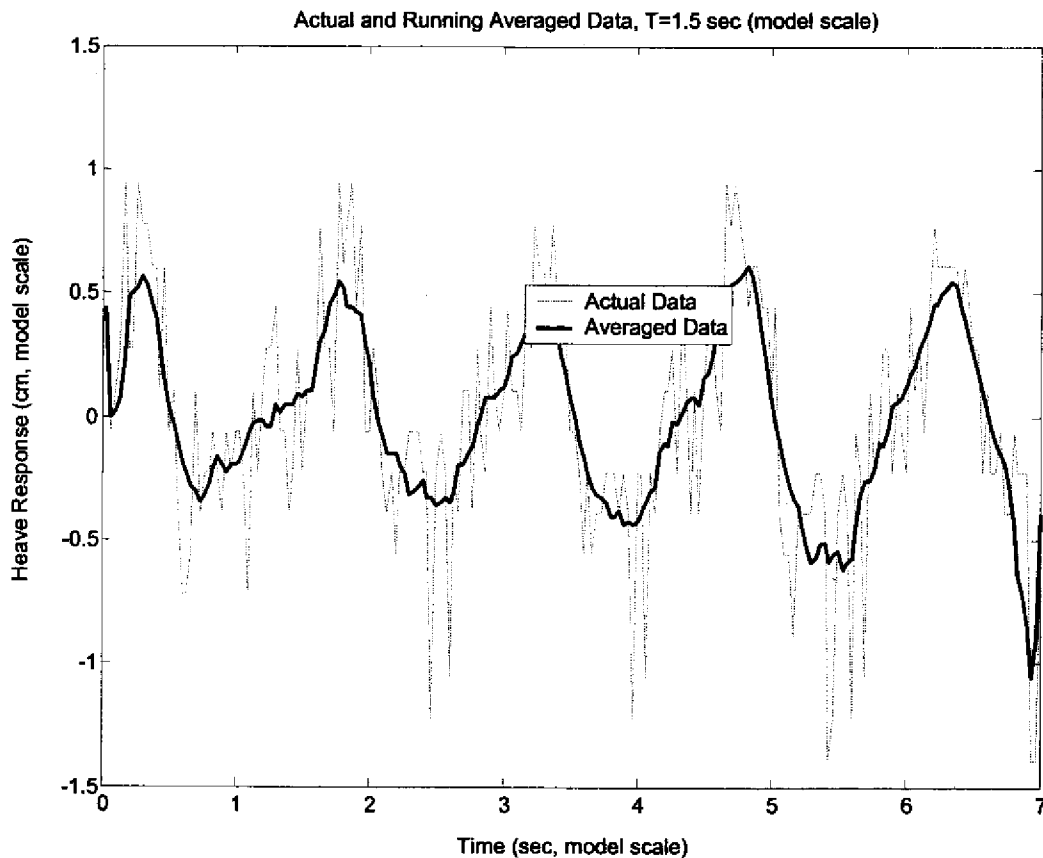


Figure 28: Comparison between the raw, noisy data, and the averaged data for the heave motion of a test with an input of $T=1.5$ seconds and $H=5$ cm, model scale.

Each data set was then analyzed for the average height (difference between the peak and the trough) of the motion. For the data sets corresponding to the wave follower ball, this indicated the wave height. The buoy heave height represented the range of vertical motion of the buoy, and the pitch “height” indicated the range of the rotation of the buoy about the vertical axis passing through its center of buoyancy. All pitch values in this section are taken

to be degrees from the vertical. Figure 29 is an example of the data recorded for a model scale period of 1.5 seconds (eight seconds full scale) and a wave height of five centimeters (1.4 meters full-scale). Figure 30 is a plot of the pitch results for the same test.

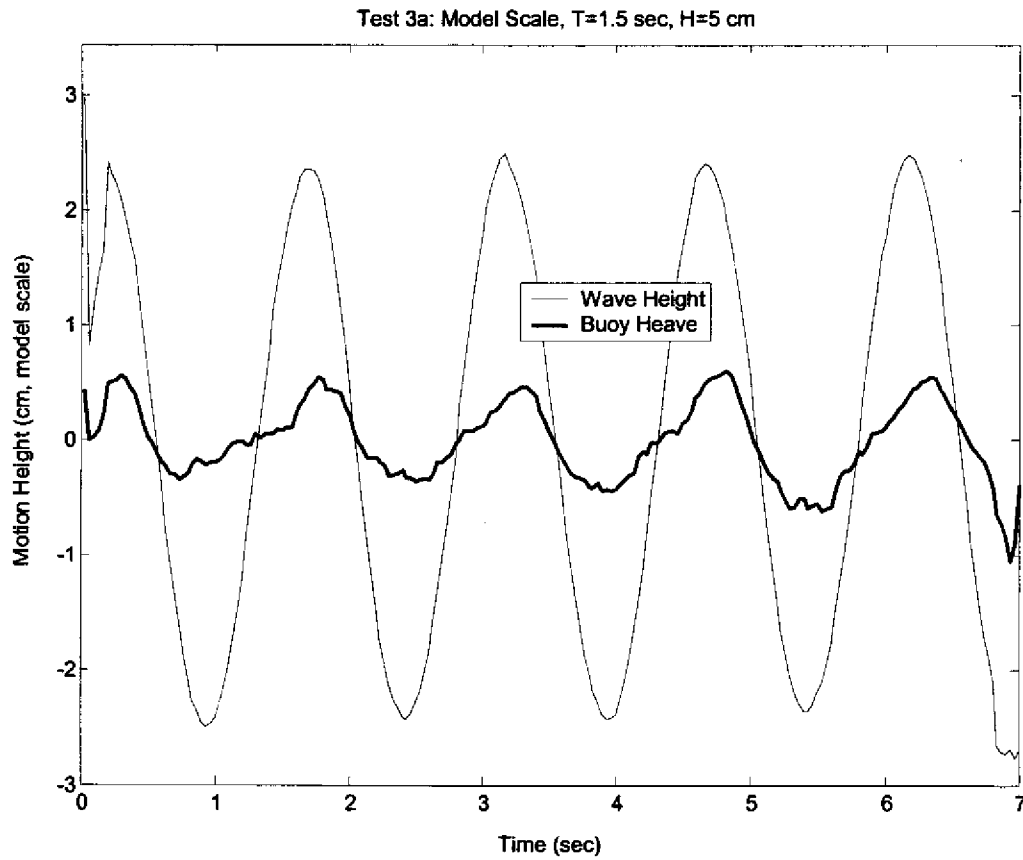


Figure 29: Results from a test at T=1.5 seconds and H=5 cm, model scale. This corresponds to an 8 second sea at 1.4 m for full scale.

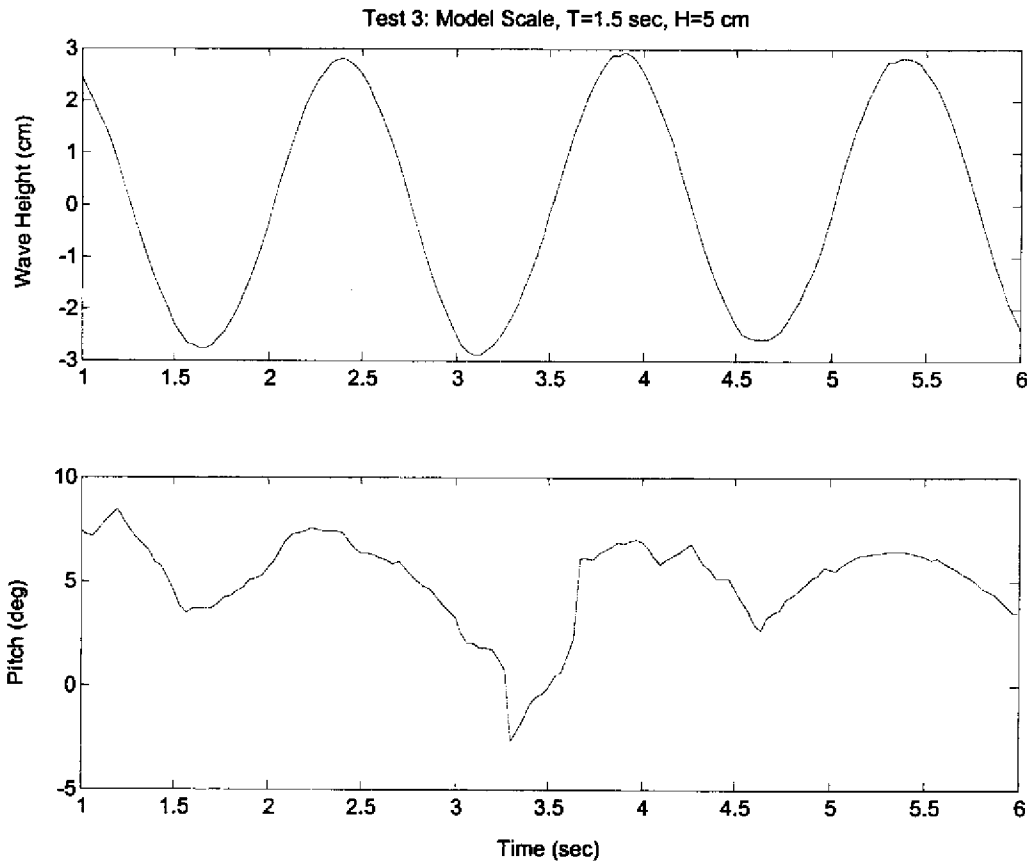


Figure 30: Pitch results corresponding to the graph in Figure 27. The test had a period of 1.5 seconds and a wave height of 8 seconds, model scale.

Figure 31 plots the heave RAO for each test and the average heave RAO for each frequency. As expected, the value of the RAO decreased with increasing frequency, a characteristic of the damping disc.

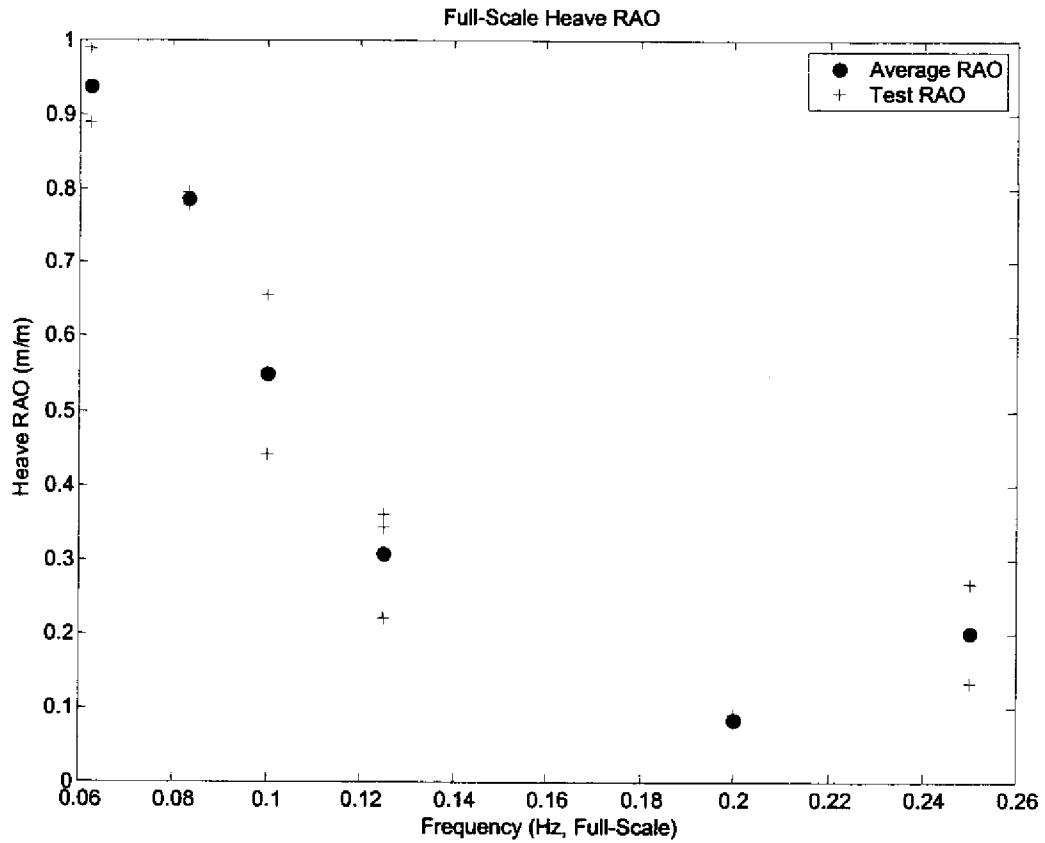


Figure 31: This plot of each test RAO and the average RAO at each frequency shows a decreasing trend in the RAO as the frequency is increased.

The pitch RAO is the ratio of the pitch angle about the vertical to the wave height. The pitch RAO is plotted in Figure 32 for each of the frequencies tested.

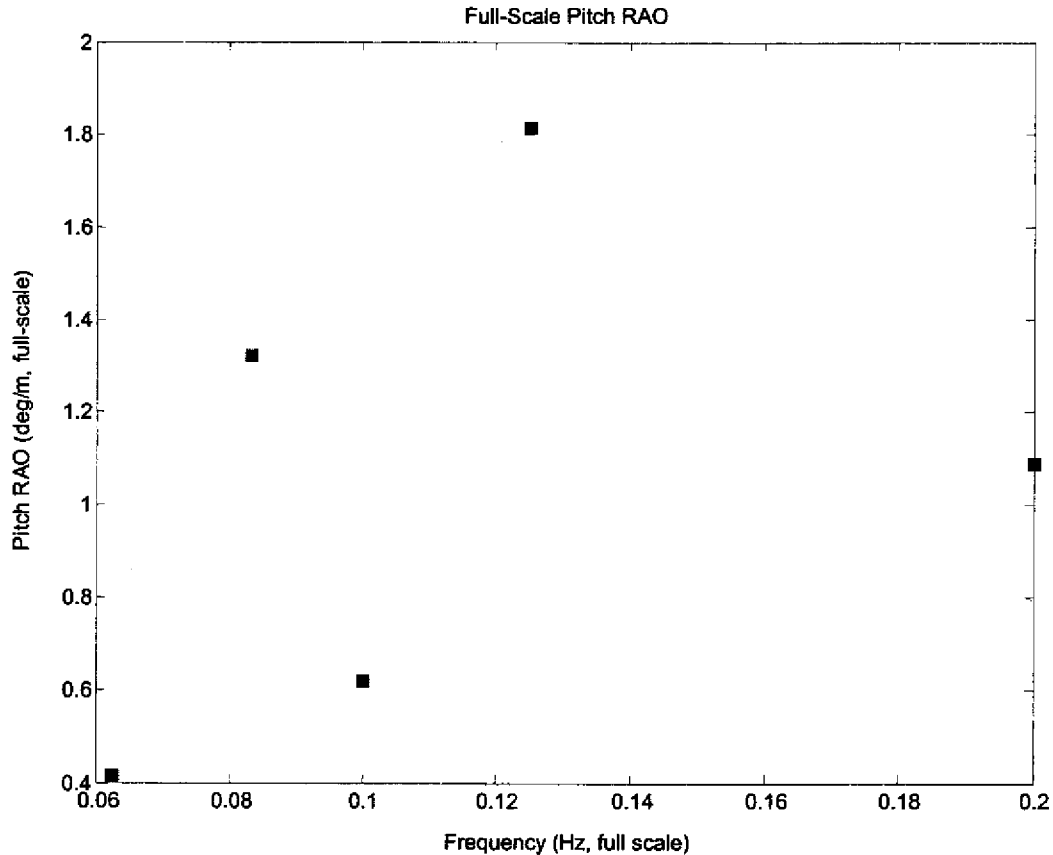


Figure 32: The transfer function of the pitch response to the wave height at each frequency can help identify a resonant situation.

Discussion

The data acquired from the sea-keeping tests is very encouraging. The RAO for the heave response is below one, which indicates that the buoy's heave motion will be quite independent of the wave heights. For the two highest frequencies, the buoy motions recorded by OPIE are actually within the error range of the measurement, and are simply noise. The RAO recorded at these frequencies is therefore a conservative value. Because OPIE looks for any dark pixel, and cannot follow the same pixel throughout the analysis, measurement error is introduced due to the size of the black spot OPIE is following. For all data this error was approximately ± 0.5 centimeters.

During testing an interesting phenomenon was observed at a frequency of 0.667 Hz model scale; the buoy had a significant response in the direction normal to wave propagation. This

frequency corresponds to a full-scale frequency of 0.125 Hz, which is the damped natural period of the spar buoy, without the damping disc. This out of plane motion also causes the pitch to be much higher at this frequency, as seen in Figure 32.

The damped natural frequency of the buoy with damping disc was found to be 0.0824 Hz. In testing this frequency displayed little resonant response in the heave; the RAO was 0.785, which follows the trend of the data for this buoy. However, the pitch RAO was slightly higher at this value.

V. Computational Modeling

This chapter will discuss the computational analysis performed on the buoy design. These analyses were done using finite element analysis software, both commercial and developed locally. A finite element analysis of the stress in the buoy structure was performed to ensure structural reliability and identify weaknesses in the design. A simulation of entire buoy and mooring system was performed under varying sea states to determine the full-scale system's response. This was investigated using the program Aqua-FE (Tsukrov et al, 2000) developed at UNH and sheds light on important characteristics that cannot be seen in scaled physical model testing.

Finite Element Analysis of Buoy Structure

Finite element analysis is necessary to finalize the design of the buoy structure. It is important to look at the stresses caused by the buoy's motion through the water. A full-scale model of the buoy structure was developed using the Finite Element software package *MSC Marc*. In developing the mesh, the buoy's overall characteristics were kept intact. The damping disc located at the base of the cylinder (spar) was modeled as a solid disc without holes for ease in creating the mesh. If the stresses within the structure are acceptable without holes, the stresses obtained with holes should be acceptable as well. There is also concern about the deflection around the edges of the damping disc as the buoy moves within the wave field.

Mesh

This finite element mesh consisted of many quadrilateral elements acting as shells. These quad elements made up the spar of the buoy. Quad elements were also used to create the damping disc and the caps on the spar; the entire mesh can be seen in Figure 33. Once the spar and the disc were completed, the gussets were added to help reduce the stress concentration at the joint between the spar and the damping disc. There are eight gussets

located equidistant around the cylinder. They are attached to the damping disc about 1.8 meters from the base and to the spar three meters above the disc.

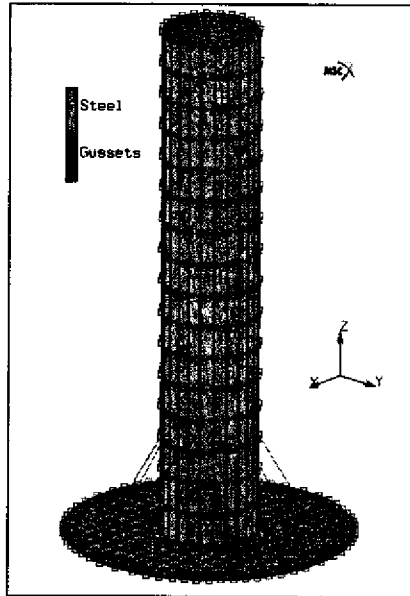


Figure 33: 3-D FEA Buoy Mesh

Load Cases

Once the buoy mesh was generated, the load cases were applied to the buoy structure. There were two main pressures considered when analyzing the buoy structure as it moved vertically in the water. The first was the pressure of the ocean water on the spar. The pressure applied to the spar by the ocean is dependant on depth. This linear function of depth was calculated along the submerged length of the spar, and applied to the proper faces. The second major loading condition was the pressure on the disc, which is induced by the velocity of the buoy as it moves vertically through the water. This loading condition was divided into two parts to be considered separately: the buoy's downward motion, and the buoy's upward motion.

Using the results from the free release heave tests, a maximum velocity was determined for each condition; the maximum full-scale velocity of the buoy in the downward direction was approximately 8.6 meters per second and the maximum velocity of the buoy in the upward direction was about 2.9 meters per second. The forces acting on the disc due to the heave motion were calculated from the experimental damping constant and the heave velocity. The forces were applied to the appropriate areas of the disc to obtain pressures. The maximum

velocities correspond to equivalent pressures of about 3,290 Pa acting on the topside of the disc (going up) and 8,708.6 Pa acting on the bottom of the disc (going down).

Figure 34 shows the loading conditions applied to the buoy as it descends through the water. This figure shows that the resistance to the buoy's motion is the pressure acting on the bottom of the disc. Figure 35 shows the loading conditions applied to the buoy as it ascends through the water with the pressure applied to the top of the disc.

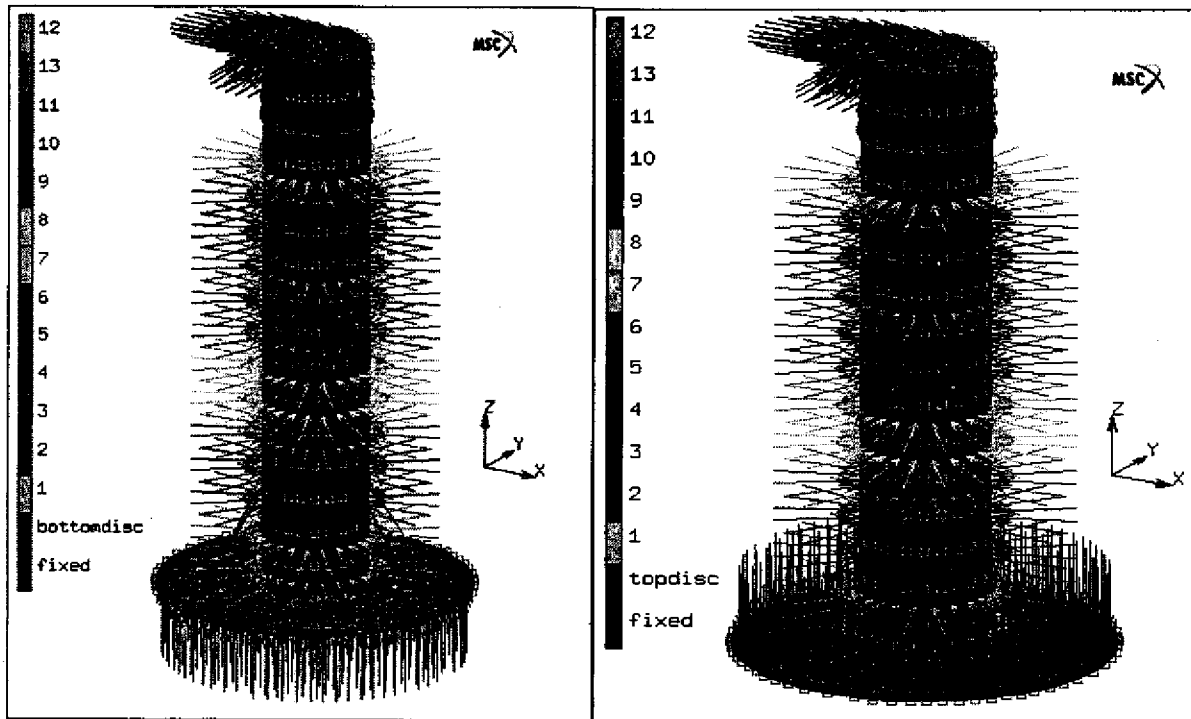


Figure 34: Downward motion

Figure 35: Upward motion

Results

These two loading conditions were run several times for two varying geometric properties. One trial kept the thickness of the disc constant at 0.05 meters and varied the thickness of the spar shell. The second analysis kept the thickness of the shell constant at 0.02 meters and varied the thickness of the disc. In each case, *Marc* calculated the maximum equivalent stress both the spar and disc according to von Mises equivalent stress formula (www.marc.com). These stresses were compared to the yield strength of steel (210 MPa for

steel) (Lardner et al, 1994). Another important result of these tests was the maximum displacement of the disc under each loading condition.

The plots of maximum equivalent stress versus the varying thickness of both the disc and shell can be seen in Figures 36 through Figure 39. In these figures, T represents the thickness. The safety factor found at each thickness is also displayed in Figures 36 through 39. The large data points shown correspond to the actual buoy design dimensions. The first two plots (36 and 37) correspond to the downward motion of the buoy. In Figure 36, the maximum stress within the disc is much greater than that of the shell. The safety factor versus thickness for the disc increases as the thickness of the shell increases.

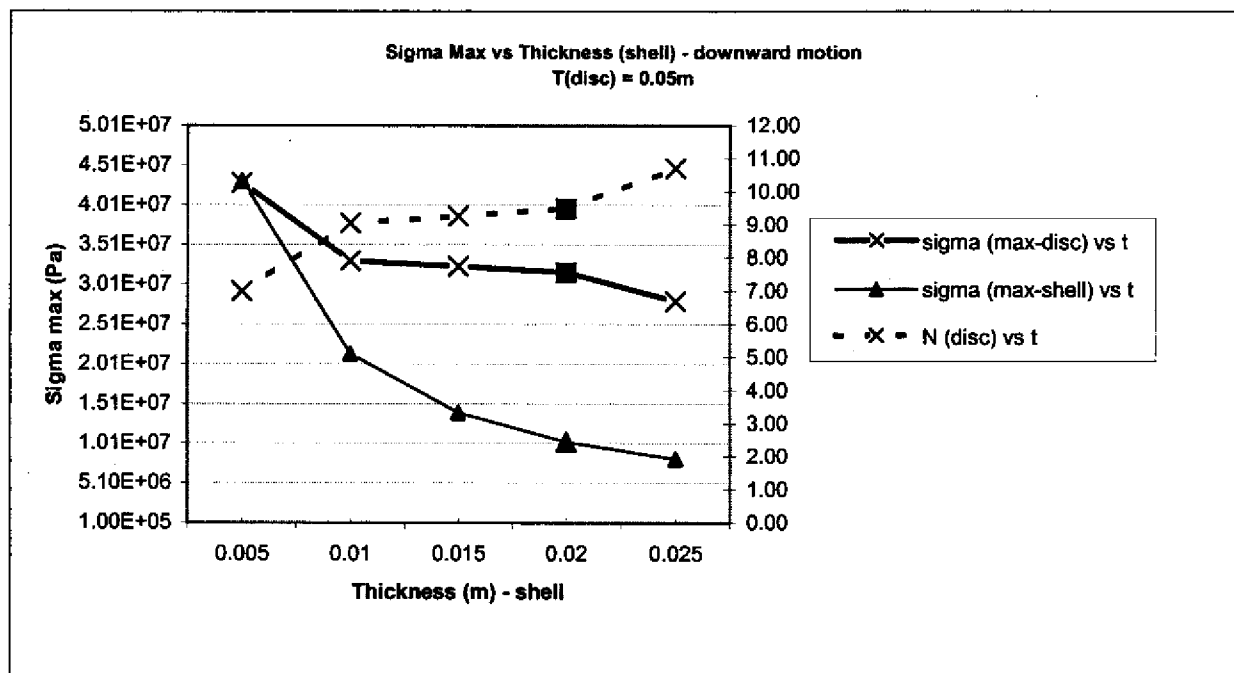


Figure 36: Sigma Max vs. Thickness of the shell ($T(\text{disc}) = 0.05\text{m}$)

Figure 37 shows a similar trend. However, as the thickness of the disc increases, the stresses within the disc are much lower than when the shell thickness was varied. The safety factor also increases with disc thickness but has a much steeper slope.

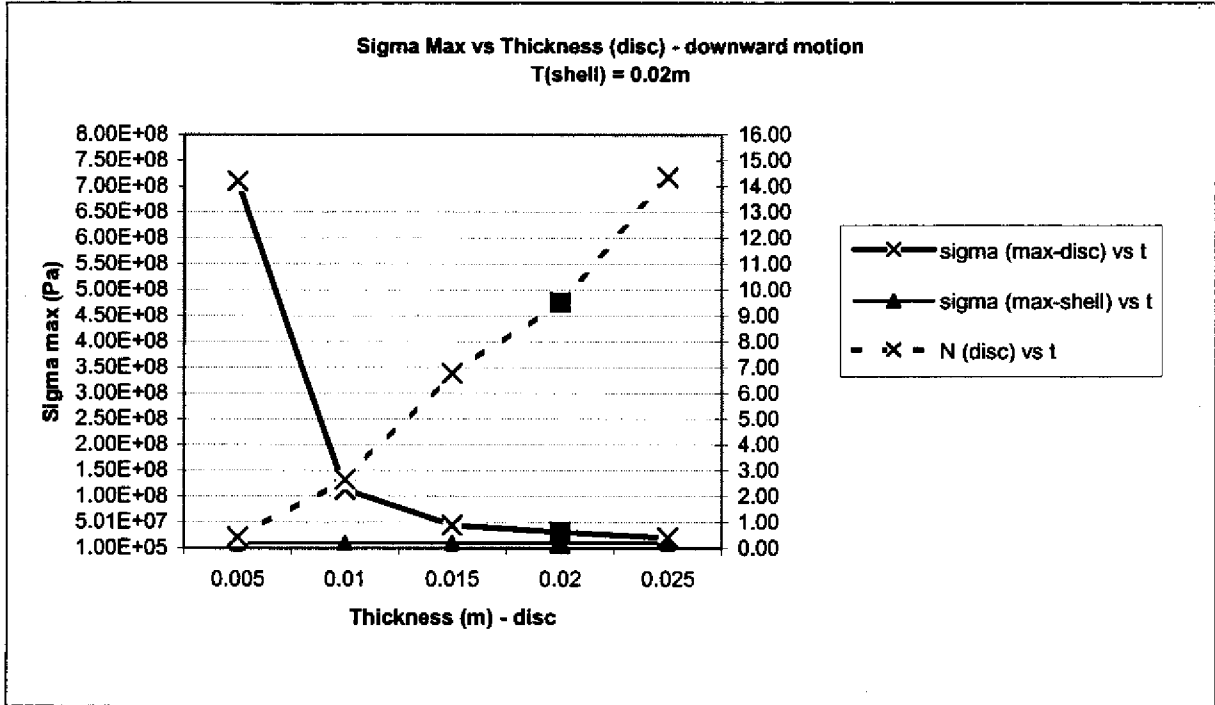


Figure 37: Sigma Max vs. Thickness of the disc (T(shell) = 0.02m)

Figures 38 and 39 correspond to the upward motion of the buoy. Figure 38 shows the same trend of decreasing stress with an increasing thickness, though the maximum stress in the shell is much greater than that of the disc.

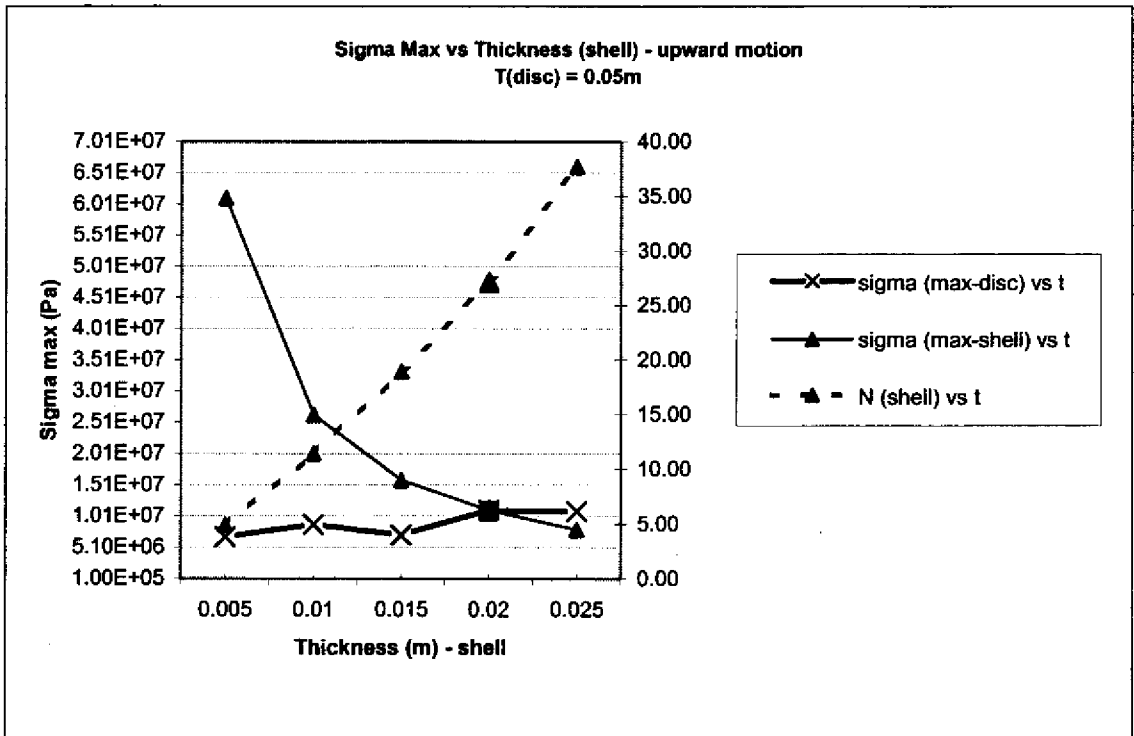


Figure 38: Sigma Max vs. Thickness of the shell (T(disc) = 0.02m)

The plot in Figure 39 shows a similar trend to Figure 37. The maximum equivalent stresses within the disc are much greater than the stresses within the shell. Similarly, the stress decreases tremendously as the thickness of the disc increases. The safety factor of the disc rises significantly with the increase in disc thickness. In all cases, the stress decreases with the increase in thickness of either structure. This corresponds to an increase in the safety factor of each case as thickness increases.

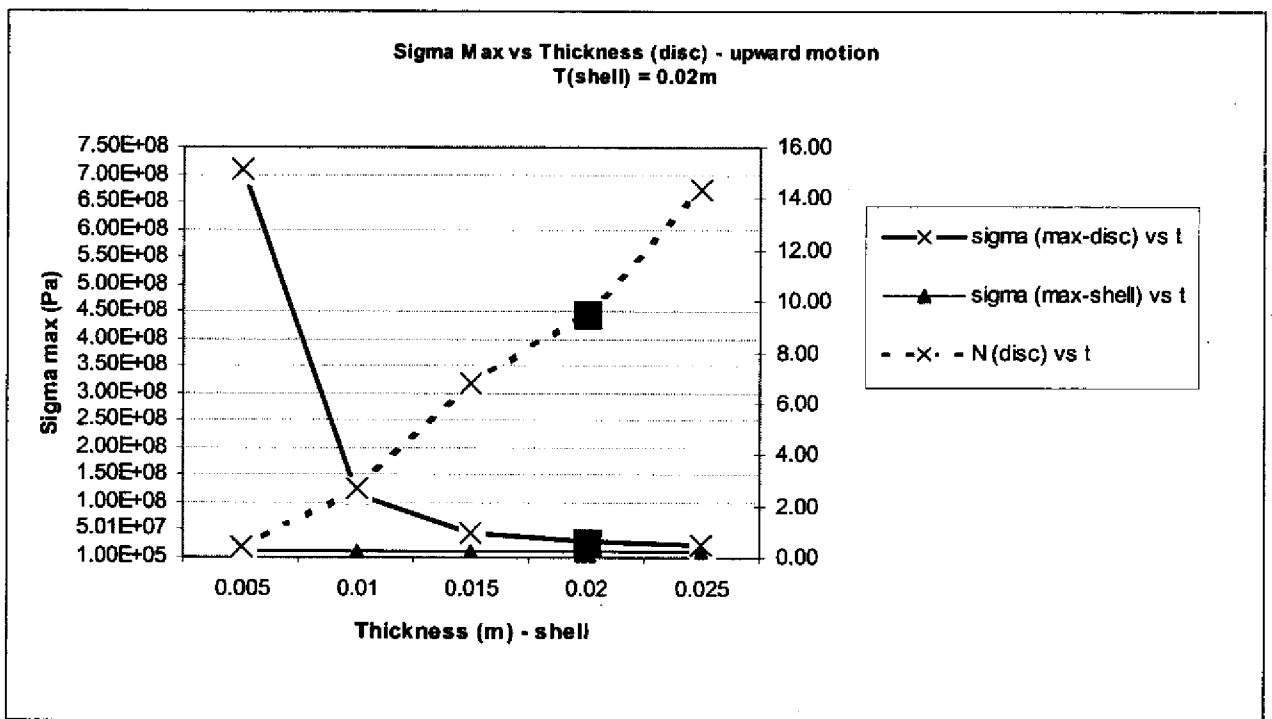


Figure 39: Sigma Max vs. Thickness of the disc (T(shell) = 0.02m)

Figures 40 and 41 are two plots of the maximum displacement of the disc under each loading condition for each analysis. Figure 40 shows the maximum displacement of the disc as the thickness of the disc increases. Figure 41 is a similar plot as the thickness of the shell varies. Both plots show a significant decrease in the maximum displacement of the disc as the thickness of both the disc and shell increase.

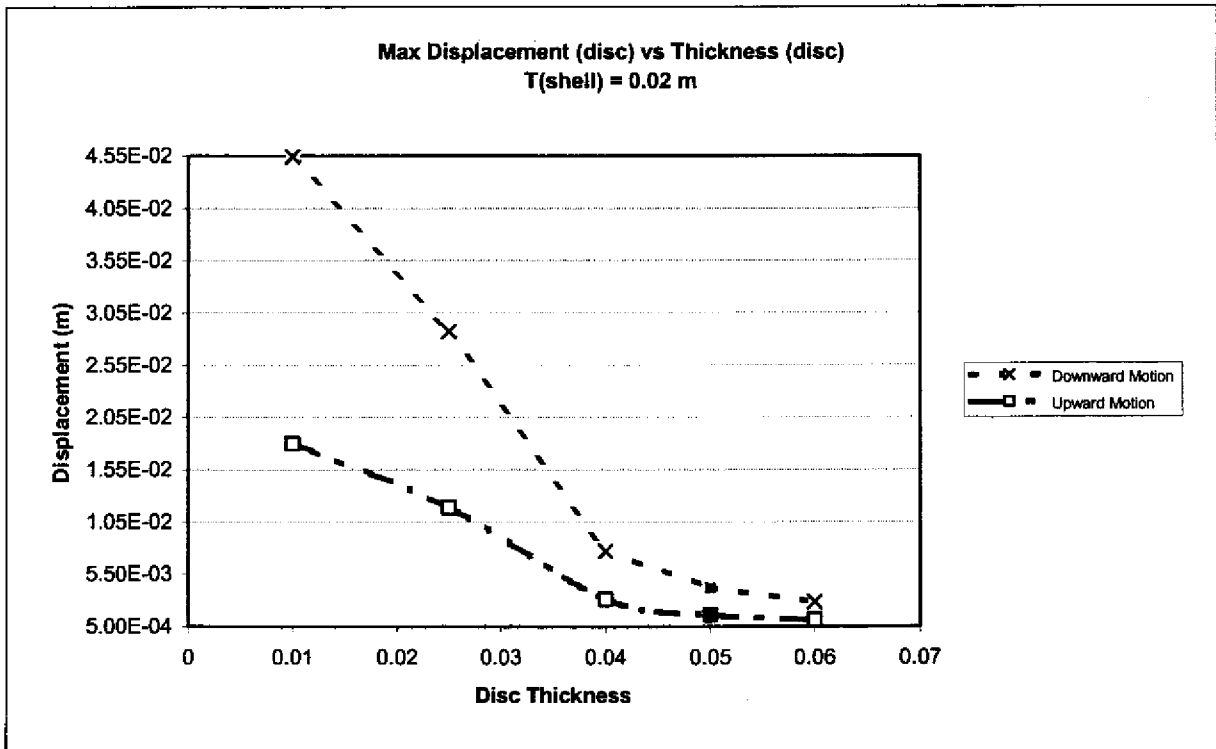


Figure 40: Max Displacement vs. Thickness of the disc (T(shell) = 0.02m)

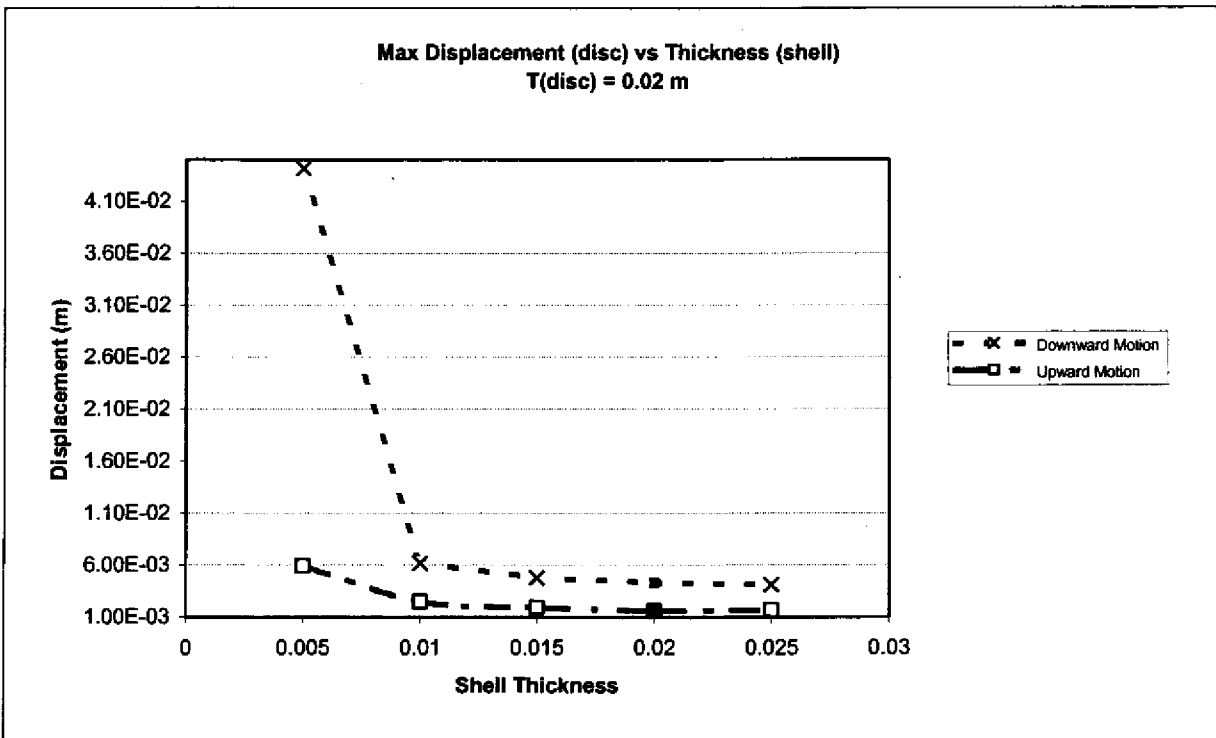


Figure 41: Max Displacement vs. Thickness of the disc (T(disc) = 0.02m)

Discussion

The results of the finite element analysis of the overall buoy structure show that the stresses in the disc and the shell associated with the prescribed loading are acceptable. The loading conditions were derived to mimic the pressures that the buoy will experience while in the ocean. The shell of the spar is designed to be 0.02 meters thick and the disc has a thickness of 0.05 meters. The results associated with these geometric parameters show that the buoy structure will be able to withstand the loading applied to it in the ocean. The maximum equivalent stress that will be placed on the buoy structure will be less than 45 MPa. Based on the results of the tests, the structure of the buoy will have a minimum safety factor of about 9.5. The maximum displacement of the disc associated with each loading condition for the designed geometric parameters was less than 4.5 mm. The desired value of displacements is not explicitly defined. The displacements should be small, however, to prevent large, repeated stresses over time and to minimize fatigue of the material. Based on this finite element study, it is concluded that the designed geometric parameters of the buoy structure will sufficiently limit the stress in the disc and spar and will minimize the displacement of the disc.

Finite Element Analysis of Mooring System

Mesh

The finite element mesh of the full-scale buoy and mooring system was created using the *MSC Marc Mentat* user interface, and analyzed using a UNH developed software called Aqua-FE, created specifically to model systems deployed in the ocean (Tsukrov et al., 2000). The model consists of 564 truss elements (Aqua-FE is only capable of analyzing truss elements), 444 of which contain mass. The remaining 120 “massless” elements are used to maintain rigidity in the structure.

The buoy was modeled by representing sections of the actual design by a series of truss elements with appropriate mass densities and cross-sectional areas; Table 11 summarizes the

geometric and material properties defined for each element. Figure 42 shows the finite element mesh of the buoy. All components of the buoy were given an elastic modulus of 2.0 GPa.

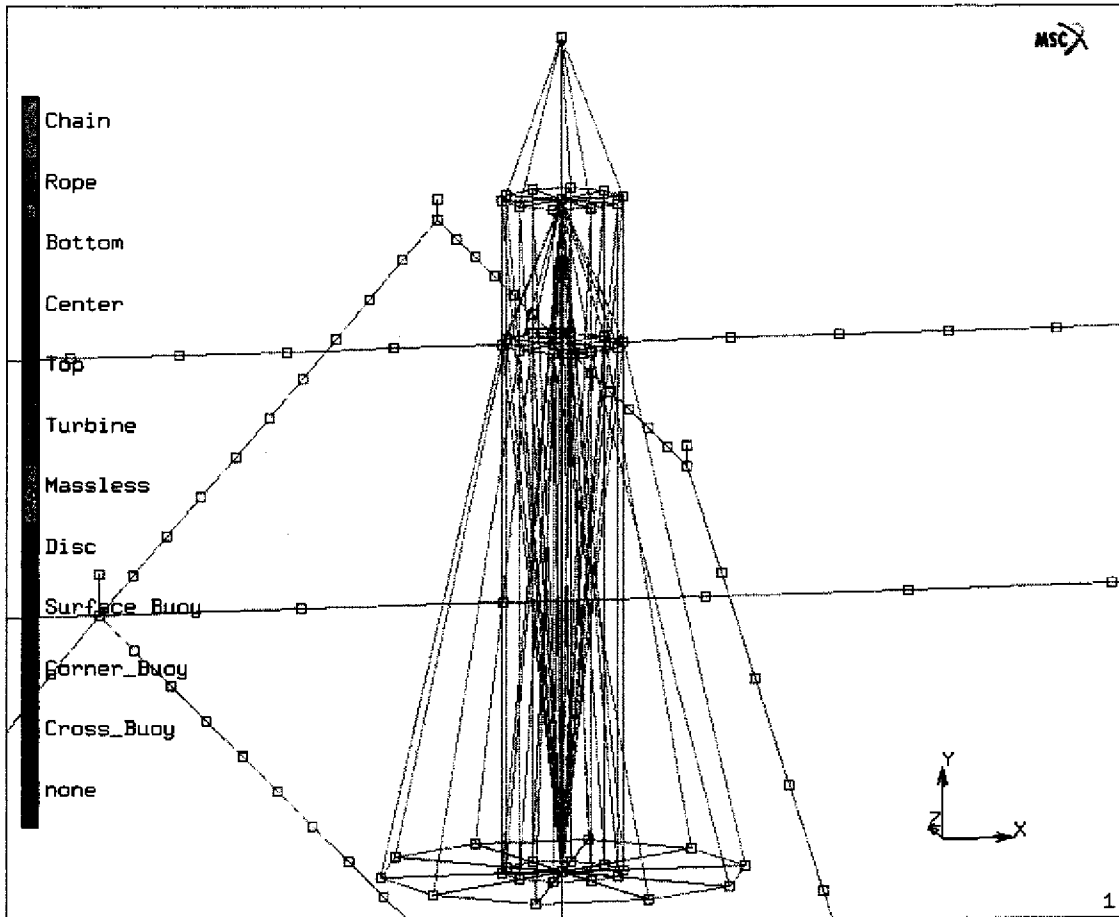


Figure 42: The finite element mesh of the buoy; the user interface is *MSC Marc Mentat*. All elements are truss elements to be used with Aqua-FE.

The grid is modeled using approximately 384 rope elements. The rope has a density of $1,025 \text{ kg/m}^3$, and a cross-sectional area of 0.0049 m^2 , with an elastic modulus of 206 MPa. A model of the full grid can be seen in Figure 43.

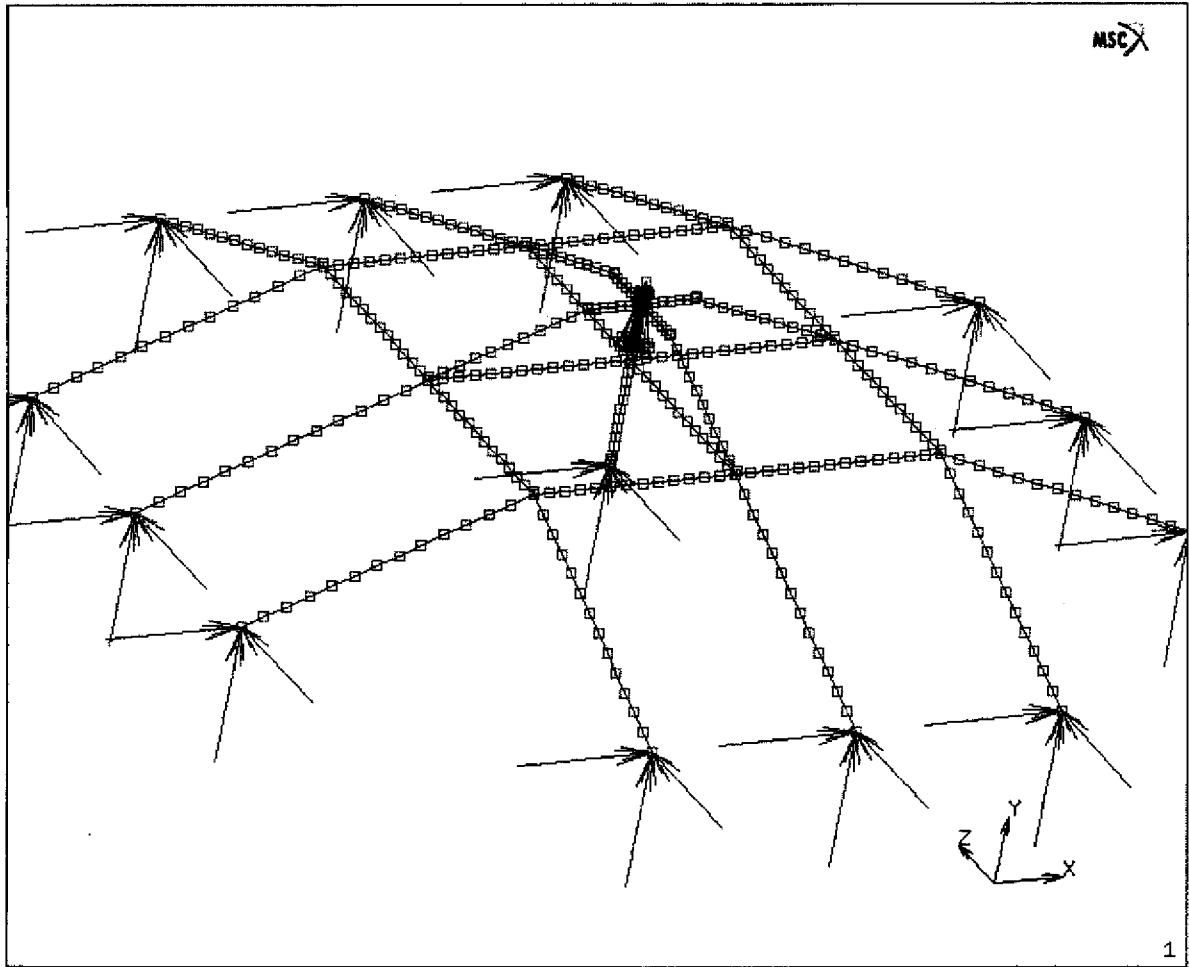


Figure 43: The full mooring grid. All the anchor points are given boundary conditions of fixed displacement (equal to 0), and the grid contains 384 elements.

The eight submerged and four surface buoys that support the grid are modeled as small cylinders with proper mass densities for their prescribed buoyant force. Buoys with a net buoyant force of 1,761.5 N (396 lbs) were used for all 12 buoys in this model, though the mooring design calls for a higher net buoyancy to be used for the submerged grid.

Table 11: Material Properties of Finite Elements Used in Mooring Mesh

	Description	Mass Density (kg/m ³)	Elastic Modulus	Cross-Sectional Area (m ²)
Chain	Lower 3m of central mooring line	291	206 MPa	0.00102
Rope	Remainder of mooring line and grid	1,025	3.58 GPa	0.0049
Bottom (of buoy)	Includes pumps, ballast locks, some auxiliary weight, bottom of the shell, and the lower bulkhead	5,199	2.00 GPa	0.2919
Center (of buoy)	Includes the cylindrical outer shell, the silo, and feed	465.2	2.00 GPa	7.069
Top (of buoy)	Includes some auxiliary weight, the batteries, the top of the shell, and the upper bulkhead	614.3	2.00 GPa	0.2919
Turbine	Wind turbine, mounted to top of buoy	21.66	2.00 GPa	3.14
Damping Disc		7,850	200 GPa	0.0415
Surface Buoys		458.4	1.00 GPa	0.1257
Submerged Buoys		321.0	1.00 GPa	0.1791
Massless	Massless elements are added for stability	0.00	200 GPa	1.29

The anchors at the base of each of the grid mooring legs were modeled using nodal fixed displacements of zero in the x, y, and z directions. The chain at the base of the central mooring line was modeled as three elastic elements; zero displacement in all directions was prescribed to the bottom node of the chain.

Load Cases

Load cases consisted of different combinations of currents and wave states. Table 12 lists the conditions tested on the computational model. The first five tests mimicked those sea states tested in the physical sea-keeping tests. The sixth test was applied a worst-case scenario with high seas at a common storm frequency, 0.125 Hz.

Table 12: Summary of Load Cases

Frequency (Hz)	Wave Height (m)	Wave Length (m)	Length of Test (sec)
0.200	1.12	16.07	6
0.125	1.4	29.12	9
0.100	1.96	43.22	11
0.083	1.4	44.10	13
0.0625	1.4	58.89	17
0.125	4.0	47.97	11

The current for the first 5 tests was 0.25 m/s (~5 knots), constant throughout the water column. The current for the “worst case” situation was 2.5 m/s (4.9 knots).

Results

Aqua-FE allows the user to identify specific node and element results of interest. The tensile stress is of particular interest in the elements that are fixed at one node. Stresses were found in the “anchored” grid leg elements, as well as the stress in the elements that share the node connecting the buoy’s vertical mooring line and the grid center. The vertical displacement of the outside edge of the grid, and the vertical displacement of the buoy were also analyzed. The displacement of the grid corners and bisecting edge points was used to verify the assumption that the grid motion is independent of the wave motion, which is utilized in the sea-keeping tests (see *IV. Physical Testing, Sea-keeping Tests*).

Table 13 gives the maximum stress at an anchored element for each of the frequencies tested. The stresses at the anchor points were well below the maximum tensile stress of the rope (215 MPa), and the stress at the bottom of the central mooring line was low for the calmer sea states. The maximum stress at the anchor points for the worst-case sea state was one order of magnitude higher than those of calm seas.

Table 13: Summary of Rope Stress at Grid Anchor Points

Frequency (Hz)	Maximum Rope Stress at Anchor (MPa)	Stress at Base of Central Mooring Line (kPa)
0.200	0.84	3.86
0.125 (small amplitude)	1.47	3.91
0.100	3.62	3.96
0.083	2.17	3.91
0.0625	2.25	3.94
0.125 (storm seas)	42.9	4.26

Due to the flexibility of the mooring system, no stress was induced in the elements surrounding the connection of the grid and the central mooring line, even in the extreme sea.

For the calm sea states the displacement of the grid was found to be minimal; the displacement was within 0.1 m (for a 1.4 m wave height), validating the assumption of small grid displacements made during physical testing (all physical tests were in relatively calm seas). Because of the strong current, the grid displacement for the storm sea was much higher; this can be seen in Figure 44.

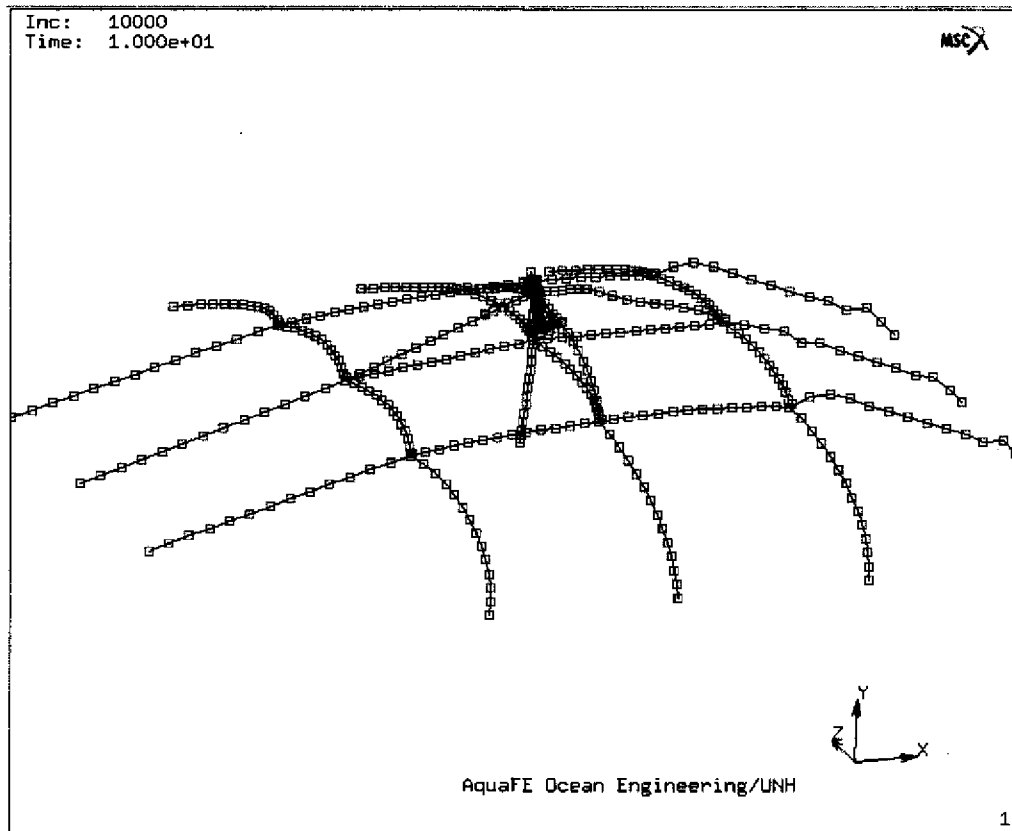


Figure 44: A frame of results of the storm sea. The current flows in the positive x direction.

The heave of the buoy is of interest because of its effect on the feed distribution system and the turbine. The heave was found to be varied, and even for tests of 60 seconds did not appear to reach steady state. For the 0.125 Hz calm seas, Figure 45 shows the buoy heave.

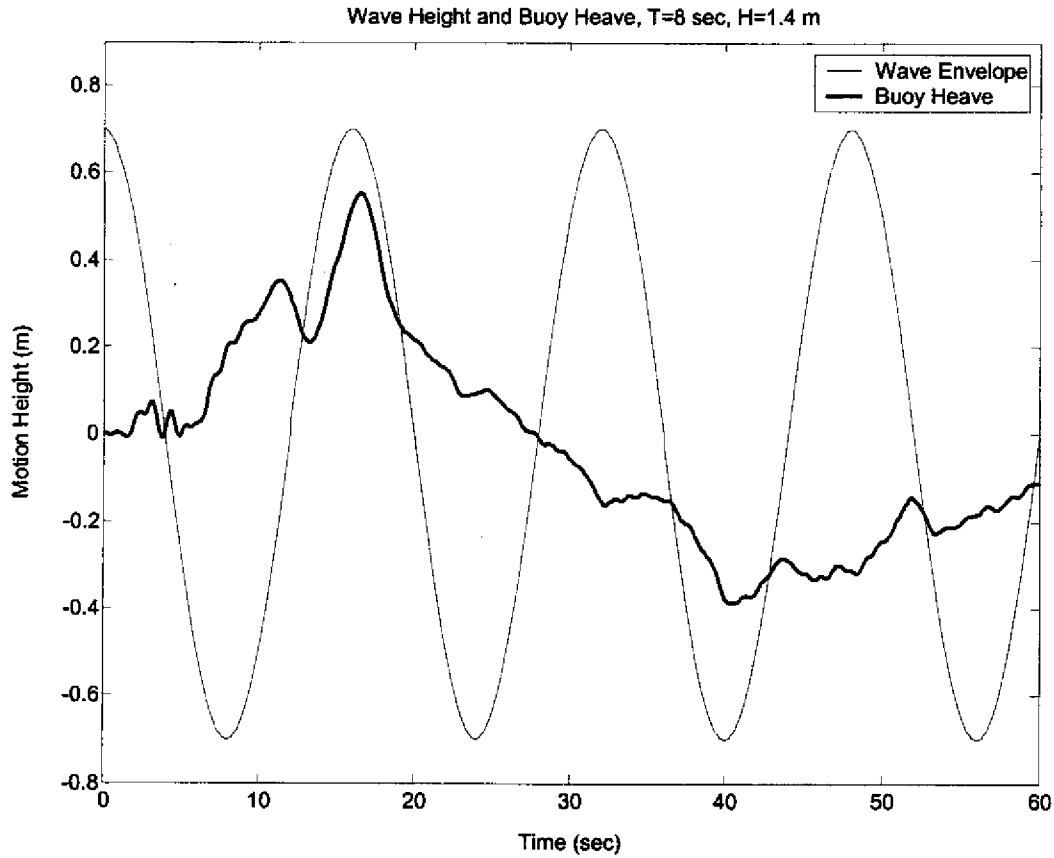


Figure 45: Input Wave Envelope and Buoy Heave as Modeled by AquaFE

The small current present in this test appears to have little effect on the motion of the buoy or grid. It is important to note that because of the constraining mooring system, however, the buoy experienced dramatic negative heave in the 11-second storm sea test.

Discussion

The maximum tensile stress of the rope is approximately 215 MPa; even in the storm seas, the maximum stress found in the rope at the anchor points was only 42.9 MPa, giving a safety factor of 5. This result indicates that the mooring grid is relatively stable. Stability in this mooring system is important for many reasons, all of which have been discussed previously in this report. Stability is very important for the buoy itself because of the power generating wind turbine mounted to it.

Through computational testing it was found that buoys with 1,761 N of buoyancy were acceptable for all submerged and surface applications. Buoys of higher buoyancy were originally applied to the submerged grid corners, and were found to be too buoyant. Computational testing also verified an assumption made during physical testing; in calmer seas the grid motion is fairly independent of buoy motion, allowing the corners of the test grid to be fixed.

The displacement of the buoy in the computational model did not quite agree with that found during physical testing. This can be due to several factors, the most obvious of which is that the computational model grid is “perfect”, while the physical grid was not exact. In addition, the computational model is analyzing the displacement of the top node of the buoy, under the assumption that a rigid structure will have the same displacement throughout, while the physical model displacement was measured towards the center of the buoy. The assumption of rigidity may be compromised by the node located at the waterline in the buoy center element, 13.66 meters above the damping disc. Final causes for the discrepancy could arise from the computational model itself. It is important to note that the computational model did mirror important characteristics that the physical modeling brought to light, particularly the pitch response at a frequency of 0.125 Hz.

One important observation that should be noted is the amount of pitch in the buoy in the storm sea state. The mooring system was designed to reduce pitch and heave motions, to keep the turbine as stable as possible, and reduce the effect of the buoy’s motion on the fish cages below. This extreme pitching motion is of concern because of damage to the turbine and disturbance to the fish cages. It is assumed that storms will be the exception, and that most sea states will induce much less pitch; this assumption is verified through the other computational tests and physical tests (see *IV. Physical Tests, Sea-keeping Tests*).

Computational modeling offers an important comparison to the physical modeling results. For this project computational modeling offered the opportunity to experiment with different grid buoys, and the ability to apply much stormier conditions than can be created in the wave tank.

VI. Conclusion

The intent of this design team was to propose a method of delivering food to four submerged cages each holding approximately 50,000 fish. The desire was service this feeder no more than once a week for restocking the feed. It was calculated that 200,000 fish could require as much as 35 metric tons per week. The space needed to store this volume of food, plus systems for delivering it, and space for ballast to be taken in to maintain a constant draft as the buoy emptied necessitated a very large design. The buoy that this group is proposing is three meters in diameter and 16.6 meters long. Admittedly this is incredibly large. To put this into perspective the mean depth of the site is 52 meters; the draft of the proposed buoy is about 25% of the total depth at the site. When originally designed the damped natural frequency of the buoy was the same as that of storm condition waves, which would have led to a resonant situation. Options for modifying the natural frequency were to decrease the diameter, increase the mass, or add something to act as a damping mechanism. A sufficient decrease in the diameter led to an unacceptably long buoy and the mass necessary to decrease the frequency of the buoy would have caused it to sink. Thus the only option to decrease the natural frequency was to add a damping mechanism, a nine-meter diameter plate on the bottom of the buoy.

The economics of a buoy of this magnitude were outside the realm of this project but from an engineering standpoint this group believes this to be feasible. Finite element analysis of the mooring system and the buoy shows that the structure is sound. The feed delivery and ballast maintenance systems can be built with “off the shelf” components. A turbine has been designed that will meet the power needs of all the systems and withstand the harsh conditions in the Gulf of Maine. Before a full scale feed buoy is built systems such as the remote control system, the pumps for adding ballast as the feed is emptied, and the feeding auger should be tested. If these tests are successful and the benefits outweigh the costs then this design group asserts that a self-sustaining buoy can be built to feed all four fish cages at the UNH Open Ocean Aquaculture site off the Isle of Shoals.

VII. References

- Aquatic Eco-Systems www.aquaticeco.com Viewed 22 Apr. 2003.
- B/C Valve www.bcvalve.com Viewed 22 Apr. 2003.
- Berteaux, H. O. (1991) Coastal and Oceanic Buoy Engineering. Berteaux: Woods Hole MA.
- Chakrabarti, S. K. (1994) Offshore Structure Modeling. World Scientific: Singapore.
- Chambers, M. (2002) Personal Conversation Regarding Feed Requirements. University of New Hampshire, Durham NH.
- Celikkol, B., D. Fredriksson, B. Fullerton, G. Rice, G. McGillicuddy, K. Baldwin, J. Ahern, M. Chambers, C. Kurgan (2002) Discussion Meeting Regarding Mooring Design. University of New Hampshire, Durham NH.
- DeCew, J. (2003) Personal Conversation Regarding Grid Buoys. University of New Hampshire, Durham NH.
- Digi-Key www.digikey.com Viewed 22 Apr. 2003.
- Fredriksson, D. W., and M. R. Swift, E. Muller, K. Baldwin, and B. Celikkol (2000) *Open Ocean Aquaculture Engineering: System Design and Physical Modeling*. Marine Technology Society Journal.
- Kerr, C. (Windstream Power System Inc.) (2003) Personal Communications Regarding Wind Turbine Design. Durham NH/ Burlington VT.
- Lardner T.J. and R.R. Archer (1994) Mechanics of Solids: An Introduction. McGraw-Hill: New York.
- McMaster-Carr www.mcmaster.com Viewed 22 Apr. 2003.
- Michelin, D and S. Stott, (1997), *Optical Positioning Instrumentation and Evaluation*. Submitted to University of New Hampshire Ocean Projects TECH 797 Course.
- National Data Buoy Center www.ndbc.noaa.gov Viewed 24 Apr.2003.
- National Oceanic and Atmospheric Administration, www.tidesonline.nos.noaa.gov, Viewed 24 Apr.2003.
- Polyform U.S. www.polyformus.com Viewed 24 Apr.2003.
- Principles of Stability* www.fas.org/man/dod-101/navy/docs/swos/dca/stg4-01.html Viewed 22 Apr. 2003.

Rolls Battery Engineering www.rollsbattery.com Viewed 24 Apr. 2003.

Savory, E. *Stability of Floating Bodies*. www.engga.uwo.ca Viewed 22 Apr. 2003.

TransTel Group, www.transtelgroup.com Viewed 24 Apr. 2003.

Tsukrov, I. I., M. Ozbay, D. Fredriksson, M. R. Swift, K. Baldwin, and B. Celikkol (2000).
Open Ocean Aquaculture Engineering: Numerical Modeling. Marine Technology
Society Journal.

University of New Hampshire Open Ocean Aquaculture Program www.ooa.unh.edu Viewed
24 Apr. 2003.

Velleman-Kit (2003) www.velleman-kit.com Viewed 22 Apr. 2003.

VIII. Appendices

The four appendices that follow contain supporting information for this design report.

Appendix A contains detailed drawings of the design. These include dimensioned drawings for the selected components. Manufacturers specifications for prefabricated materials called for in the buoy design are located in Appendix B. Specific processes for deploying the feed can be seen in Appendix C. Appendix D contains the raw data (in graphical form) from the physical model tests. Graphs of the heave and pitch response for both the free-release tests and the sea-keeping tests are included.

A. Detail Drawings

Buoy Assembly..... A-2

Top Section..... A-3

Middle Section..... A-4

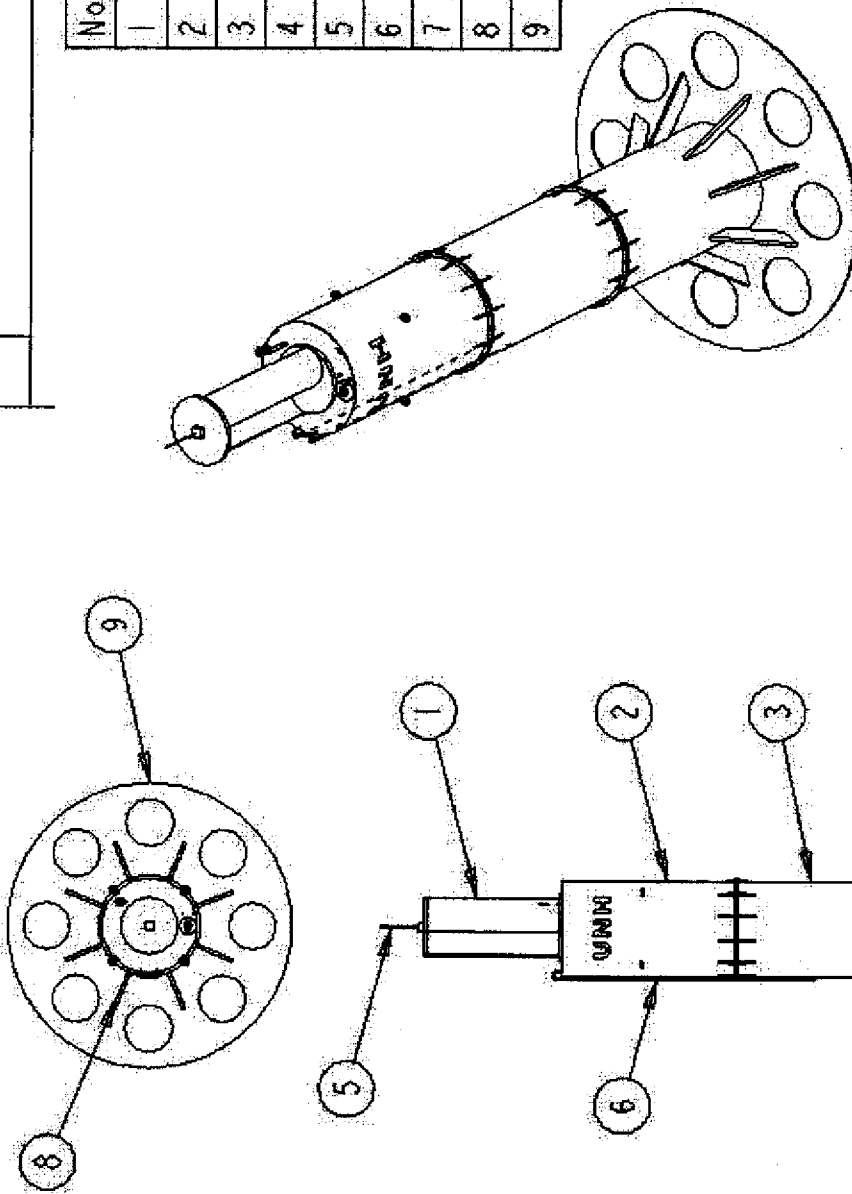
Bottom Section.....A-5

Feed Silo.....A-6

Helius Turbine..... A-7

The University of New Hampshire

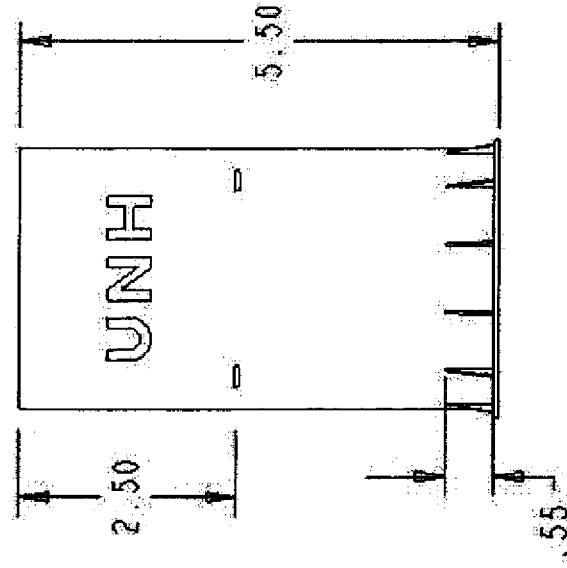
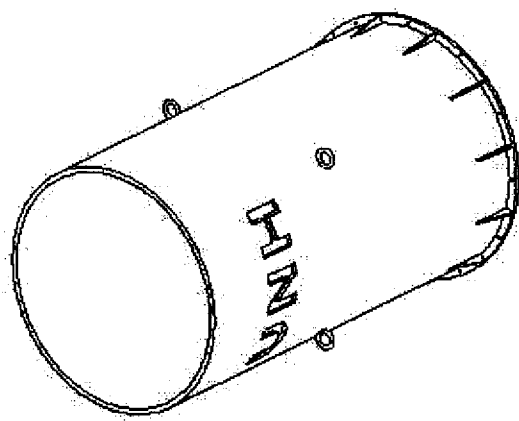
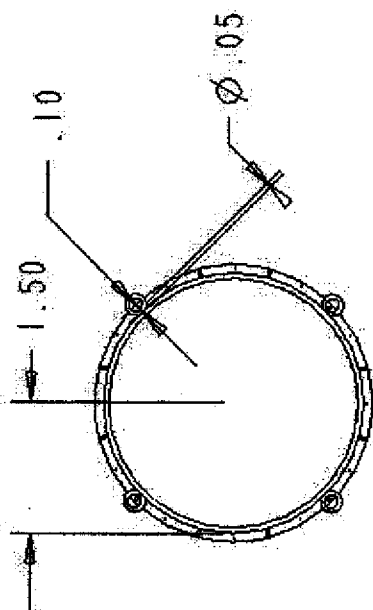
No.	Feature
1	Wind Turbine
2	Top Section
3	Middle Section
4	Bottom Section
5	Antenna
6	Ladder
7	Mooring Hook
8	Gusset
9	Damping Disc



Buoy Assembly	
OSWEB	
04/25/03	TECH 797 Modeled by PRP

SCALE : 0.1:1 TYPE : ASSEM NAME : BUOY SIZE : A

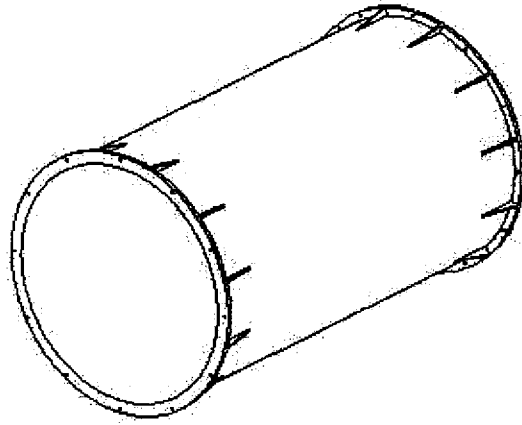
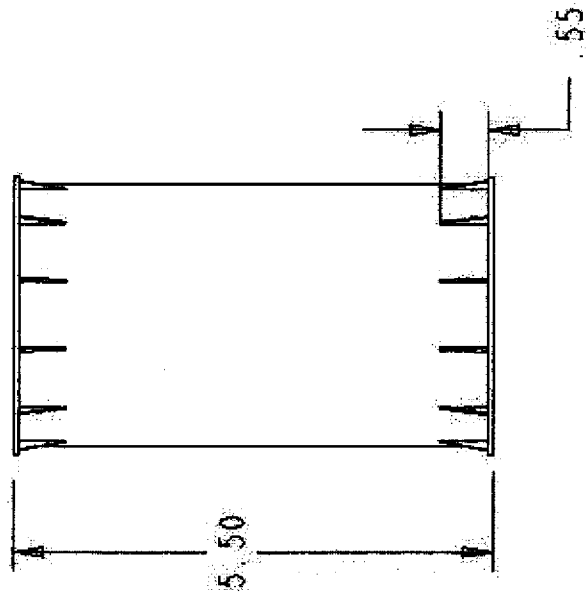
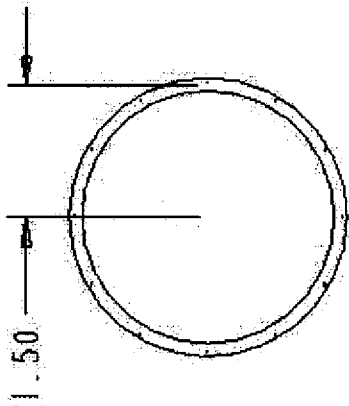
The University of New Hampshire



Top Section	
OSWEB	
Dim. in Meters	TECH 797 Modeled by PRP
04/25/03	

SCALE : 0.333 TYPE : PART NAME : TOPSECTION SIZE : A

The University of New Hampshire



Middle Section

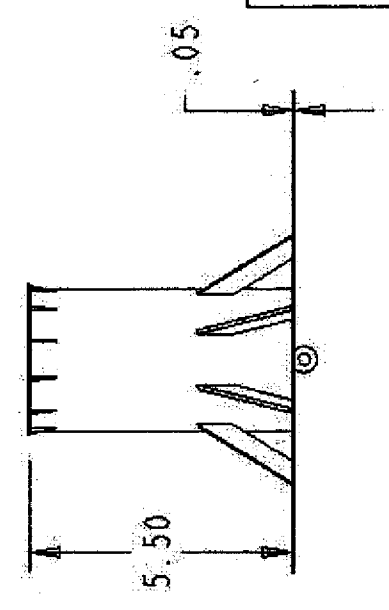
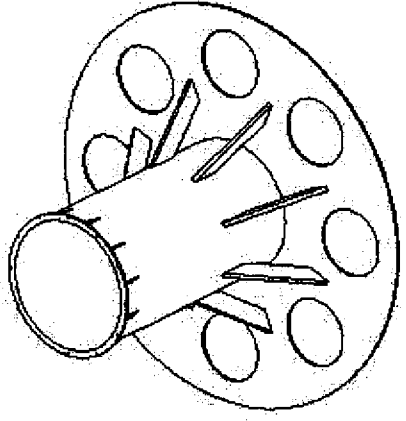
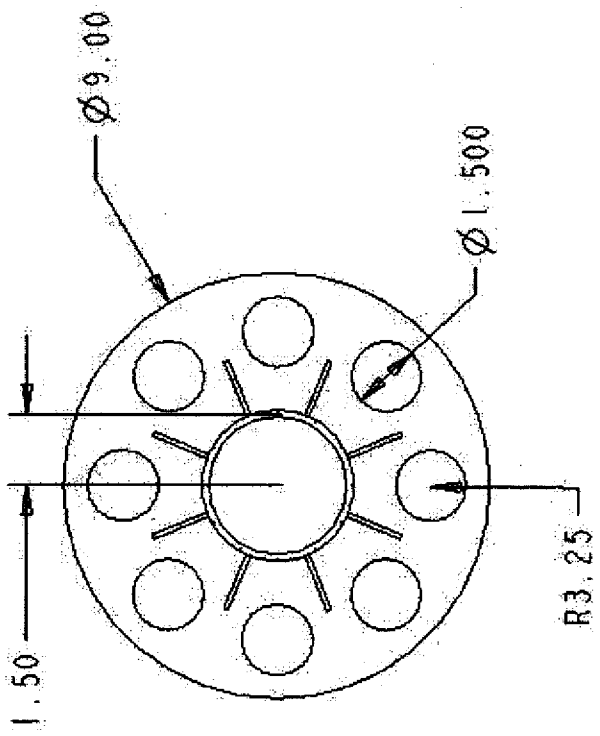
OSWEB

Dim. in Meters

04/25/03

TECH 797 Modeled by PRP

The University of New Hampshire



Bottom Section	
OSWEB	
Dim. in Meters	
04/25/03	TECH 797
	Modeled by PRP

The University of New Hampshire

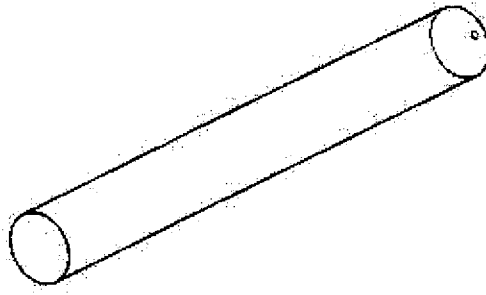
THICKNESS .005

$\varnothing 1.60$

R.085

14.800

.50



Feed Silo

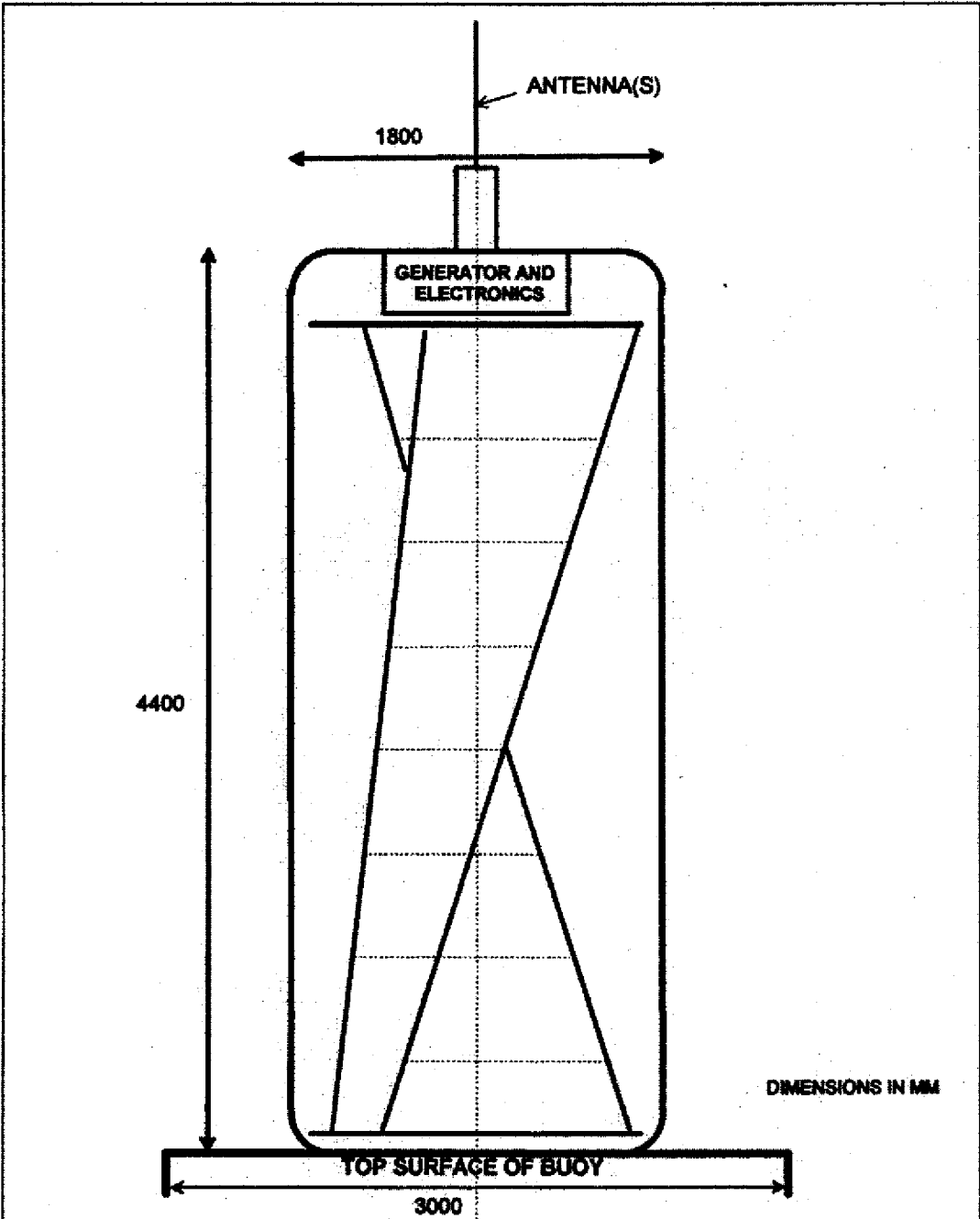
OSWEB

Dim. in Meters

04/25/03

TECH 797 Modeled by PRP

SCALE : 0.200 TYPE : PART NAME : SILO SIZE : A



030408 HELIUS WIND TURBINE LAYOUT

SPECIFICATIONS SUBJECT TO CHANGE WITHOUT NOTICE

**WINDSTREAM POWER SYSTEMS
INCORPORATED**
Independent Power Systems Throughout the World

PO BOX 1804 / BURLINGTON, VERMONT 05402-1804 / USA
TEL 802 855 0075 FAX 802 855 1088
EMAIL engineering@windstreampower.com
WEB www.windstreampower.com

B. Buoy Feed System Operating Procedures

To begin feeding:

1. Be sure ballast discharge valve is closed, it is normally closed. (Turn switch "B" to off).
2. Be sure the feedwater intake valve is open, it is normally open. (Turn switch "C" to off).
3. Open one and only one of the cage selector valves. (Turn switch "F", "G", "H", or "I" to on).
4. Turn on the main pump motor and main pumpside feed line valve. (Turn switch "D" to on).
5. Turn on the screw/auger silo emptier. (Turn switch "N" to on).

To feed a different cage, once feeding has begun:

1. Open the cage selector valve to the cage you want to start feeding. (Turn switch "F", "G", "H", or "I" to on).
2. Close the cage selector valve to the cage you want to stop feeding. (Turn switch "F", "G", "H", or "I" to off).

To stop feeding:

1. Turn off the screw/auger silo emptier. (Turn switch "N" to off).
2. Turn off the main pump motor and main pumpside feed line valve. (Turn switch "D" to off).
3. Close all cage selector valves. (Turn switch "F", "G", "H", and "I" to off).

To take on ballast:

1. Be sure ballast discharge valve is closed, it is normally closed. (Turn switch "B" to off).
2. Open the ballast intake valve. (Turn switch "A" to on.)
3. Close the ballast intake valve after taking on the appropriate amount of ballast. (Turn switch "A" to on.)

To discharge ballast:

1. Be sure the feedwater intake valve is open, it is normally open. (Turn switch "C" to off).
2. Open one of the cage selector valves. (Turn switch "F", "G", "H", or "I" to on).
3. Turn on the main pump motor and main pumpside feed line valve. (Turn switch "D" to on).
4. Open the ballast discharge valve. (Turn switch "B" to on).

5. Close the feedwater intake valve. (Turn switch "C" to on.)
6. When tank is empty, open feedwater intake valve. (Turn switch "C" to off).
7. Close the ballast discharge valve. (Turn switch "B" to off).
8. Turn off the main pump motor and main pumpside feed line valve. (Turn switch "D" to off).

Close all cage selector valves. (Turn switch "F", "G", "H", and "I" to off).

C. Prefabricated Component Specifications

Main and Backup Pump Motor.....	C-2
Main and Backup Pump.....	C-4
Solenoid Valves.....	C-6
Feed Lines.....	C-9
Velleman Device Controller.....	C-10
RTS AutoPak Wireless Modem.....	C-11
MOSFET's.....	C-12
Screw/Auger Feeder.....	C-13
Electrical Enclosure.....	C-14
Helius Turbine.....	C-15

DC Motors & Gearmotors

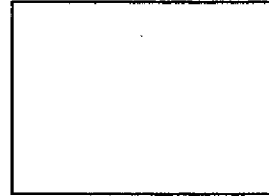
For information about electric motors, see [page 888](#).

DC Motors

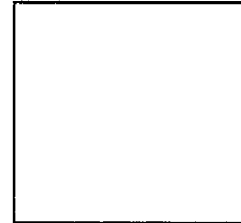
The permanent magnet design means that the motor field is supported by magnets instead of copper windings, giving you a lighter weight motor that's more economical to operate. With linear speed/torque characteristics over the entire speed range, these motors can be used with a control for applications that require adjustable speed *and* constant torque. For adjustable speed controls, see 7729K on [page 771](#) for 12 and 24 VDC motors; see 7793K on [page 771](#) for 0-180 VDC motors. Great for braking and reversing applications. All motors have permanently lubricated ball bearings. The brush/spring assembly is easy to access for trouble-free maintenance. Housing is steel. End shields are die cast aluminum. Rotation is reversible. Rated for continuous duty. Motors have Class F insulation and a side junction box, except as noted.

NEMA C-Face motors offer direct mounting to equipment with the matching configuration and also include a removable steel bolt-on base for mounting versatility. *12 VDC and 24 VDC* motors are great for mobile and generator-powered applications. They have a totally enclosed nonventilated (TENV) enclosure, except as noted. *90 VDC and 180 VDC* motors offer a high starting torque for heavy loads. They have a totally enclosed fan-cooled (TEFC) enclosure.

Square-flange motors operate on 12 VDC to 24 VDC and have a totally enclosed nonventilated (TENV) enclosure.



NEMA C-Face Mount



Square-Flange Mount

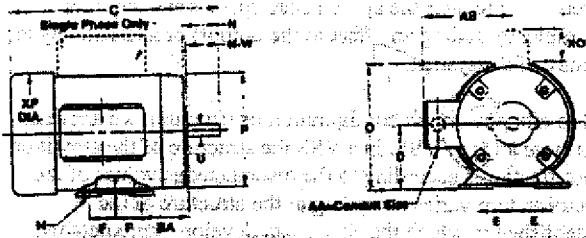
NEMA C-Face Mount

hp	rpm	Torque, in.-lbs.	NEMA Frame	Full Load Amps	Overall Lg.	Each

Motor Dimensions

DIMENSIONS NEMA STEEL FRAME MOTORS

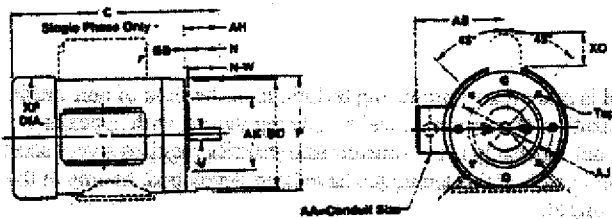
RIGID MOUNT



The condensed dimensions shown on these pages are for general reference only and are not for construction. The overall length or "C" dimension for each catalog item is included in this catalog.

Certified drawings of all ratings are available for construction purposes.

C FACE



NEMA SHAFT AND KEYWAY DIMENSIONS (Inches)

NEMA SHAFT SIZE	KEYWAY DIMENSIONS	NEMA SHAFT SIZE	KEYWAY DIMENSIONS
Ø	W x D	Ø	W x D
1/2	3/16 x 3/16	1-1/2	3/8 x 3/8
3/4	1/4 x 1/4	1-3/4	7/16 x 7/16
1	5/16 x 5/16	2	1/2 x 1/2
1-1/4	3/8 x 3/8	2-1/4	5/8 x 5/8
1-1/2	7/16 x 7/16	2-1/2	3/4 x 3/4
1-3/4	1/2 x 1/2	2-3/4	7/8 x 7/8
2	5/8 x 5/8	3	1 x 1

Ø is keyway width.
D is keyway depth.

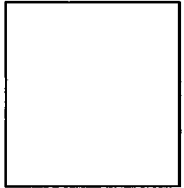
NEMA STEEL FRAME DIMENSIONS (Inches)

Frame Size A	B	E	F	H	I	O	P	U	W	AA	AB	AE	AH	AJ	AK	BA	BB	BD	BO	XP	XP	XP	XP
40	2 1/2	1 1/2	1 1/4	1 1/2	1 1/2	1 1/2	1 1/2	1 1/2	1 1/2	1 1/2	4 1/2	1 1/2	1 1/2	1 1/2	3	2 1/2	1 1/2	1 1/2	1 1/2	1 1/2	1 1/2	1 1/2	1 1/2
48	3	2 1/4	1 1/2	1 1/2	1 1/2	1 1/2	1 1/2	1 1/2	1 1/2	1 1/2	4 1/2	1 1/2	1 1/2	1 1/2	3	2 1/2	1 1/2	1 1/2	1 1/2	1 1/2	1 1/2	1 1/2	1 1/2
56	3 1/2	2 1/2	1 1/2	1 1/2	1 1/2	1 1/2	1 1/2	1 1/2	1 1/2	1 1/2	4 1/2	1 1/2	1 1/2	1 1/2	3	2 1/2	1 1/2	1 1/2	1 1/2	1 1/2	1 1/2	1 1/2	1 1/2
63	4	3	1 1/2	1 1/2	1 1/2	1 1/2	1 1/2	1 1/2	1 1/2	1 1/2	4 1/2	1 1/2	1 1/2	1 1/2	3	2 1/2	1 1/2	1 1/2	1 1/2	1 1/2	1 1/2	1 1/2	1 1/2
71	4 1/2	3 1/2	1 1/2	1 1/2	1 1/2	1 1/2	1 1/2	1 1/2	1 1/2	1 1/2	4 1/2	1 1/2	1 1/2	1 1/2	3	2 1/2	1 1/2	1 1/2	1 1/2	1 1/2	1 1/2	1 1/2	1 1/2
80	5	4	1 1/2	1 1/2	1 1/2	1 1/2	1 1/2	1 1/2	1 1/2	1 1/2	4 1/2	1 1/2	1 1/2	1 1/2	3	2 1/2	1 1/2	1 1/2	1 1/2	1 1/2	1 1/2	1 1/2	1 1/2
90	5 1/2	4 1/2	1 1/2	1 1/2	1 1/2	1 1/2	1 1/2	1 1/2	1 1/2	1 1/2	4 1/2	1 1/2	1 1/2	1 1/2	3	2 1/2	1 1/2	1 1/2	1 1/2	1 1/2	1 1/2	1 1/2	1 1/2
100	6	5	1 1/2	1 1/2	1 1/2	1 1/2	1 1/2	1 1/2	1 1/2	1 1/2	4 1/2	1 1/2	1 1/2	1 1/2	3	2 1/2	1 1/2	1 1/2	1 1/2	1 1/2	1 1/2	1 1/2	1 1/2
112	6 1/2	5 1/2	1 1/2	1 1/2	1 1/2	1 1/2	1 1/2	1 1/2	1 1/2	1 1/2	4 1/2	1 1/2	1 1/2	1 1/2	3	2 1/2	1 1/2	1 1/2	1 1/2	1 1/2	1 1/2	1 1/2	1 1/2
125	7	6	1 1/2	1 1/2	1 1/2	1 1/2	1 1/2	1 1/2	1 1/2	1 1/2	4 1/2	1 1/2	1 1/2	1 1/2	3	2 1/2	1 1/2	1 1/2	1 1/2	1 1/2	1 1/2	1 1/2	1 1/2
140	7 1/2	6 1/2	1 1/2	1 1/2	1 1/2	1 1/2	1 1/2	1 1/2	1 1/2	1 1/2	4 1/2	1 1/2	1 1/2	1 1/2	3	2 1/2	1 1/2	1 1/2	1 1/2	1 1/2	1 1/2	1 1/2	1 1/2
160	8 1/2	7 1/2	1 1/2	1 1/2	1 1/2	1 1/2	1 1/2	1 1/2	1 1/2	1 1/2	4 1/2	1 1/2	1 1/2	1 1/2	3	2 1/2	1 1/2	1 1/2	1 1/2	1 1/2	1 1/2	1 1/2	1 1/2
180	9 1/2	8 1/2	1 1/2	1 1/2	1 1/2	1 1/2	1 1/2	1 1/2	1 1/2	1 1/2	4 1/2	1 1/2	1 1/2	1 1/2	3	2 1/2	1 1/2	1 1/2	1 1/2	1 1/2	1 1/2	1 1/2	1 1/2
200	10 1/2	9 1/2	1 1/2	1 1/2	1 1/2	1 1/2	1 1/2	1 1/2	1 1/2	1 1/2	4 1/2	1 1/2	1 1/2	1 1/2	3	2 1/2	1 1/2	1 1/2	1 1/2	1 1/2	1 1/2	1 1/2	1 1/2
225	11 1/2	10 1/2	1 1/2	1 1/2	1 1/2	1 1/2	1 1/2	1 1/2	1 1/2	1 1/2	4 1/2	1 1/2	1 1/2	1 1/2	3	2 1/2	1 1/2	1 1/2	1 1/2	1 1/2	1 1/2	1 1/2	1 1/2
250	12 1/2	11 1/2	1 1/2	1 1/2	1 1/2	1 1/2	1 1/2	1 1/2	1 1/2	1 1/2	4 1/2	1 1/2	1 1/2	1 1/2	3	2 1/2	1 1/2	1 1/2	1 1/2	1 1/2	1 1/2	1 1/2	1 1/2
280	13 1/2	12 1/2	1 1/2	1 1/2	1 1/2	1 1/2	1 1/2	1 1/2	1 1/2	1 1/2	4 1/2	1 1/2	1 1/2	1 1/2	3	2 1/2	1 1/2	1 1/2	1 1/2	1 1/2	1 1/2	1 1/2	1 1/2
315	14 1/2	13 1/2	1 1/2	1 1/2	1 1/2	1 1/2	1 1/2	1 1/2	1 1/2	1 1/2	4 1/2	1 1/2	1 1/2	1 1/2	3	2 1/2	1 1/2	1 1/2	1 1/2	1 1/2	1 1/2	1 1/2	1 1/2
350	15 1/2	14 1/2	1 1/2	1 1/2	1 1/2	1 1/2	1 1/2	1 1/2	1 1/2	1 1/2	4 1/2	1 1/2	1 1/2	1 1/2	3	2 1/2	1 1/2	1 1/2	1 1/2	1 1/2	1 1/2	1 1/2	1 1/2
400	16 1/2	15 1/2	1 1/2	1 1/2	1 1/2	1 1/2	1 1/2	1 1/2	1 1/2	1 1/2	4 1/2	1 1/2	1 1/2	1 1/2	3	2 1/2	1 1/2	1 1/2	1 1/2	1 1/2	1 1/2	1 1/2	1 1/2
450	17 1/2	16 1/2	1 1/2	1 1/2	1 1/2	1 1/2	1 1/2	1 1/2	1 1/2	1 1/2	4 1/2	1 1/2	1 1/2	1 1/2	3	2 1/2	1 1/2	1 1/2	1 1/2	1 1/2	1 1/2	1 1/2	1 1/2
500	18 1/2	17 1/2	1 1/2	1 1/2	1 1/2	1 1/2	1 1/2	1 1/2	1 1/2	1 1/2	4 1/2	1 1/2	1 1/2	1 1/2	3	2 1/2	1 1/2	1 1/2	1 1/2	1 1/2	1 1/2	1 1/2	1 1/2
560	19 1/2	18 1/2	1 1/2	1 1/2	1 1/2	1 1/2	1 1/2	1 1/2	1 1/2	1 1/2	4 1/2	1 1/2	1 1/2	1 1/2	3	2 1/2	1 1/2	1 1/2	1 1/2	1 1/2	1 1/2	1 1/2	1 1/2
630	20 1/2	19 1/2	1 1/2	1 1/2	1 1/2	1 1/2	1 1/2	1 1/2	1 1/2	1 1/2	4 1/2	1 1/2	1 1/2	1 1/2	3	2 1/2	1 1/2	1 1/2	1 1/2	1 1/2	1 1/2	1 1/2	1 1/2
710	21 1/2	20 1/2	1 1/2	1 1/2	1 1/2	1 1/2	1 1/2	1 1/2	1 1/2	1 1/2	4 1/2	1 1/2	1 1/2	1 1/2	3	2 1/2	1 1/2	1 1/2	1 1/2	1 1/2	1 1/2	1 1/2	1 1/2
800	22 1/2	21 1/2	1 1/2	1 1/2	1 1/2	1 1/2	1 1/2	1 1/2	1 1/2	1 1/2	4 1/2	1 1/2	1 1/2	1 1/2	3	2 1/2	1 1/2	1 1/2	1 1/2	1 1/2	1 1/2	1 1/2	1 1/2
900	23 1/2	22 1/2	1 1/2	1 1/2	1 1/2	1 1/2	1 1/2	1 1/2	1 1/2	1 1/2	4 1/2	1 1/2	1 1/2	1 1/2	3	2 1/2	1 1/2	1 1/2	1 1/2	1 1/2	1 1/2	1 1/2	1 1/2
1000	24 1/2	23 1/2	1 1/2	1 1/2	1 1/2	1 1/2	1 1/2	1 1/2	1 1/2	1 1/2	4 1/2	1 1/2	1 1/2	1 1/2	3	2 1/2	1 1/2	1 1/2	1 1/2	1 1/2	1 1/2	1 1/2	1 1/2

* 140-47C NEMA C face BA dimension is 2 1/4". 180-47C NEMA C face BA dimension is 2 1/2". 210-57C NEMA C face BA dimension is 4 1/4".
 ** 280-7C and smaller have A mounting holes as NEMA C face. 280-7C and larger have B mounting holes.
 A. Shaft mounting device dimensions comply with NEMA standard MS1.

Pedestal-Mount Bronze Centrifugal Pumps without Motor

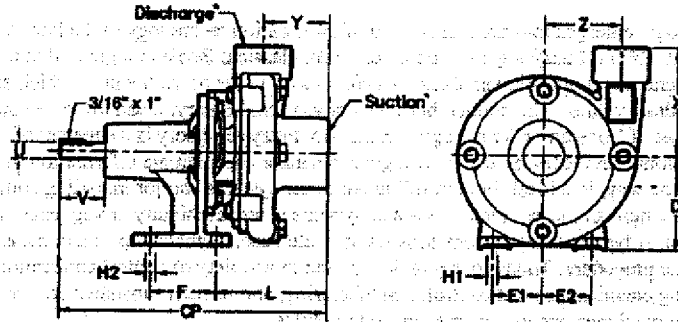
Connect these pumps to your motor, gear reducer, or belt drive to transfer and circulate water. They have a bronze housing and open brass impeller. Shaft is Type 303 stainless steel, 5/8" diameter, and has self-lubricating double ball bearings. Maximum temperature is 210° F. Fluids must be compatible with wetted parts (materials in contact with solution). Wetted parts are bronze, Buna-N, carbon, ceramic, Type 303 stainless steel, and Vellumoid.



██████████ [Click here \(See top of page for details\)](#)

PUMP PERFORMANCE, gpm @ ft. of head										Connections,		
When Used with 3450 rpm, 60 Hz Motor					When Used with 1725 rpm, 60 Hz Motor					NPT female		
Req'd hp	5 ft.	20 ft.	50 ft.	Shutoff, ft.	Req'd hp	1 ft.	5 ft.	10 ft.	Shutoff, ft.	Intake	Discharge	Each
1/3	37	27	—	47	1/4	16	10	3	11	3/4"	1/2"	4284K2 \$158.30
3/4	61	50	9	56	1/3	36	28	17	13	1"	3/4"	4284K7 186.07
1 1/2	102	86	42	67	█	█	█	█	█	█	█	█

Straight Centrifugal Pedestal Pumps



Pump Dimensional Data

Model No.	SUC*	DIS*	CP	D	E1	E2	F	H1	H2	L	U	V	X	Y	Z	BHP Required @3450 RPM	(-95) Cast Iron Ship. Wt.	(-97) Bronze Ship. Wt.	(-98) S. Steel Ship. Wt.
GENERAL SERVICE MODELS																			
3682-9x	3/4"	1/2"	3.6	3.2	1.5	1.5	N/A	0.3	0.3	3.0	0.8	1.3	1.9	1.4	1.9	0.58	9 Lbs.	10 Lbs.	9 Lbs.
3704-9x	1"	3/4"	3.7	3.2	1.5	1.5	N/A	0.3	0.3	3.0	0.8	1.3	2.4	1.4	2.1	1.13	10 Lbs.	11 Lbs.	10 Lbs.
3954-9x	1-1/4"	1"	3.7	3.2	1.5	1.5	N/A	0.3	0.3	3.0	0.8	1.3	2.5	1.3	2.0	1.95	12 Lbs.	13 Lbs.	12 Lbs.
HIGH HEAD MODELS																			
4897-9x	1-1/4"	1"	1.5	4.2	2.2	2.2	3.0	0.5	0.5	4.4	0.7	1.9	4.8	2.1	3.3	1.13	34 Lbs.	36 Lbs.	34 Lbs.
4906-9x	1-1/2"	1-1/4"	12.1	4.2	2.2	2.2	3.0	0.5	0.5	4.9	0.7	1.9	4.9	3.0	3.5	3.45	36 Lbs.	40 Lbs.	36 Lbs.

(* Standard NPT (female) pipe thread)

NOTE: Dimensions have a tolerance of ± .005

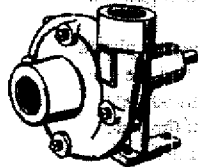
When Ordering Add the Correct -9x Suffix to Model Number Indicating Material Selection:

XCI (-95) = Cast Iron Construction with Stainless Steel Impeller and Buna N Seals, Max. Temperature 180... F

XCB (-97) = Cast Bronze Construction with Viton® Seals, Max. Temperature 200... F

XSS (-98) = Investment Cast 316 Stainless Steel Construction with Viton® Seals, Max. Temperature 200... F

Standard Features



✓ Stainless Steel Fitted Cast Iron, Cast Bronze or Investment Cast 316 Stainless Steel Construction

✓ Maximum Temperature

Buna N 180... F
Viton® 200... F

✓ 3/4" to 1-1/2" NPT Suction Ports

✓ Maximum Flow 118 GPM

✓ 1/2" to 1-1/4" NPT Discharge Ports

✓ Maximum Head 148 Ft.

✓ Maximum Working Pressure

General Service 75 PSI
High Head 150 PSI

✓ Discharge Port Rotates in 90... Increments on High Head Units

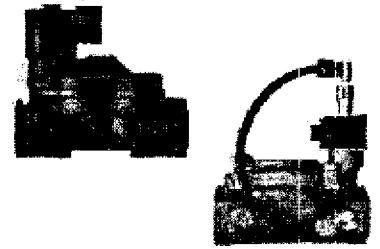
✓ Self-cleaning Impellers on General Service Models

✓ Epoxy Coated Pedestal Drive on High Head Models

368 PES-CP / 1999

Solenoid Valves Specifications

Series 31 2-Way Piloted Diaphragm General Service Solenoid Valves Brass and Polymer Bodies » 3/4" - 3" NPT



GENERAL INFORMATION:

The Economy Line of valves offers a reliable low cost, lightweight and compact alternative to the Industrial Line. These valves are well suited for humid environments and can be inexpensively modified to meet specific requirements.

(These valves are not intended for use in medical life-support, combustion, aerospace or similar applications)

Mounting Position:

Any Position (best if vertical and upright)

Actuation Response Time:

1 second - 6 seconds is typical

ELECTRICAL SPECIFICATIONS:

Standard Voltages:

AC 50/60 Hz: 6, 12, 24, 120, 240
DC: 6, 12, 24
DC Latching: 12

Coil Rating:

Continuous duty totally encapsulated
Class A Rated 105°C; 221°F

Voltage Tolerances:

±10% of applicable voltage

Standard Lead Length: 18" or 24"

DC Latching Valves:

2-Wire (std): 30-50 ms pulse is required for activation; a reversed polarity pulse is required for deactivation. Pulses longer than 50 ms may cause the valve to re-actuate.

NOMINAL AMBIENT TEMPERATURE

RANGES:

0°C to 49°C; 32°F to 120°F

ENCLOSURE OPTIONS:

1/2" FPT Conduit (std) - Epoxy potted coil in a glass filled polypropylene housing with integral female conduit connection and 24" leads

1/2" MPT Conduit (120, 240 VAC std) - Fully molded coil in a Valox housing with integral male conduit connection (Class F Rated)

Spade Terminals - Two 1/4" spade terminals integrally molded in a Thermoplastic Polyester housing and open frame design

Din Connection - Form "B" style connection

Canister - Epoxy potted coil in a glass filled nylon canister with two 18" leads wires (custom wire configurations available)

OPERATING MODES AVAILABLE:

Normally Closed - Closed when de-energized, open when energized

Normally Open - Open when de-energized, closed when energized

VALVE PARTS IN CONTACT WITH MEDIA:

Body - Brass or 30% Glass Filled Nylon

Internals - Brass Valves - Brass, S/S
Polymer Valves - Acetal

Base Nut - Brass (std)

Core Tube - S/S T305

Plunger and Core Plug - S/S T430F

Shading Ring (AC unites only) - Copper (std); Silver (special order only)

Springs - S/S T302

Seals - Nitrile (std)

Diaphragm - Nylon Reinforced Nitrile

OPTIONS:

• Latching Solenoids



Other voltages, coil constructions, lead lengths and materials are available to meet special requirements.

Technical Data, Mounting Holes, Flow Patterns

Valve Specifications													Solenoid Specification			
Port Size (in)	Orifice Size (in)	Cv Factor	Operating Press						Max. Operating Temp		Coil Wattage		Brass	30% GF Nylon	Voltage	Enclosure/Termination
			AC Air/Gas/Water Max. (MOPD)		DC Air/Gas/Water Max. (MOPD)		°F	°C	AC	DC						
			Min. (psi)	(bar)	(psi)	(bar)										

NORMALLY CLOSED (CLOSED WHEN DE-ENERGIZED)

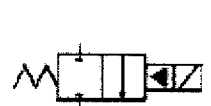
3/4	1	10	10	.7	150	10.5	125	8.5	180	82.2	5	10	-	AC	A205 - SA -	24-50/60 Spade
-----	---	----	----	----	-----	------	-----	-----	-----	------	---	----	---	----	-------------	----------------

1	10	15	1.2	300	21.0			180	82.2	5	10	3108B-672CN	-	24-50/60	Spade	
1	14	10	.7	150	10.5	125	8.5	180	65.5	5	10	-	3110N-662CN	A210 -	Term.	
1	1	14	10	.7	180	12.6	125	8.5	180	82.2	5	10	3110B-662CN	-	110/50- 120/60	LL - Din "B"
1	14	15	1.2	300	21.0			180	82.2	5	10	3110B-672CN	-			
1-1/2	1-1/2	40	10	.7	150	10.5	125	8.5	180	82.2	5	10	3116B-692CN	3116N-692CN	A223 -	CB -
2	2	56	10	.7	150	10.5	125	8.5	180	82.2	5	10	3120B-712CN	3120N-712CN	220/50- 240/60	1/2" MPT
															DC -	
NORMALLY OPEN (OPEN WHEN DE-ENERGIZED)															DC	
3/4	1	10	10	.7	150	12.6	125	8.5	180	82.2	5	10	-	3108N-662ON	12 VDC	CN -
1	1	10	10	.7	150	12.6	125	8.5	180	82.2	5	10	3110B-662ON	3110N-662ON	A375-	Canister
1-1/2	1-1/2	10	10	.7	150	12.6	125	8.5	180	82.2	5	10	3116B-692ON	3116N-662ON	24 VDC	
2	2	10	10	.7	150	12.6	125	8.5	180	82.2	5	10	3120B-712ON	3120N-712ON		
																

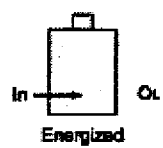
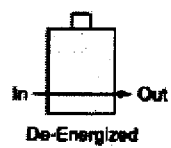
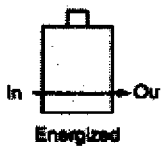
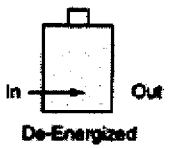
Technical Information

Operational Sequence / Flow Patterns:

2-Way Normally Closed



2-Way Normally Open



Wattage Rating / Power Consumption:

DC		AC		
Wattage	Voltage (60Hz)	Wattage	Inrush Current V ma	Holding Current V ma
	24	5	385	200
6	120	5	97	65
	240	5	58	37

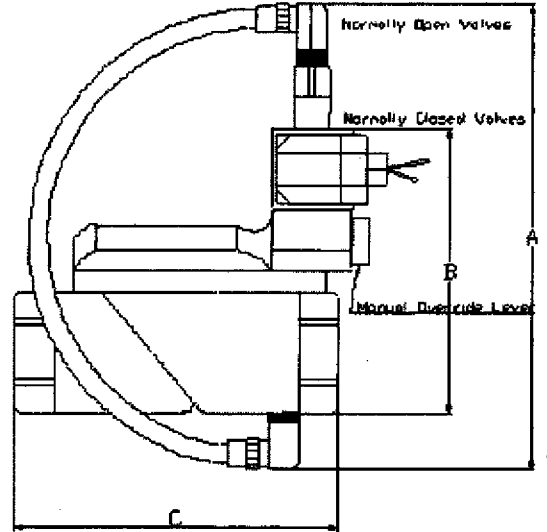
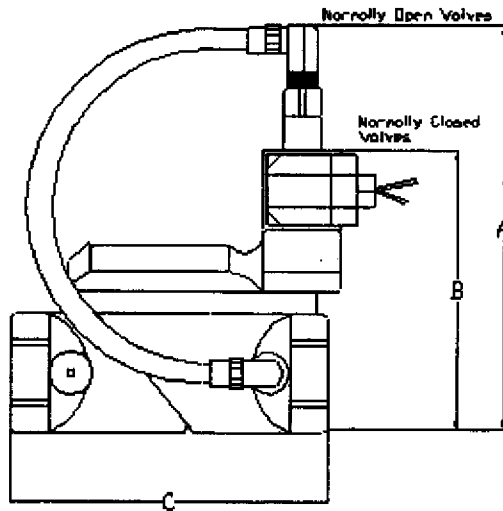
AC
 Inrush Amps = Volt-Amp Inrush / Voltage
 Holding Amps = volt-amp Holding / Voltage

DC
 Since DC valves have no Inrush current, the amp rating can be determined:
 Amps = Watts (DC) / Voltage

Valve Dimensions:

Brass Valves

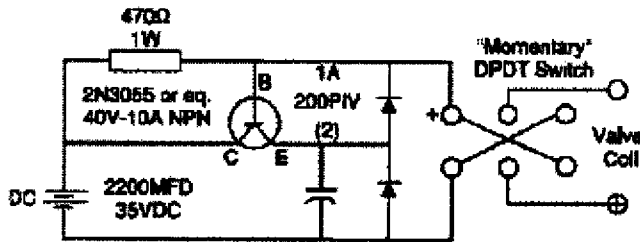
GF Nylon Valves



Pipe Size	A	B	C	Weight (lbs.)
3/4"	n/a	3.8	4.2	1.8
1"	5.3	4.0	4.4	2.5
1-1/2"	7.3	5.1	6.1	6.8
2"	7.3	5.6	7.0	8.5
3"	11.7	10.0	11.7	38.0

Pipe Size	A	B	C	Weight (lbs.)
3/4"	5.98	4.1	4.35	.75
1"	5.98	4.1	4.35	.75
1-1/2"	7.2	7.2	6.3	2.2
2"	7.4	7.4	6.8	2.4

Latching Valve 2-Wire Circuit:



Lead Wires:

Red (+) is for Latching;
Black (-) is common

Current Pulse:

the

A 12 VDC 30-50 ms pulse is required to latch actuator in

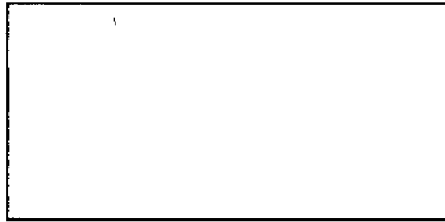
open or closed position. A pulse longer than 50 ms may cause the armature to re-

actuate.

Other configurations and materials are available for special requirements. Please contact the factory or fill out the custom application form with your requirements.

Pure Gum Rubber Tubing

- Temperature Range: -70° to +160° F
- Color: Tan
- Durometer, Shore A: 45
- Tensile Strength: 3000 psi
- Elongation: 700%
- Sterilization: Not rated
- Material Meets: FDA (food and beverage), Fed. Spec. ZZ-T-831D
- Fittings: Barbed (see pages 111-118)



Smooth Finish



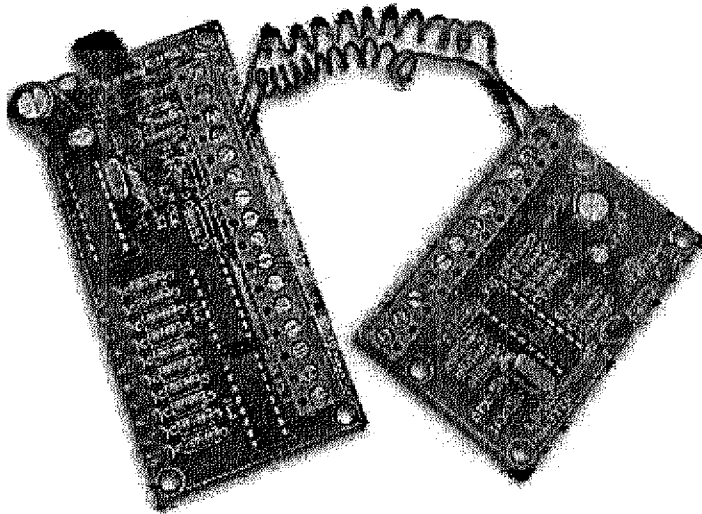
Rough Finish

This natural rubber heavy-wall tubing has a rough-textured finish (except where noted). Provides excellent abrasion resistance, yet isn't as resilient, soft, or smooth as latex rubber tubing. Use for abrasive media, air, chemical, food, and beverage transfer lines. Not pressure rated; use for gravity flow applications. Not rated for bend radius. **Vacuum-rated** tubing withstands vacuum up to 29.9" Hg at 70° F.

ID	OD	Wall	Available Lengths, ft.		Per Ft.
Standard					
1 1/4"	1 3/4"	1/4"	Up to 50	5546K11	5.00
1 1/2"	2 1/2"	1/2"	Up to 20	5546K12	9.73
2"	2 1/4"	1/8"	Up to 12	5546K13	4.59
2"	2 1/2"	1/4"	Up to 12	5546K14	7.57
2"	3"	1/2"	Up to 12	5546K19	13.82
2 1/4"	2 3/4"	1/4"	Up to 12	5546K16	8.78
2 1/2"	3"	1/4"	Up to 12	5546K17	9.46
‡ Smooth finish.					

10-CHANNEL, 2-WIRE REMOTE CONTROL

Order Code : K8023



This kit allows you to control up to 10 devices using only 2 wires at a long distance. Microprocessor controlled. Inputs can be push-buttons, switches or open collector outputs from another device. The receiver section provides 10 open collector outputs that allow you to control relays directly. Terminal block connectors for all input and output connections are included. All outputs are provided with LED indication. Can be used with our kits : [K6711](#), [K8000](#), [K8006](#),... Can be connected to our standard relay card : [K6714](#) or [K6714-16](#).

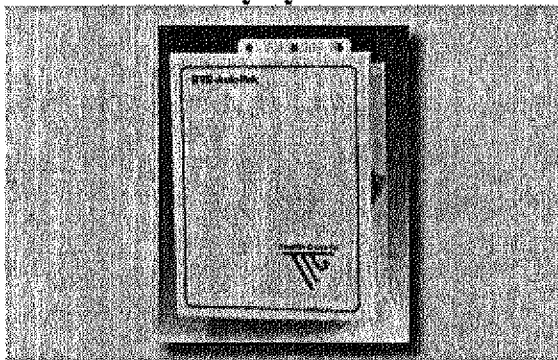
Specifications

- 10 open collector outputs : 50V / 100mA
- tested to a distance of up to 50m (55 yards) between control- and receiver section
- operating voltage : single 12-15V AC or DC, 300mA
- dimensions :
 - control pcb : 70 x 50 x 16mm (2.7" x 2.0" x 0.6")
 - receiver pcb : 103 x 50 x 24mm (4.0" x 2.0" x 1.0")
- recommended adapter : [PS1205](#)

Last Update: 11 Mar 2003

© 2000 Velleman® Components N.V.
Also visit the [main Velleman Website](#)

Remote Telemetry System AutoPak



- Transceiver:** Motorola Series IV Cellular Radio - rated at nominal 3 watts maximum power output, TNC antenna connector
Terminal block with dry-contact closure for indicating loss of cellular signal
Motorola messenger receiver; TNC antenna connector.
- Power Supply:** Keyed connector with cable for 12-VDC input from storage battery
Low voltage and thermal protection of cellular transceiver
Selection of optional batteries and complete solar assemblies for a wide range of applications
Optional AC input supplies for special requirements
Varistor and RFI filtering, transient and overcurrent protection for RJ11 connections
External ground lug.
- User Interface:** RJ11 Jack for data or voice, RJ45 jack for programming, testing, and antenna setup
AutoSafe automatic transceiver activation
Two wire, loop start
Ring voltage, 25 Hz, 60 Vrms, 150 V p-p
Dial Tone: 350 Hz/440 Hz square wave
Maximum REN=3
- RTS-SPM Power Management Module
- Environmental:** NEMA 3R weatherproof enclosure
Thermal shutoff protection
-40C to 60C (-40F to 140F) operating,
-40C to 80C (-40F to 176F) storage
5% to 95% percent relative humidity, non-condensing
- Mechanical:** Punch-outs for 1/2-inch conduit to accommodate electrical and telephone wires, securable latch
Size: 11 inches H x 8.5 inches W x 5 inches D
Weight Approximately 8.5 pounds (including battery)
Optional bracket for mounting cellular antenna

MOSFET

12/2003 WED 07:56 FAX DIGI-KEY

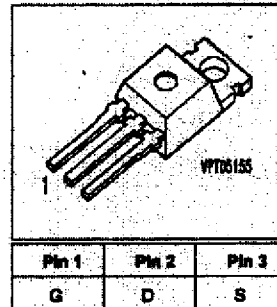
002/009



SiPMOS Power Transistor

- N channel
- Enhancement mode
- Avalanche-rated

BUZ 21



Type	V _{DS}	I _D	R _{DS(on)}	Package	Ordering Code
BUZ 21	100 V	21 A	0.085 Ω	TO-220 AB	C67078-S1308-A2

Parameter	Symbol	Value	Unit
Continuous drain current T _C = 25 °C	I _D	21	A
Pulsed drain current T _C = 25 °C	I _{D(pulse)}	84	A
Avalanche current, limited by T _{Jmax}	I _{AR}	21	A
Avalanche energy, periodic, limited by T _{Jmax}	E _{AR}	11	mJ
Avalanche energy, single pulse I _D = 21 A, V _{DD} = 25 V, R _{GS} = 25 Ω L = 340 μH, T _J = 25 °C	E _{AS}	100	mJ
Gate source voltage	V _{GS}	± 20	V
Power dissipation T _C = 25 °C	P _{tot}	75	W
Operating temperature	T _J	-55 ... + 150	°C
Storage temperature	T _{stg}	-55 ... + 150	°C
Thermal resistance, chip case	R _{θJC}	≤ 1.87	K/W
Thermal resistance, chip to ambient	R _{θJA}	75	K/W
DIN humidity category, DIN 40 040		E	
IEC climatic category, DIN IEC 68-1		55 / 150 / 55	

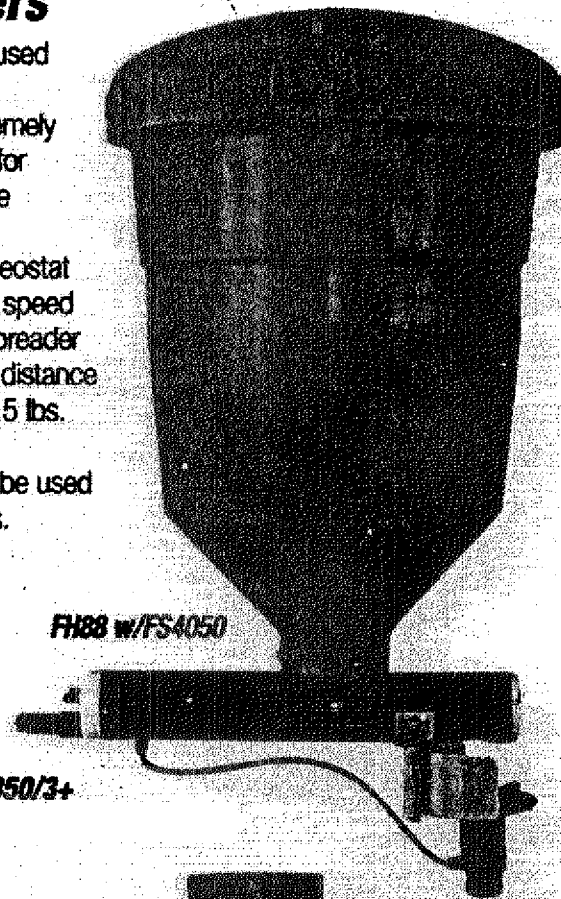
Data Sheet

1

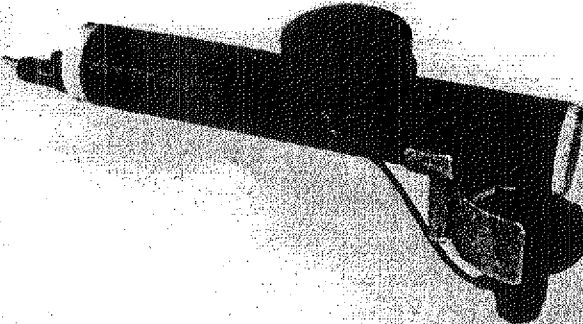
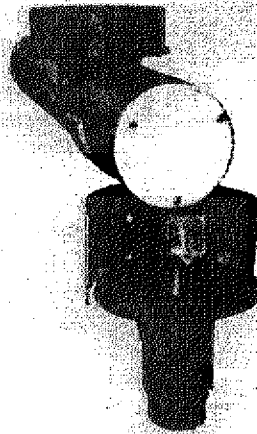
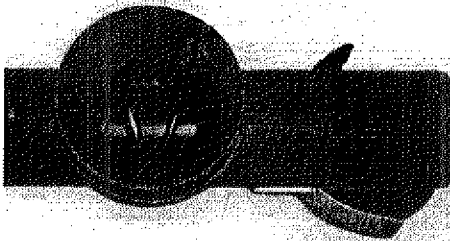
05.99

Screw/Auger Feeders

These new screw-style feeders are used throughout the world in commercial aquaculture facilities. They are extremely well built, durable and can be used for both indoor and outdoor aquaculture applications. Designed for accurate dispensing of feed, they feature a rheostat adjustable auger that can be set for speed and duration. **FS4050** includes a spreader plate with a rheostat adjustment for distance and weighs 8 lbs. **FS4059** weighs 5 lbs. Screw feeders are 12V and draw approximately 0.5 amps. They can be used with any of the Lucky Pond hoppers.



FS4059 Screw Feeder **\$369** **\$350/3+**



Fiberglass Enclosures

For information about NEMA enclosure ratings, see page 718.

NEMA 6P Fiberglass Enclosures

All have urethane-gasketed covers with stainless steel hinges and four 0.31" flanged mounting holes. Working depth (area available for component mounting) is approximately 3/4" less than the enclosure depth. UL and C-UL listed.

Color-Coded Enclosures with Standard Covers— With Screw Seal— Have two stainless steel captive screws for closing. **With Padlock Hasp—** Have a stainless steel hasp (3/8" shackle dia.) for padlocking.

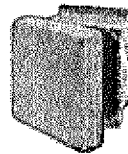
Please specify enclosure color: gray, red, white, or yellow.

Gray Enclosures with Link-Lock Latch— Have a stainless steel cam-actuated link-lock latch.

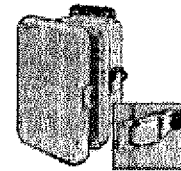
Gray Enclosures with Raised Covers— Provide additional depth. Offered with a stainless steel hasp (3/8" shackle dia.) for padlocking or with a cam-actuated link-lock latch.

Please specify hasp or link-lock latch.

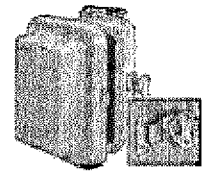
Removable inner component mounting **panels** are sold separately below.



Screw Seal with Standard Cover



Padlock Hasp with Standard Cover



Link-Lock Latch with Raised Cover

Overall Size, Ht. x Wd. x Dp.	COLOR-CODED ENCLOSURES		GRAY ENCLOSURES		GRAY ENCLOSURES		PANELS	
	w/Screw Seal Each	w/Padlock Hasp Each	w/Link-Lock Latch Each	with Raised Cover Wd. x Dp.	Each	Ht. x Wd.	Each	
7.5" x 5.4" x 4.8"	7583K1 \$32.50	7740K11 \$48.87	6917K31 \$48.87	5.5" x 6.2"	6918K51 \$49.37	4.9" x 2.9"	6917K11 \$5.26	
7.5" x 7.5" x 4.8"	7583K2 37.28	7740K12 50.73	6917K32 50.73	7.5" x 6.2"	6918K52 51.21	4.9" x 4.9"	6917K12 5.44	
9.6" x 7.5" x 4.8"	7583K3 38.51	7740K13 51.38	6917K33 51.38	7.5" x 6.2"	6918K53 51.88	6.9" x 4.9"	6917K13 6.75	
11.6" x 9.4" x 4.3"	7583K4 45.15	7740K14 51.98	6917K34 51.98	9.4" x 6.6"	6918K54 52.50	8.9" x 6.9"	6917K14 9.52	
13.6" x 11.4" x 5.2"	7583K5 52.91	7740K15 59.94	6917K35 59.94	11.4" x 6.6"	6918K55 60.54	10.9" x 8.9"	6917K15 10.31	
15.5" x 13.5" x 6.3"	7583K6 61.32	7740K16 80.65	6917K36 77.67	13.4" x 7.7"	6918K56 78.71	12.9" x 10.9"	6917K16 12.31	
17.5" x 15.5" x 6.3"	7583K7 70.46	7740K17 87.71	6917K37 84.46	15.4" x 7.7"	6918K57 85.58	14.9" x 12.9"	6917K17 15.94	
		7740K18 113.98	6917K38 103.98	17.5" x 10.6"	6918K58 111.21	16.9" x 14.9"	6917K18 20.41	

BUOY-MOUNTED HELIUS VERTICAL AXIS WIND TURBINE

**For - David V. Parker
Department of Mechanical Engineering
University of New Hampshire**

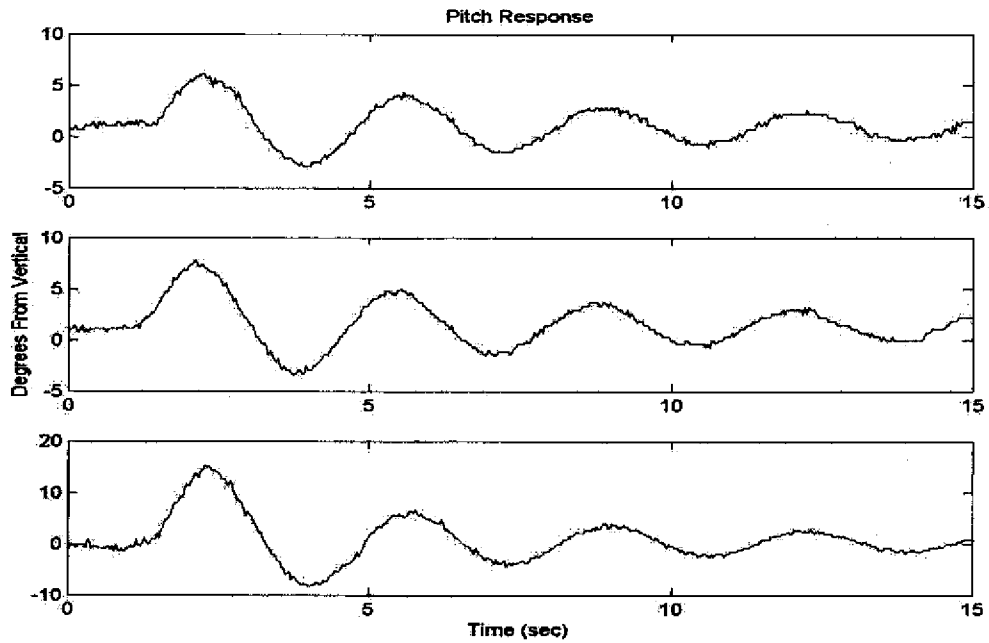
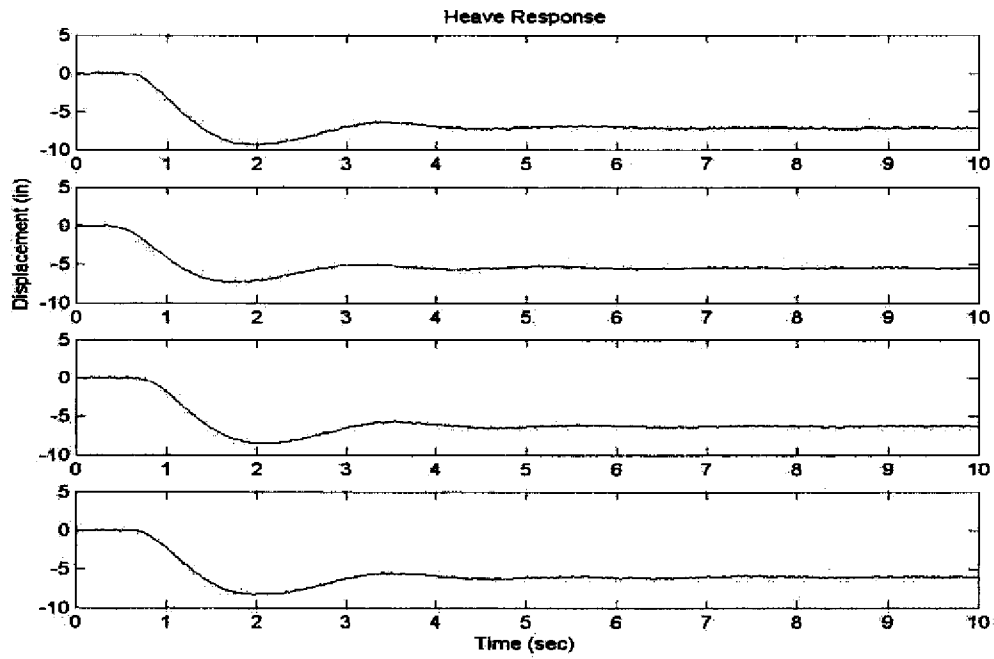
030408

Specifications:

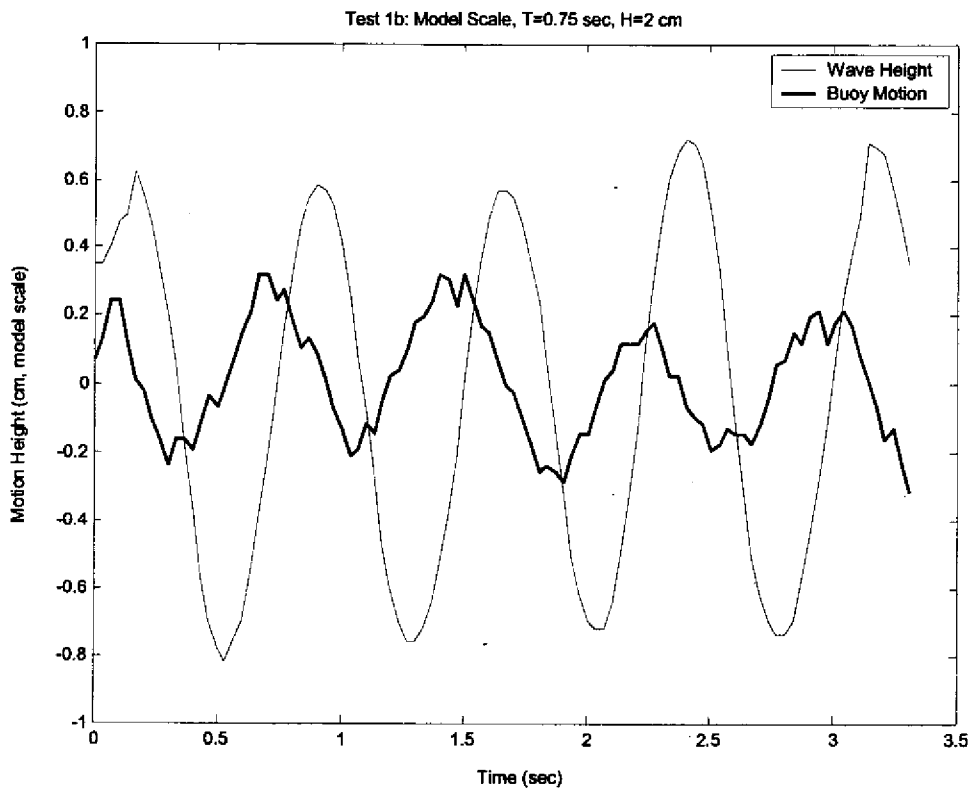
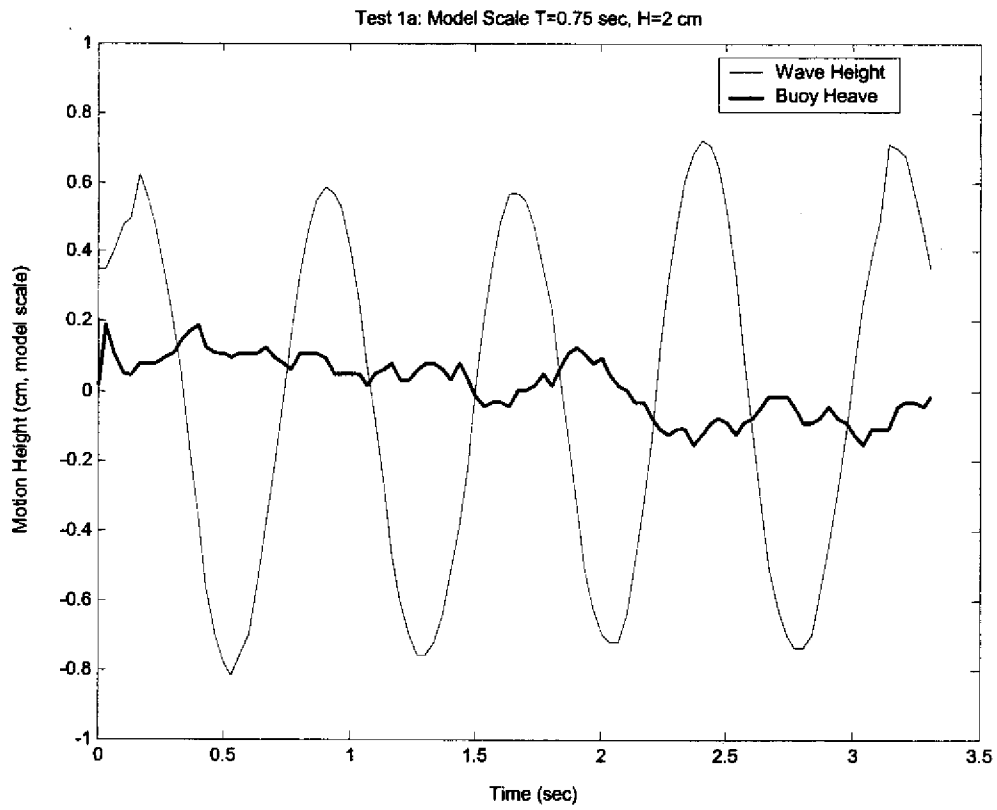
Rated power	250 watts (10.4 amperes at 24 volts nominal).
Rated windspeed	18 m/sec.
Power production	2.9kWh/day (20kWh/week) at 6m/sec average wind speed.
Power output	24 volts dc nominal (27.6 v regulated float voltage) for charging 24 volt battery pack.
Voltage regulation	Electronic voltage regulator included.
Generator	Direct drive encapsulated three phase brushless permanent magnet alternator.
Overspeed control	Integral
Weight	Aluminum construction - 600kg. Stainless steel construction - 980kg.
Dimensions	Height - 4.4m. Outside diameter (frame) 1.8m.
Mounting	On 3m wide buoy.
Antenna mounting	On top of turbine.
Price (single unit) :	Aluminum construction - \$11,980. Stainless steel construction - \$15,100.

D. Raw Data Plots of Physical Test Results

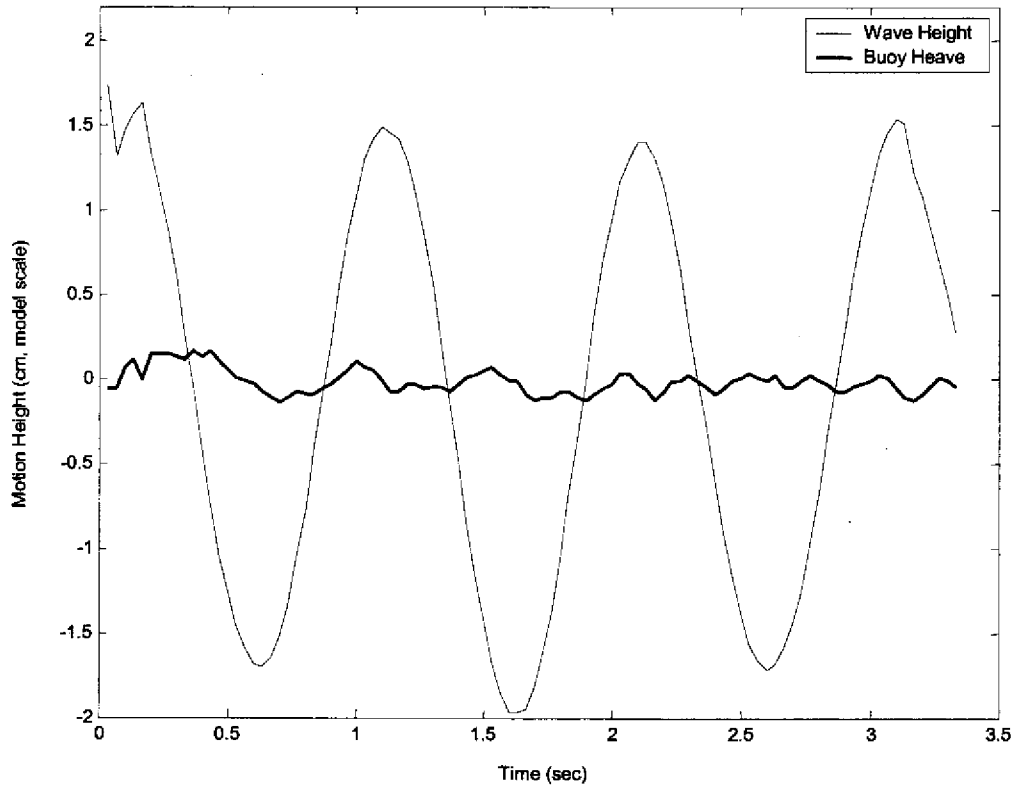
Free Release Tests for Heave and Pitch



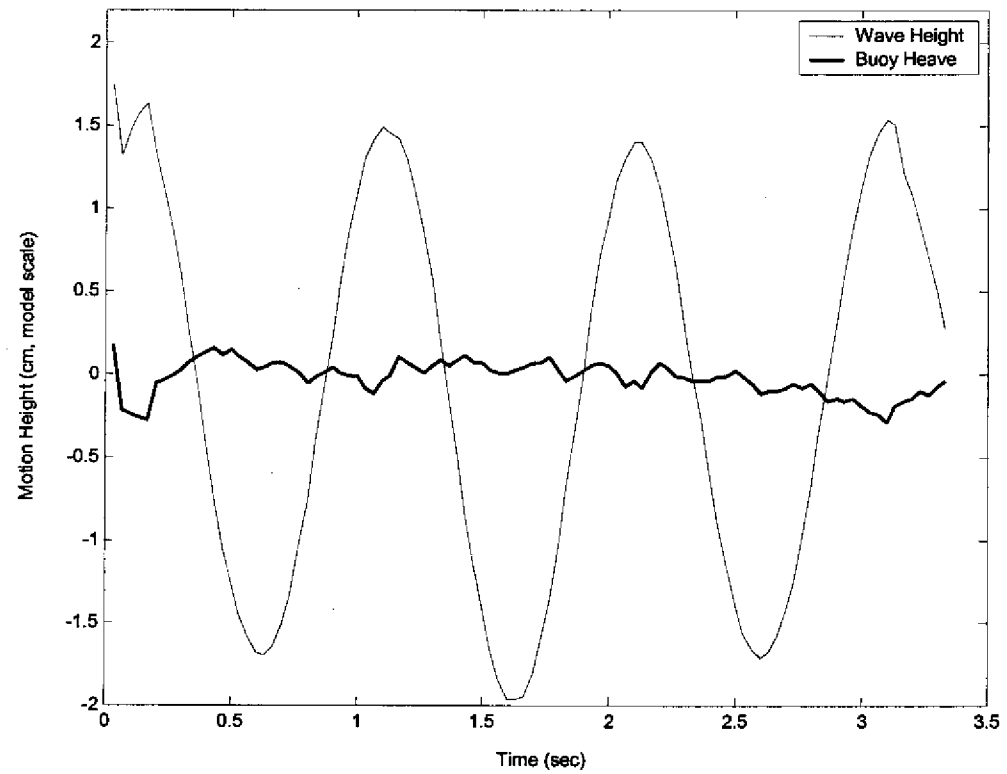
Moored Sea-Keeping Tests



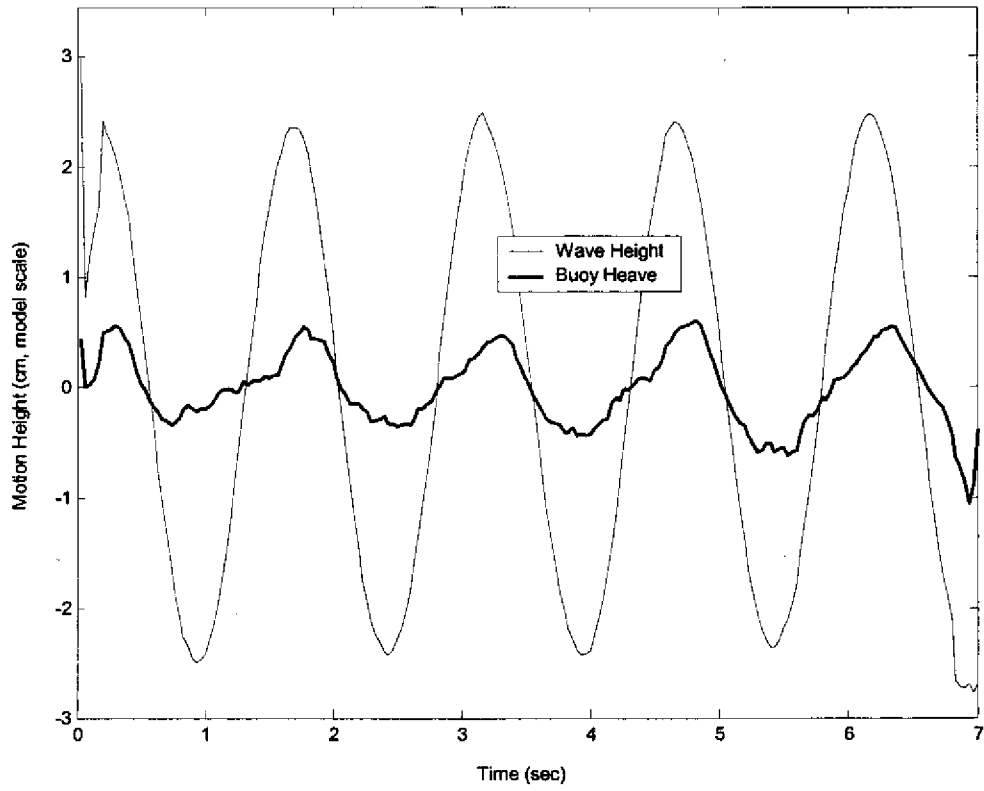
Test 2a: Model Scale, T=1 sec, H=4 cm



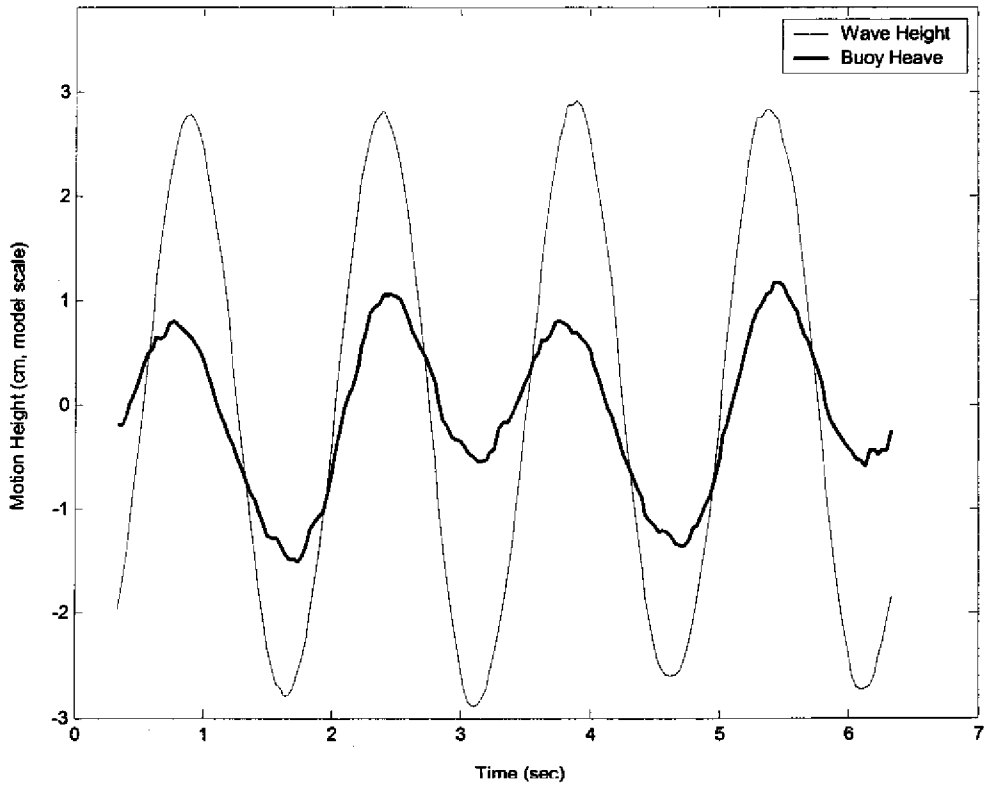
Test 2b: Model Scale, T=1 sec, H=4 cm



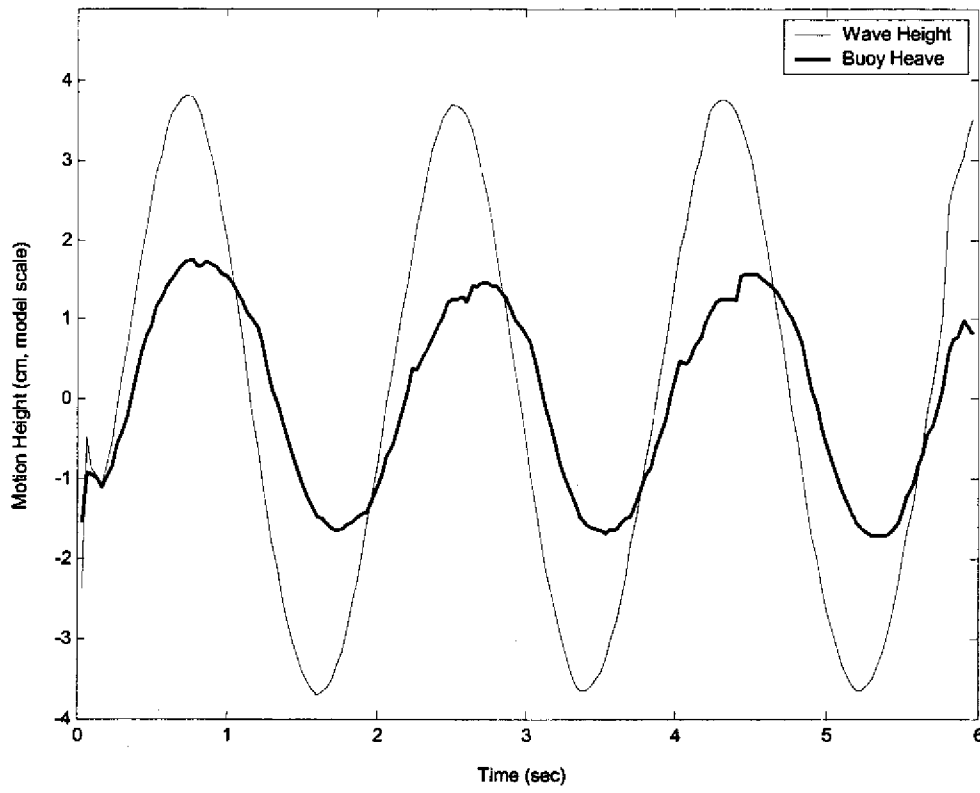
Test 3a: Model Scale, T=1.5 sec, H=5 cm



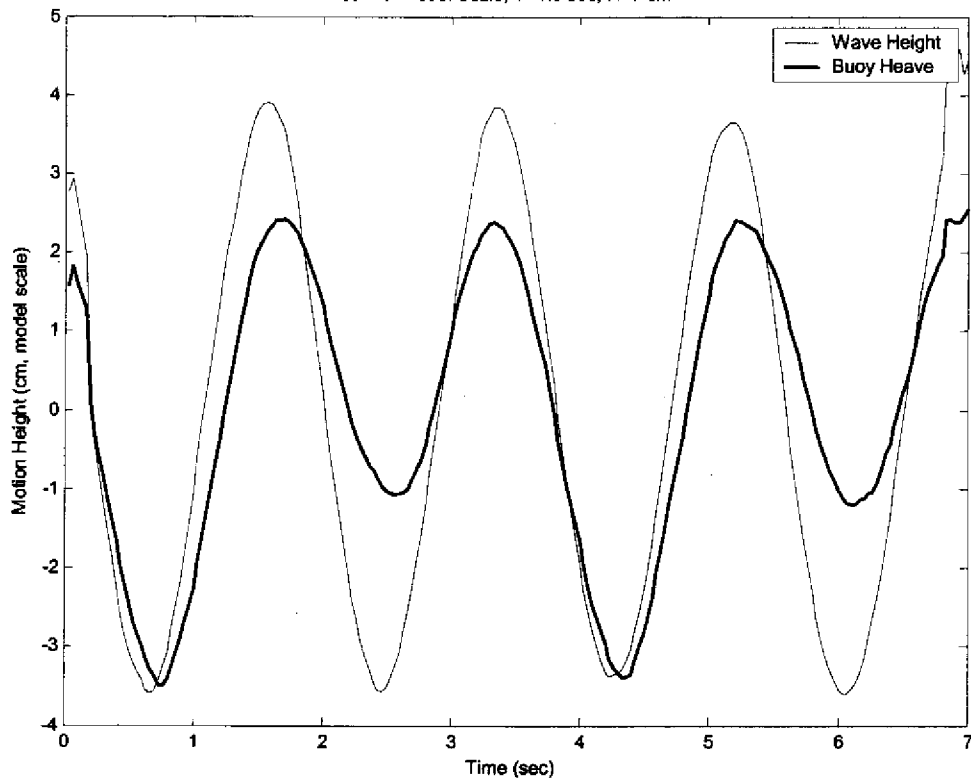
Test 3b: Model Scale, T=1.5, H=5 cm



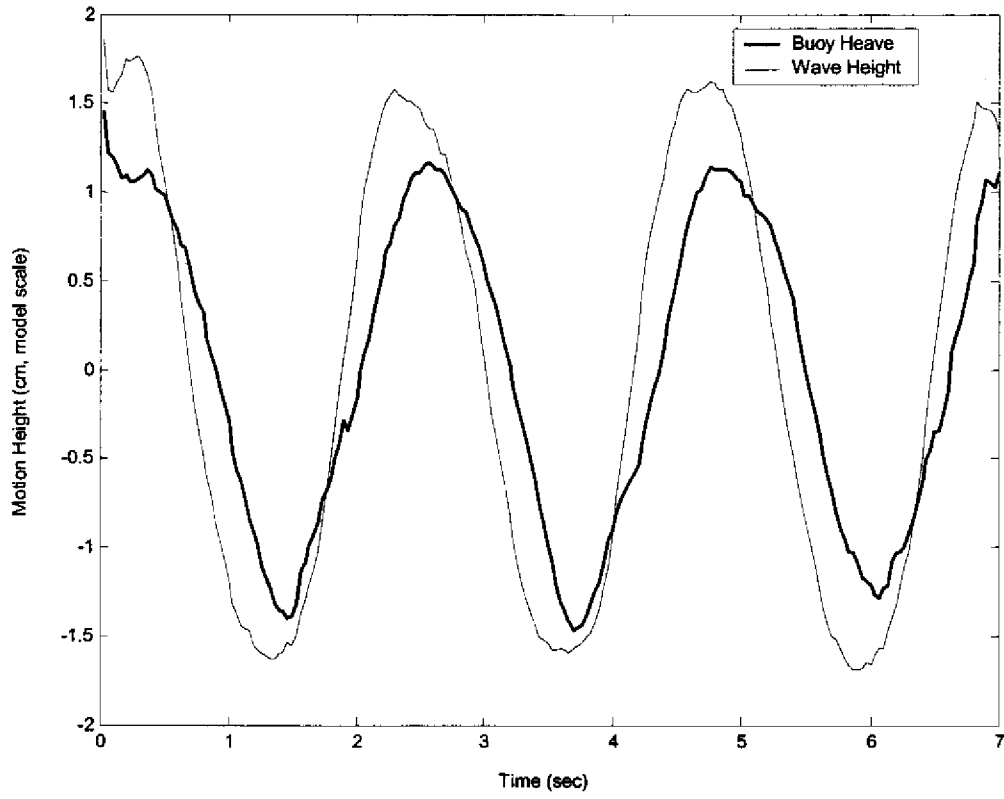
Test 4a: Model Scale, T=1.8 sec, H=7 cm



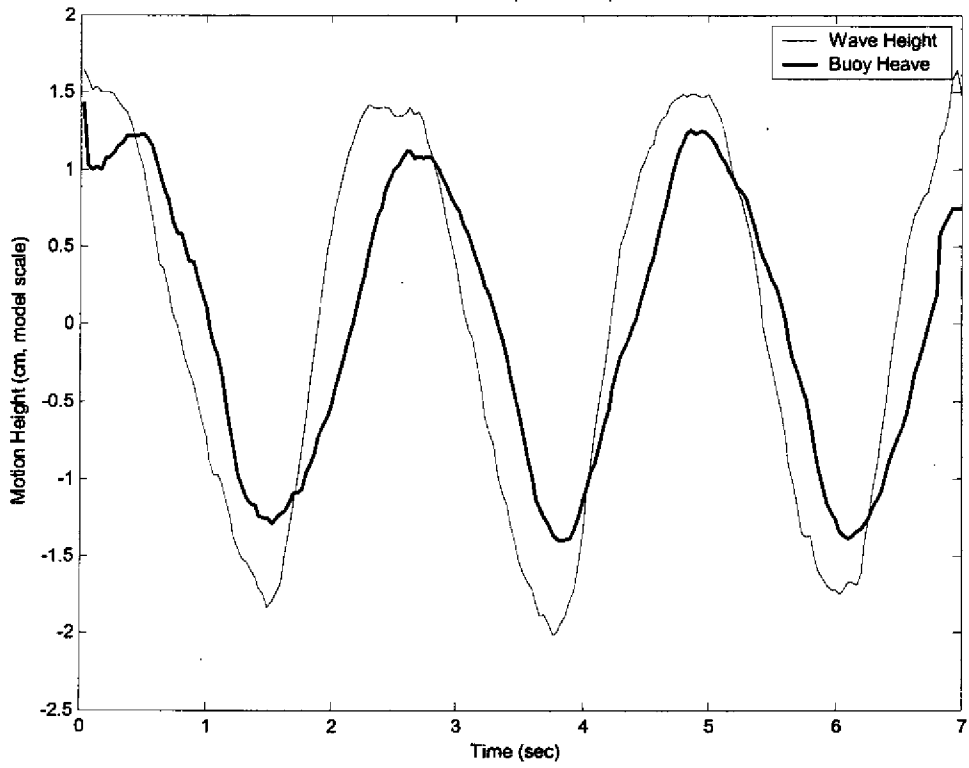
Test 4b: Model Scale, T=1.8 sec, H=7 cm



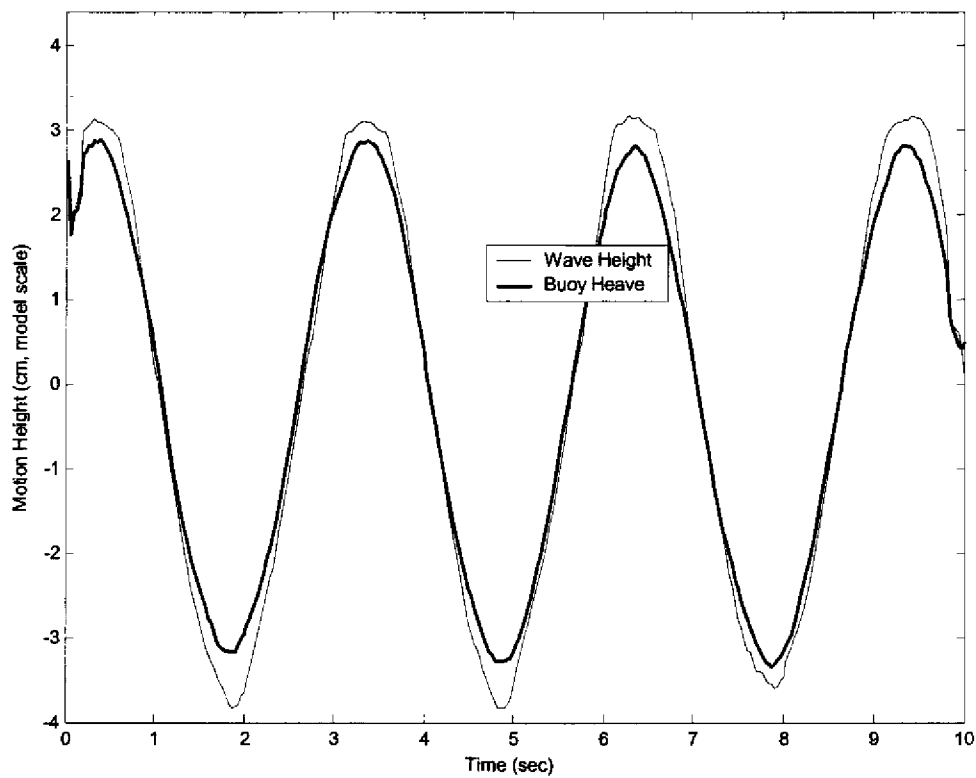
Test 5a: Model Scale, T=2.3, H=5 cm



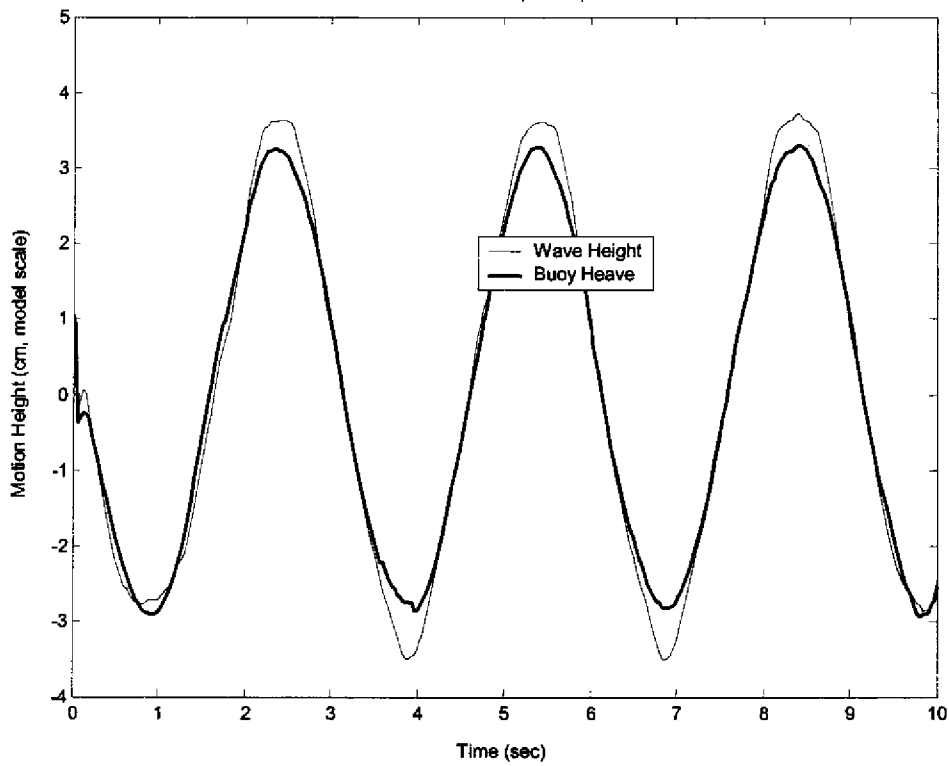
Test 5b: Model Scale, T=2.3 sec, H=3 cm

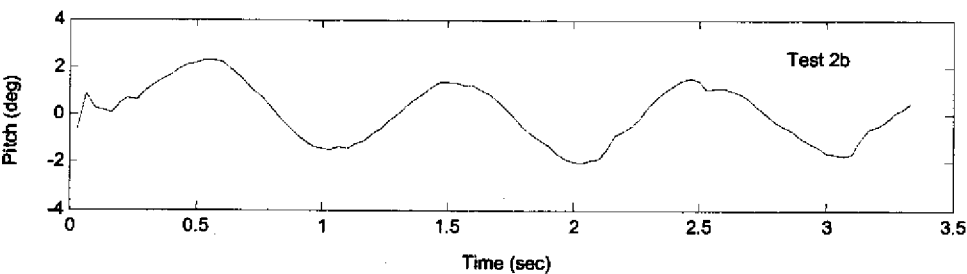
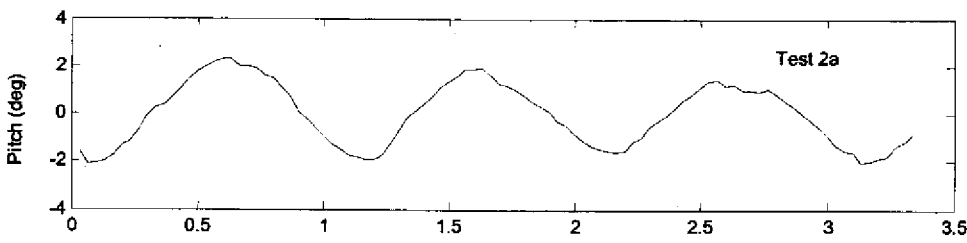
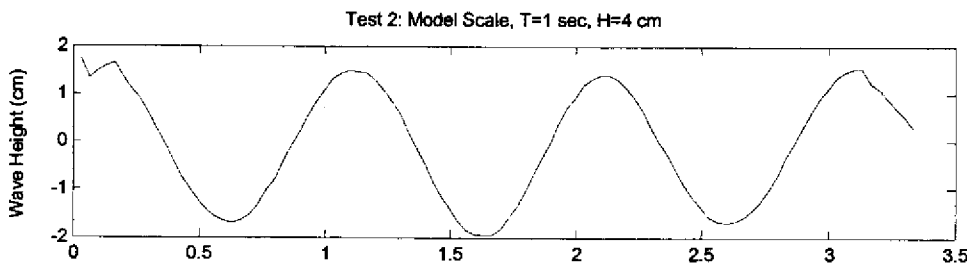
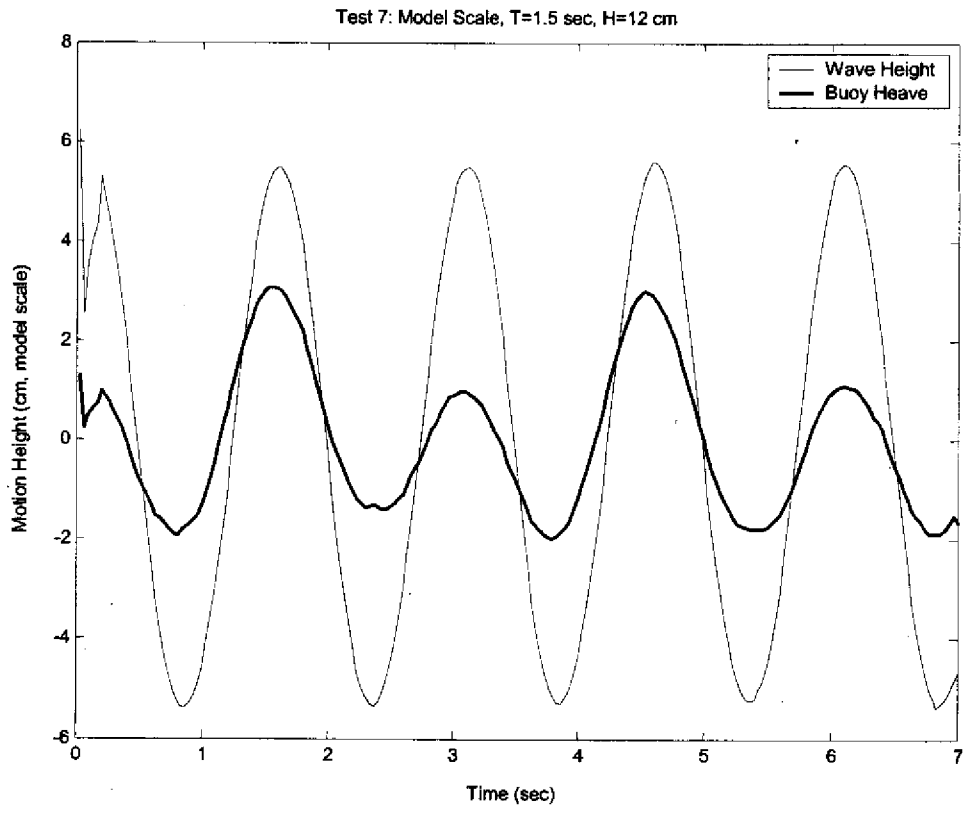


Test 6a: Model Scale, T=3 sec, H=5 cm

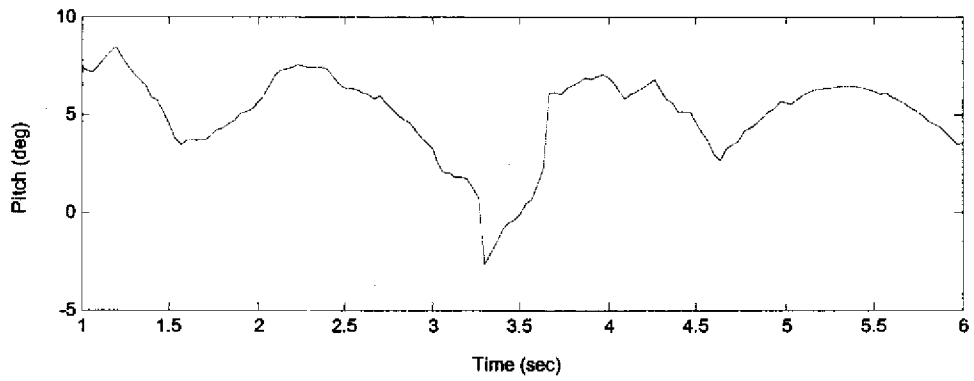
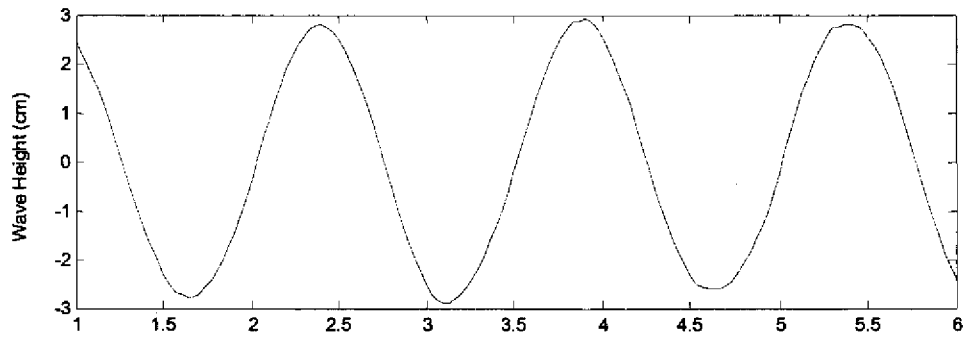


Test 6b: Model Scale, T=3.0, H=5 cm

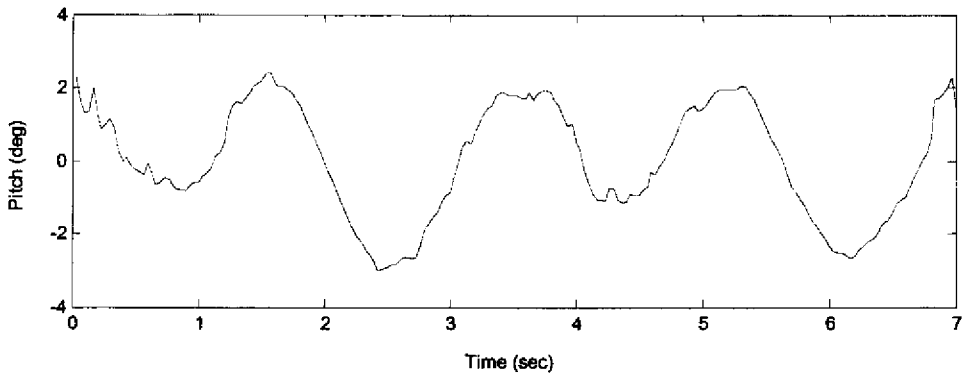
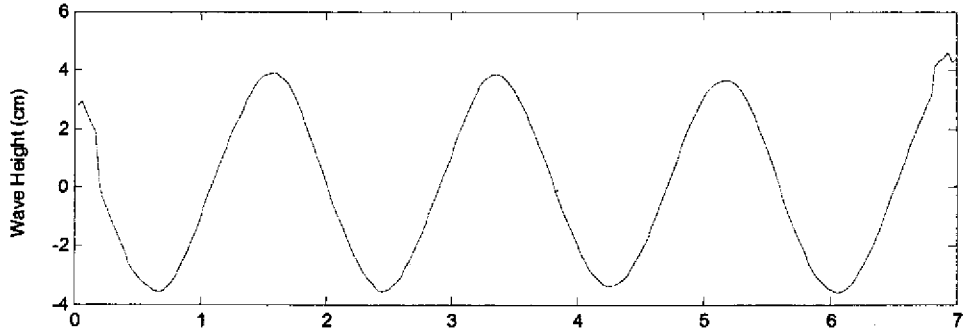




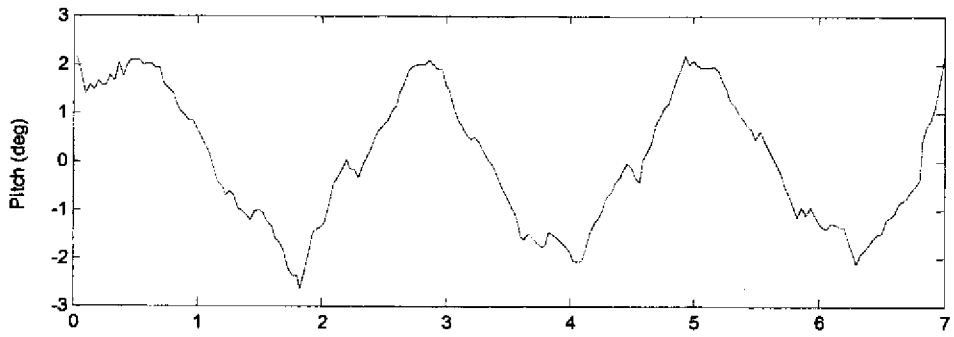
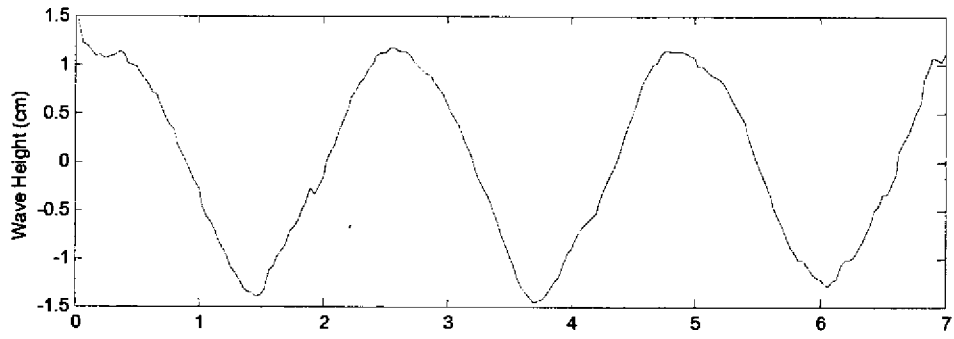
Test 3: Model Scale, T=1.5 sec, H=5 cm



Test 4: Model Scale, T=1.8 sec, H=7 cm



Test 5: Model Scale, T=2.3, H=3 cm



Test 6: Model Scale, T=3 sec, H=5 cm

